Stony Brook University

Investigation of the dynamics of QPX, a pathogen of the hard clam

***Mercenaria mercenaria,* in the environment and clams**

A Dissertation Presented

By

Qianqian Liu

to

The Graduate School

In Partial Fulfillment of the

Requirements

for the Degree of

Doctor of Philosophy

in

Marine and Atmospheric Science

Stony Brook University

May 2010

Stony Brook University

The Graduate School

Qianqian Liu

We, the dissertation committee for the above candidate for the

Doctor of Philosophy degree, hereby recommend

acceptance of this dissertation

Jackie L. Collier – Dissertation Advisor
Assistant Professor, School of Marine and Atmospheric Sciences

Bassem Allam – Dissertation Advisor
Associate Professor, School of Marine and Atmospheric Sciences

Christopher J. Gobler – Chairperson of Defense
Associate Professor, School of Marine and Atmospheric Sciences

Robert M. Cerrato
Associate Professor, School of Marine and Atmospheric Sciences

Susan Ford
Professor Emeritus, Haskin Shellfish Research Laboratory
Rutgers, the State University of New Jersey

This dissertation is accepted by the Graduate School

Lawrence Martin
Dean of the Graduate School

Investigation of the dynamics of QPX, a pathogen of the hard clam *Mercenaria mercenaria,* in the environment and clams

By

Qianqian Liu

Doctor of Philosophy

in

Marine and Atmospheric Science

Stony Brook University

2010

Quahog Parasite Unknown (QPX) is a potentially lethal pathogen of the hard clam *Mercenaria mercenaria* along the northeastern coast of the United States. To enumerate QPX in clams and in environmental samples, a SYBR Green real-time quantitative PCR (qPCR) assay targeting the ITS region of the QPX rRNA operon was developed. The qPCR assay was used to test samples collected in 2006 from the site of a recent QPX disease outbreak in Raritan Bay, NY, and from a site where QPX has not been detected in Peconic estuary, NY. No QPX was detected in any seawater sample analyzed while QPX was detected at abundance between 34 and 215 cells mg^{-1} in four sediment samples. At the three Raritan Bay sites studied in 2006, QPX prevalence and infection intensity in clams examined by both histological and qPCR assays showed a temporal pattern, suggesting a relationship between QPX infection and temperature. Laboratory-based experiments were conducted to study the effect of temperature on parasite abundance and mortality in experimentally and naturally infected clams. Clams kept at 13 °C always showed higher mortality as well as higher QPX prevalence and weighted prevalence compared to those at 21 and 27 °C after 2 or 4 months incubation, suggesting that under lab conditions, low temperature could be more advantageous for QPX than clams in the host-pathogen interaction. The transmission experiments conducted in this study also revealed that low temperature may promote QPX transmission between cohabited infected clams and susceptible clams. At 13 °C, some susceptible clams acquired QPX cells at rare to moderate levels of abundance after 2 to 3 month cohabitation with naturally infected clams, while no QPX was detected by qPCR in susceptible clams after being co-incubated with naturally infected clams at 21°C. The labyrinthulomycetes, the larger phylogenetic group to which QPX belongs, are a group of ubiquitous but rather poorly understood marine protists. 18S rRNA gene-based qPCR assay and terminal restriction fragment length polymorphism (T-RFLP) analysis were developed to assess the abundance and diversity of labyrinthulomycetes in sediment and seawater samples

collected from Raritan and Peconic Bays in 2006. T-RFLP analysis revealed temporal changes in labyrinthulomycete community structure in both sediment and seawater samples, although the pattern was more distinct in seawater. The composition of labyrinthulomycete communities in sediment was significantly different from those in seawater samples. Labyrinthulomycete community structure was not related to the prevalence of QPX disease in clams collected along with the sediment and seawater samples.

Table of Contents

List of figures

List of tables

Acknowledgement

Background

Hard clam and QPX disease

The hard clam or northern quahog, *Mercenaria mercenaria*, is a native species of marine bivalve along the eastern coast of North America, ranging from the Maritime Provinces of Canada to Florida and the Gulf of Mexico in U.S., and has also been introduced to California and Europe. As a popular seafood item, the hard clam is a very important component of the shellfish fisheries in the U.S. In the State of New York, particularly, the hard clam is the most important fishery (23% of NY fisheries resources combined) in terms of both production (4950 metric tons, 24% of national production) and economic value ($10.7 million) according to the National Marine Fisheries Service (NMFS) report in 2004.

QPX is a parasite of hard clam. The association of QPX with hard clam mortality was initially found in New Brunswick, Canada in the early 1960s (Drinnan and Henderson, 1963). In the late 1980s, high hard clam mortality attributed to the same or similar organisms occurred in a shellfish hatchery located on Prince Edward Island, Canada, where this protistan pathogen was named Quahog Parasite Unknown (QPX) (Whyte *et al.*, 1994). QPX disease has been documented to be present in aquaculture and wild clam populations in various locations of the American and Canadian coasts (Ragone Calvo *et al.*, 1998; Smolowitz *et al.*, 1998; MacCallum and McGladdery, 2000; Ford *et al.*, 2002). As the death of clams usually occurs when the clams are approaching market size (Smolowitz *et al.*, 1998), QPX enzootics have resulted in cessation of local aquaculture development in some regions. In the summer of 2002, the first reported QPX outbreak in New York emerged and caused severe clam mortality in a wild clam population in Raritan Bay (Dove *et al.*, 2004). In response, New York State's Department of Environmental Conservation (NYDEC) suspended the Raritan Bay Shellfish Transplant Program to protect wild hard clams in Peconic Bay from introduction of QPX from infected clams from Raritan Bay. The transplant program, which allowed clams harvested in uncertified areas in Raritan Bay to be depurated in certified waters within the Peconic estuary, had previously represented more than 40% of annual clam production in the state. Since then, the Marine Animal Disease Laboratory in Stony Brook University, in cooperation with NYDEC, has been monitoring QPX distribution and prevalence in hard clam populations in different parts of NY's marine district.

Morphological and molecular evidence have shown that QPX belongs to the protistan phylum Labyrinthulomycota as a member of the thraustochytrid group (Whyte *et al.*, 1994; Maas *et al.*, 1999; Ragan *et al.*, 2000; Stokes *et al.*, 2002; Qian *et al.*, 2007; Collado-Mercado *et al.*, 2010). Three life stages of QPX have been observed in infected clam tissue and in culture. Thalli (2-20 micron in diameter) are single-nucleate cells which mature to form sporangia that contain many vegetative endospores. When the sporangia rupture, endospores are released and in turn mature to form thalli (Kleinschuster *et al.*, 1998). *In vitro* cultured QPX produce mucoid material that envelops QPX cells and allows them to adhere to each other. Evidence of this mucoid material is also seen in histopathological examination of QPX-infected clams, in which QPX thalli are surrounded by clear areas that likely were filled with QPX-produced mucoid material that was removed during histological processing (Smolowitz *et al.*, 1998). It has been hypothesized that this mucus plays a role in the ability of QPX to resist host antimicrobial agents (Anderson *et al.*, 2003).

Developing methods for QPX detection

Currently, the standard technique for QPX infection diagnosis in clams is based on histopathology. Most of the available QPX prevalence data (expressed as the percentage of

QPX infections found in a sample of clams) are from histological examination. However, the histological technique appears to underestimate QPX prevalence in clams because histology can yield a high number of "false" negatives if the infection site is missed by the tissue section. It also cannot be used in environmental samples such as seawater, sediment, and macroalgae detritus. In contrast, the sensitivity of PCR (Polymerase Chain Reaction) amplification for revealing trace quantities of target nucleic acid in heterogeneous samples makes this technology an ideal choice for detecting infectious agents. PCR has been used as a diagnostic tool to study protistan pathogens in bivalves (Carnegie *et al.*, 2000; Kleeman and Adlard, 2000) and has been shown to be more sensitive than histology in detecting pathogens (Marsh *et al.*, 1995; Stokes and Burreson, 1995). A set of QPX –specific primers, QPX-F and QPX-R2, was developed by Stokes *et al.* (2002) and was able to amplify a nearly 670 bp region of the QPX 18S rRNA from QPX isolates with different geographic origins. Our preliminary results showed that PCR with the Stokes QPX-specific primers was able to detect QPX in 17 of 45 examined clams, while histology only found three to be QPX-positive (Liu unpublished data). Recently, Lyons *et al*. (2005) used *in situ* hybridization assays to successfully detect the presence of QPX in marine aggregates collected from an area near infected clam beds. Using one set of thraustochytrid-specific 18S rRNA primers reported by Mo *et al*. (2002) and another set reported by Stokes *et al.* (2002), Gast *et al.* (2006) developed a nested PCR and DGGE (denaturing gradient gel electrophoresis) -based detection method for QPX. Although this DGGE method had a relatively low detection limit (10 to 100 QPX cells in 1 liter of water, 1 gram of sediment and 100 mg of clam tissue), it required about 90 PCR cycles, which are time-consuming and necessitate multiple transfers of post-PCR products, which provides opportunity for cross-contamination. Also its conventional end-point PCR does not provide precise quantification of QPX in the starting material. Therefore, a rapid, specific and reliable technique is still needed for the detection and enumeration of QPX.

Molecular techniques have been used to investigate the genetic variability of QPX strains isolated from infected clams. The initial identification of QPX was done by using universal primers to amplify 18S rDNA from QPX cultures isolated from infected clams (Maas *et al.*, 1999; Ragan *et al.*, 2000). Further studies found no 18S rDNA sequence variation among QPX isolates recovered from infected clams collected from different geographic locations (Stokes *et al.*, 2002; Qian *et al.*, 2007). The rRNA operon ITS region, including the Internal Transcribed Spacers (ITS1 and ITS2) and 5.8S rRNA gene that separates ITS1 and ITS2, is a common target to look for genetic variability. ITS1 and ITS2 are more variable than the conserved 18S, 5.8S and 28S rRNA genes and can be used to distinguish closely related species and strains. QPX was found to have a high ITS sequence variability, but similar variation was observed not only among isolates but within isolates, which is believed to be the consequence of non-concerted evolution of rRNA operons in QPX (Qian *et al.*, 2007). To date, the rRNA-based (18S and ITS) genetic studies suggest that QPX isolated from different geographic locations are closely related and QPX disease is probably caused by a single species of organism everywhere it occurs. This conclusion supports the development and application of species-specific QPX diagnostic techniques. Based on our previously reported rRNA sequences for several QPX isolates from Massachusetts and New York (Qian *et al.*, 2007), a real-time quantitative PCR (qPCR) assay for QPX targeting the ITS region of the rRNA operon was developed in this study. This

method will provide an essential tool for further study of QPX dynamics in clams and in the environment.

Influence of environmental factors on QPX disease

Environmental factors may play a critical role in determining the prevalence and severity of QPX infections and associated hard clam mortalities. Temperature and salinity have been suggested to be the main environmental factors that significantly influence host-pathogen dynamics in many bivalve infectious diseases (Ragone and Burreson, 1993; Ragone Calvo *et al.*, 2003). The effect of the environment on a disease can be by a direct impact on either the pathogen or host, or on both, that results in an unbalanced host-pathogen interaction that favors the pathogen (or the host) leading to disease and subsequent mortality (or to healing). Monitoring of QPX infections in the Raritan Bay wild clam population in New York demonstrated a cyclic pattern: QPX prevalence in clams increased from the late spring, peaked in the summer, and declined in the fall (Fig.1) (Allam and Pawagi, 2005). However, such a seasonal trend was not observed in other reports on QPX infections in wild clam populations. MacCallum and McGladdery (2000) reported QPX prevalence ranging from 3.3 to 20% for Canadian clam samples, but found no correlations between QPX prevalence and temperature or salinity at the time of collection. Compared with wild populations, there have been more studies of QPX infections in cultured clam beds (Ragone Calvo *et al.*, 1998; Ford *et al.*, 2002; Lyons *et al.*, 2007; Ragone Calvo *et al.*, 2007). QPX infections were present in cultured clams collected throughout the year, and there was not a seasonal trend in QPX prevalence due to high variability of mean prevalence among months (Lyons *et al.*, 2007). In terms of geographic distribution, QPX-related clam mortality has been reported from Atlantic Canada to coastal Virginia, and no QPX-associated clam mortality has been reported south of Virginia. It is yet unknown if the absence of major QPX disease in the southern states is associated to their relative higher annual water temperature or other factors.

The effect of salinity on QPX disease is not well studied. Most reports of QPX disease have been from areas with moderate to high salinity (20-32 psu in MacCallum and McGladdery (2000) and 28-33 psu in Ragone Calvo *et al.* (2007)). Ragone Calvo *et al* (1998) reported an absence of QPX disease in areas of Chesapeake Bay with moderate salinities (15-25 psu) and suggested a stronger negative effect of low salinity on QPX than on clams.

Generally, organisms which are stressed by some factor(s) are believed to be more susceptible to infection and more negatively affected by parasites. Stress associated with high clam densities and/or poor husbandry conditions can enhance the risk of QPX disease. Positive correlations between clam density and QPX prevalence have been reported in wild (Allam and Pawagi, 2004) and aquacultured (Ford *et al.*, 2002) clams, but published reports have not detected a statistically significant effect of planting density (in cultured clams) on mortality caused by QPX disease (Kraeuter *et al.*, 1998; MacCallum and McGladdery, 2000; Ford *et al.*, 2002). Another factor that affects QPX disease development is the strain of the clam host. Clams originating from southern locations (South Carolina and Florida) and planted in northern states (New Jersey, Virginia or New York) showed higher QPX prevalence and heavier mortalities than northern clams (from Virginia, New Jersey, Massachusetts or New York) (Ragone Calvo *et al.*, 2007; Dahl *et al.*, 2010). Dahl *et al.*, (2008) used laboratory-based transmission experiments to demonstrate that Florida clam seeds had consistently the highest susceptibility among four strains of clam seeds (from NY, MA, VA, and FL) when challenged by different QPX isolates (two from NY and one from MA).

Transmission of QPX disease

The transmission mechanism of QPX disease is currently a subject of scientific debate. Based on the evidence that QPX is widely present in clam populations in different geographic locations, but at a low level of prevalence in most cases, the prevailing theory suggests that QPX is an opportunistic or facultative pathogen: QPX can live independently in the natural environment (with or without clams), or coexist with clams without causing disease; an outbreak of QPX disease is triggered when the clam immune system is compromised by environmental or physiological stress (Ford *et al.* 2002). The detection of QPX in seawater, sediment, marine aggregates, and in association with other invertebrates and macrophytes by using *in situ* hybridization (Lyons *et al.*, 2005), real-time PCR (Lyons *et al.*, 2006) and nested PCR followed by DGGE (Gast *et al.*, 2008) further support this theory.

As an endoparasite, QPX must breach host barriers to establish an infection and survive the host's internal defenses to proliferate. Histopathology results show that typical QPX infection primarily occurs in pallial organs (e.g. mantle, gill and siphon) (Smolowitz *et al.*, 1998; Ford *et al.*, 2002; Dove *et al.*, 2004) indicating a direct transmission from the environment because these organs are directly exposed to seawater and may be the portals of entry for QPX from the environment. However, experimental transmission is currently based on the injection of *in vitro* cultured QPX cells into clam tissue. The attempts to "naturally" transmit QPX parasite by adding QPX cells to water in tanks with clams or by cohabitating infected adult clams with naïve seed clams did not induce detectable infections (Dahl and Allam, 2007). One of the reasons behind these frustrations may be the lack of environmental reservoir(s) or vector(s) required to facilitate the transmission of QPX. There is still limited knowledge of many basic aspects of the biology and ecology of QPX in the environment, including such questions as whether and where QPX could grow and become infectious outside of host clams, how QPX are transported outside their hosts and transmitted into them, and whether there is a threshold of QPX abundance to initiate infection and cause epizootic disease in clam populations.

Buggé and Allam (2007) studied the ability of QPX to grow outside clams and found that QPX growth was not supported by natural seawater under laboratory conditions. Some morphological changes have been observed in all life stages of QPX when growth medium was replaced by seawater (Kleinschuster *et al.*, 1998), but the significance of these changes for QPX survival and infectivity is unknown. Buggé and Allam (2007) also found that QPX growth *in vitro* was supported by several macroalgae species when their products (e.g. fresh or decomposed macroalgae homogenates) were used as growth media, but was inhibited by others. Whether a particular species of macroalgae supports or inhibits QPX growth is likely due to the antimicrobial properties of these algae. This study suggested the possibility of macroalgae as a substrate for QPX to survive or grow outside clam hosts, but their roles as environmental reservoirs for QPX need to be further studied. Recently, QPX has been detected in a variety of environmental samples by molecular techniques (Lyons *et al.*, 2005; Gast *et al.*, 2008), but the ability of QPX to survive and grow on these substrates and the role of these habitats for QPX disease transmission is still unclear.

Infected hosts (clams or other possible intermediate hosts) may be another important source of QPX parasites. For many lethal parasites, decay of infected tissue, with consequent release of parasites into the environment, has been considered the main source of infective cells for transmission (Burreson and Ragone Calvo, 1996; Ragone Calvo *et al.*, 2003; Audemard *et al.*, 2006). Another important source of infective stages can be from the feces or

pseudofeces of a living, infected host. For parasites that do not always cause immediate mortality, such as *Perkinsus marinus* in oyster, the latter may be the principal mode of pathogen release and provide a reservoir between transmissions (Bushek *et al.*, 2002). The coincidence of highest QPX prevalence occurring in the densest clam populations (Allam and Pawagi, 2004; Ford *et al.*, 2002) also suggests shedding of viable parasites from infected clams could be an important source of transmission for this pathogen. However, the release and uptake mechanisms, if any, between infected (living or dead) and uninfected clams are yet unknown.

Labyrinthulomycete community in marine environments

Labyrinthulomycetes, including the group of thraustochytrids to which QPX belongs, represent one of the most unexplored components of marine food webs. One of the factors that hinder our understanding of the QPX organism is the limited knowledge of the biology and ecology of organisms related to QPX.

Labyrinthulomycetes are sometimes described as "marine slime molds" because they use a unique organelle known as a bothrosome or sagenosome to produce an ectoplasmic network. Although they are very common in a variety of marine habitats all over the world, their taxonomy and evolutionary relationships are only now being clarified. For example, they have only recently been correctly classified as heterokonts, not fungi (Cavalier-Smith *et al.*, 1994). The Heterokonta, sometimes called stramenopiles, also includes a variety of chromophyte algae such as diatoms, brown algae, chrysophytes, yellow-green algae and others. The classification within the labyrinthulomycetes is still in flux, with at least two systems having been proposed. Cavalier-Smith *et al*. (1994) classified labyrinthulomycetes as two families: Thraustochytridae and Labyrinthulidae, while Leander and Porter (2001) argued that aplanochytrids (which belonged to family Labyrinthulidae in early reports) may deserve a family status as well and that the three families are distinguished by the structure of the ectoplasmic network and mobility of vegetative cells and spores. Based on 18S rDNA sequences, Honda *et al*. (1999) divided the labyrinthulomycetes into two groups: the thraustochytrid phylogenetic group (TPG) and the labyrinthulid phylogenetic group (LPG), generally consistent with the families Thraustochytridae and Labyrinthulidae, with aplanochytrids falling within the LPG.

Labyrinthulomycetes are ubiquitous in the water column and sediments of marine and estuarine environments. Most labyrinthulomycetes are nonpathogenic and associated with degrading organic detritus, although many of them are observed living in or on marine organisms such as sponges, corals, bivalves, octopus, squids, nudibranches, and echinoids as parasites, commensals or mutualists (Raghukumar 2002 and reference therein). Recently, these protists are receiving more attention from researchers because of their roles as pathogens in mollusk diseases (Bower, 1987; Whyte *et al.*, 1994; Anderson *et al.*, 2003) and potential as sources for valuable bioactive compounds (Lewis *et al.*, 1998; Bowles *et al.*, 1999). Labyrinthulomycetes have also been reported as predominant contaminants of marine invertebrate cell cultures; for example, Rinkevich (1999) reviewed 21 confirmed and suspicious cases during the last decade, suggesting the association of thraustochytrids with marine animals may be broader and more common than what we now appreciate..

In the water column, a significant correlation was found between particulate organic carbon (POC) and thraustochytrid densities by Raghukumar *et al*. (2001). Numbers of thraustochytrids ranged from levels below detection ($< 1 \, l^{-1}$) to a few hundred per liter in coastal and oceanic water (Raghukumar 2002) depending on the season. Thraustochytrids are

also important members of sediment microbial communities, reported at abundances from 40-100 ml^{-1} in sandy sediments and up to several thousand g^{-1} in more organic-rich conditions, such as seagrass meadows and decaying mangrove leaves (Raghukumar *et al.*, 1995; Santangelo *et al.*, 2000; Bongiorni and Dini, 2002). A positive relationship between thraustochytrid abundance and sediment organic matter content has also been reported (Bongiorni and Dini, 2002). Thraustochytrids attain higher population densities in estuarine areas than offshore, possibly owing to the higher load of organic matter and nutrients in the estuary (Gaertner and Raghukumar, 1980).

For a long time, the detection and quantification of labyrinthulomycetes (thraustochytrids) has been based on two methods: Most Probable Number (MPN) technique incorporating the pine pollen baiting method (Gaertner, 1968) and acriflavine direct detection (AfDD) epifluorescence microscopy (Raghukumar and Schaumann, 1993). Pine pollen can bait those thraustochytrids whose ectoplasmic net elements are able to penetrate the sporopollenin layer of the pine pollen to obtain nutrients for growth. AfDD appears to detect higher numbers than MPN assay when performed on the same sample (Raghukumar *et al.*, 2001), which suggested that clumping of cells; inefficient cultivation and other artifacts may limit the accuracy of the MPN assay. Acriflavin stains DNA in the nucleus and the cell wall of thraustochytrids differently, so that they fluorescence greenish and red, respectively. The AfDD assay may also underestimate labyrinthulomycete abundance because zoospores and small vegetative cells lack thick enough cell walls to be detected (Raghukumar and Schaumann, 1993; Santangelo *et al.*, 2000; Kimura *et al.*, 1999). Both MPN and AfDD assays are time-consuming and require a great deal of experience in identifying morphological characteristics of thraustochytrids and other protists. Classifying labyrinthulomycetes in environmental samples and cultures is also very difficult because some features used for species identification can change with growth conditions (Leander *et al.*, 2004). In the available quantitative data based on AfDD assay, it is unclear whether what the authors called "thraustochytrids" also included labyrinthulids and aplanochytrids. Until now, the only available studies describing the changes in species composition of labyrinthulomycete communities have been based on differences in the size of the thraustochytrids: Raghukumar *et al.* (2001) demonstrated a strong seasonality of thraustochytrid abundance and species composition in the Arabian Sea; and Bongiorni *et al.* (2005) observed the average size of thraustochytrid cells differed among sites and with the impact of fish farm wastes, suggesting possible changes in thraustochytrid species composition.

Recently, molecular techniques based on 18S rRNA sequences have been used to overcome the difficulties of the cultivation-dependent and morphology-based detection methods (MPN and AfDD), both to detect new species and classify current species of labyrinthulomycetes (Honda *et al.*, 1999; Maas *et al.*, 1999; Ragan *et al.*, 2000; Mo *et al.*, 2002). Some genera and species named based on morphological characteristics are not consistent with 18S rRNA sequence-based phylogenetic relationships (Honda *et al.*, 1999). Molecular-based methods enable a more thorough characterization of labyrinthulomycete diversity over a wider range of sampling locations in comparison to culture-dependent or microscopic techniques. New labyrinthulomycete sequences have been recovered in recent studies describing the diversity of protists in various marine habitats (Stoeck *et al.*, 2003; Collado-Mercado *et al.*, 2010). Based on the database of 18S rRNA labyrinthulomycete sequences recovered from strains currently in culture and from environmental clone libraries

(Collado-Mercado *et al.*, 2010), and the existing "labyrinthulomycete-specific" primers Laby-A and Laby-Y (Stokes *et al.*, 2002), the development of new 18S rRNA-based molecular methods would allow us to accurately assess the abundance and diversity of labyrinthulomycete communities and would improve our understanding about the relationships between QPX, QPX disease and broader labyrinthulomycete community.

Objectives

The focus of this project is to investigate the dynamics of QPX in hard clams and in the natural environment. The specific objectives are:

1. To develop a quantitative PCR technique for detection and quantification of QPX in clam and environmental samples. The aim is to develop a quantitative real-time PCR method to specifically detect and quantify the QPX organism. The new technique was optimized to allow sensitive detection of QPX in clam tissues and environmental samples.
2. To investigate the dynamics of QPX abundance in hard clams and in the natural environment and the environmental factors affecting the pattern of QPX prevalence and infection intensity in a clam population. Based on the results of the field study, the effect of temperature on the development and progression of QPX disease was further investigated in laboratory-controlled experiments.
3. To investigate the dynamics of QPX in cohabited infected and susceptible naïve clams and in potential environmental reservoirs in laboratory-based transmission experiments under different temperature conditions. The aim is to provide information for a better understanding of parasite release and uptake by clams during disease transmission.
4. To investigate the temporal and spatial patterns of labyrinthulomycete community structure in QPX enzootic areas. The aim is to study the relationship between labyrinthulomycete community structure (abundance and diversity) and prevailing environmental factors in enzootic areas in Raritan Bay, to gain a better understanding of the natural dynamics of QPX as a component of the microbial community.
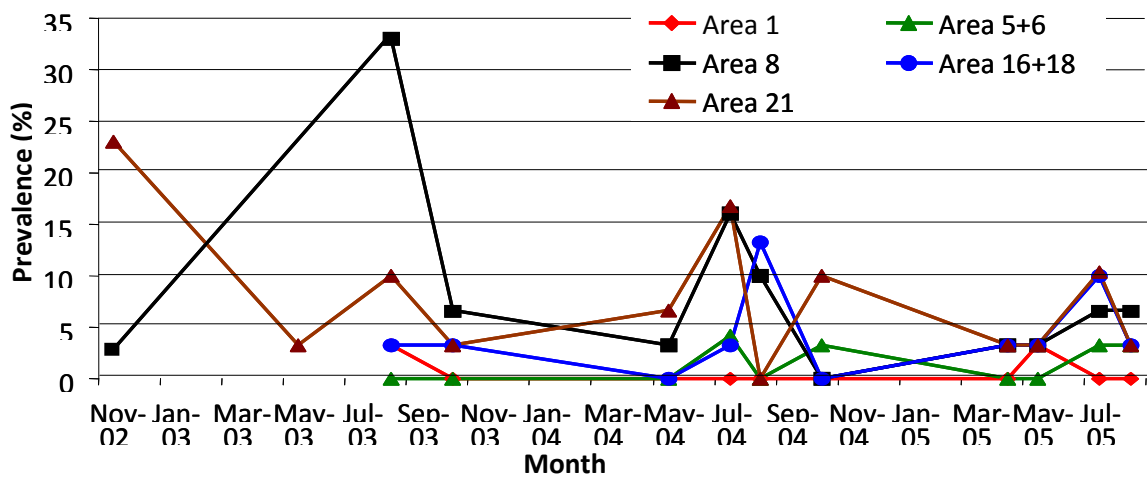
Figure 1. QPX prevalence (determined by histology) in Raritan Bay clams from 2002 to 2005 (Allam and Pawagi, 2005).

Chapter 1: Development of a real-time quantitative PCR (qPCR) assay for detection and quantification of QPX in clam and environmental samples

(Most content of this chapter has been published as Liu *et al*. (2009))

Introduction

In the 1960's, a protistan disease was reported in wild hard clams from New Brunswick, Canada. Since then, the protist has been identified as a thraustochytrid now called QPX, and QPX disease has caused high mortalities in hatchery-reared clams from Prince Edward Island (Canada) and in commercially harvested clam populations from Virginia, Massachusetts and New Jersey (USA) (Whyte *et al.*, 1994; Ragone Calvo *et al.*, 1998; Smolowitz *et al.*, 1998; MacCallum and McGladdery, 2000; Ford *et al.*, 2002). In the summer of 2002, QPX infections suddenly appeared in the Raritan Bay wild clam population, causing significant clam mortality and closure of the fishery (Dove *et al.*, 2004).

Current techniques for QPX diagnosis in clam tissue are based on histopathology. This technique involves the diagnosis of clams by microscopic examination of a transversal histological section for the presence of QPX cells. Although this histological method provides important information regarding the distribution and presentation of QPX infection in various tissue types, it is not only time-consuming, but also has a major flaw for monitoring QPX in clams because of the focal nature of QPX disease: histology can yield a high number of false negatives if the infection site is missed by the section. Standard PCR (polymerase chain reaction) can also be used to determine the presence or absence of QPX cells in a clam (Stokes *et al*. 2002), but is also limited since it cannot be used to accurately determine the number of QPX cells present.

QPX is thought to be an opportunistic pathogen, capable of growing outside its host. However, there is limited knowledge about alternate habitats or substrates that might support QPX organisms outside of hard clams. The ability to detect and enumerate QPX cells in potential reservoirs would offer new insight into fundamental questions about the natural transmission mechanisms of the infection. Among the available techniques for detection of QPX, histology cannot be used for environmental samples, such as seawater or sediment. Although molecular methods such as in *situ* hybridization and denaturing gradient gel electrophoresis (DGGE) have been used to detect QPX in environmental samples (Lyons *et al*. 2005, Gast *et al*. 2008) and have provided new and important information on potential environmental reservoirs of the QPX organism, none of them were quantitative. There is still a need for a rapid, specific and consistent technique for detecting and enumerating QPX in clam and environmental samples.

Real-time PCR was first reported in 1993 (Higuchi *et al.*, 1993) and has since become an emerging technique for the detection and quantification of microorganisms in the environment (Ginzinger, 2002; Zhang and Fang, 2006). During typical PCR reactions, the target fragment of double-stranded DNA templates is amplified over a number of denaturation-annealing-extension cycles. During the early steps of a PCR reaction, amplification products accumulate exponentially. Due to reagent limitation, accumulation of inhibitors or inactivation of the polymerase, usually after 30-40 cycles, a PCR reaction is no longer generating amplicons at an exponential rate (otherwise known as the "plateau phase"). In a standard PCR, only the end-point product is examined by electrophoresis and detection by a double stranded DNA (dsDNA)-specific intercalating dye (ethidium bromide is a common choice of dye), and the initial presence of template is determined as

"positive/negative". In contrast, in real-time PCR, the accumulation of amplification products is measured by a fluorescence-based technique at each thermal cycle as the amplification progresses, which allows determination of the initial template abundance to be based on the fluorescence signal during the exponential phase of amplification.

SYBR Green is a fluorescent dye that binds to dsDNA and can be used to monitor real-time PCR reactions. In SYBR Green-based real-time PCR, the specificity of the reaction is determined entirely by the specificity of the primers, so primers must be carefully designed and tested. It is critical to minimize the effects of any side-reaction product, such as the extension of primer bound to non-target DNA sequences, primer dimer formation, etc. This issue becomes more prominent at low target concentrations. In SYBR Green-based assays, the amplification of the desired product can be confirmed by a dissociation profile generated after amplification. To construct the dissociation curve, PCR samples are subjected to a stepwise increase in temperature from 55 to 95 degrees; as the temperature increases, the amplification products in each tube will melt according to their composition, and fluorescence is measured at every temperature increment. If primer dimer or nonspecific products were made during the amplification step, they will melt at a different (lower) temperature than the desired products. The dissociation curve analysis can be a very powerful tool in the interpretation of fluorescence data obtained during real-time PCR. Quantification of the initial template abundance is achieved by threshold analysis. The threshold (C_T) is defined as the cycle at which fluorescence is significantly above background. The threshold cycle has been shown to be inversely proportional to the log of the initial target template copy number; that is, the more template is initially present, the fewer cycles it takes to accumulate enough fluorescence signal to cross the threshold.

Previous studies have demonstrated that the 18S rDNA primer pair QPX-F and QPX-R2 can be used in a standard PCR assay to detect the presence of QPX DNA in clam tissue samples (Stokes *et al.*, 2002). Unfortunately, this primer pair produces amplicons that are too long (~650 base pairs), and often with too much primer dimer, to meet the requirements of a SYBR Green real-time qPCR assay. The low sequence variability in 18S rDNA made it difficult to design other 18S rDNA primers specific for QPX. Compared to the rRNA - encoding genes (18S, 5.8S and 28S), the regions of ITS1 and ITS2 are much more variable, offering greater flexibility for development of species-specific primers (Alvarez and Wendel, 2003). In this study, based on previously reported QPX ITS region sequences for several QPX isolates from Massachusetts and New York (Qian *et al.*, 2007), a SYBR Green-based real-time quantitative PCR (qPCR) assay was developed targeting the ITS region of the rRNA operon of QPX.

The sensitivity of the qPCR assay for detecting QPX in clam and environmental samples can be strongly affected both by the PCR inhibition effect in template DNA and by the recovery of QPX DNA from field samples. Although optimization of DNA extraction procedures has been included in previous reports of qPCR assay development (Haugland *et al.*, 2002; Cook and Britt, 2007), little quantitative evaluation has been done of the PCR inhibition effect or of the recovery rate of target DNA from environmental samples. Therefore, one aim in this study is to test and quantitatively evaluate various DNA extraction and purification methods for reducing PCR inhibition in template DNA and recovering QPX DNA from clam, sediment and seawater samples. The methods which provide the highest DNA recovery rate for QPX in each type of sample will be applied to samples collected from experiments described in Chapter 2 to 5 in this study.

Materials and methods

DNA from QPX and other thraustochytrid cultures

The QPX isolates used in this study were cultured as reported previously (Qian *et al.*, 2007) in modified MEM medium (Kleinschuster *et al.*, 1998) at 23 °C under ambient atmosphere. To provide known numbers of cells, 8 to 10 QPX cultures (5 mL each) growing in the exponential phase were pooled. The mucoid material enveloping QPX aggregates was dissociated from the cells by adding sterile artificial seawater and slowly aspirating and ejecting several times through a 20-gauge needle. After centrifugation at $5000 \times g$ for 5 min, the supernatant (containing mucoid material) was carefully removed and the cell pellet was resuspended in sterile artificial seawater. QPX cells were counted in a hemocytometer (Hausser Scientific, Horsham, PA) at $400 \times$ magnification. The counting repeated 8 to 10 times until the total volume of counted cell suspension reached 1.5 to 2 µl. For measuring the recovery of QPX DNA from clam and environmental samples, 1.0×10^5 or 2.0×10^5 QPX cells were spiked immediately into Sterivex filter units (seawater samples), weighed sediment subsamples, and clam tissue homogenate. For DNA content measurements, 1.0×10^6 QPX cells were collected by centrifugation and stored at -80°C. DNA was extracted from QPX cell pellets by resuspending in 250 µl of T1 lysis buffer from the BD Nucleospin tissue kit (BD Biosciences, Macery-Nagel, Germany), following the manufacturer's instructions, and eluting in 150 µl EB elution buffer.

The thraustochytrids *Schizochytrium aggregatum* (ATCC28209), *Schizochytrium limacinum* (ATCCMYA-1381), and *Thraustochytrium aureum* (ATCC34304) were acquired from the American Type Culture Collection (ATCC, Manassas, VA) and maintained in medium 790 By+ at 23°C. Genomic DNA was extracted from these cultures using the BD Nucleospin tissue kit.

Clam and environmental sample collection

Seawater and sediment samples were collected from between seven and eleven sites in Raritan Bay along with one site in Hashamomuck Pond in Peconic estuary (both in New York, USA; Fig. 2.1) at 6-week intervals from April to September 2006. The sampling at Hashamomuck Pond was usually performed during the same or following week of each Raritan Bay sampling. From three Raritan Bay sites (sites 8, 18 and 21) during the 5 sampling dates and from site 20 in Raritan Bay in May and August in 2006, clams (~30 clams per group) were collected and analyzed by both histological and qPCR methods. The details about clam and environmental sample collection are further described in Chapter 2.

DNA extraction from clam tissue samples

Ethanol-preserved clam tissues were washed twice using phosphate-buffered saline (PBS) and mechanically homogenized in 10 volumes of PBS (e.g., 1 g tissue in 10 ml PBS). A 1 ml aliquot of homogenate of each clam, containing 100 mg clam tissue, was transferred to a 1.5 ml centrifuge tube. The cells were harvested by centrifugation at $12,000 \times g$ for 10 min and resuspended in 250 µl T1 lysis buffer and 25 µl proteinase K (20 mg ml^{-1}) provided by the BD Nucleospin tissue kit, followed by incubation at 56 °C overnight (16-18 hr). The sample was processed further by following the manufacturer's protocol. At the final step, to recover a high yield of DNA the column was eluted twice with 75 µl of pre-heated EB elution buffer and the two eluates were combined and stored at -20 °C.

To determine the recovery rate of QPX DNA by this procedure, DNA was extracted side by side from aliquots of clam tissue homogenate spiked with 1.0×10^5 QPX cells and aliquots to which no QPX cells were added. The difference between "spiked" and "unspiked"

samples in number of QPX cells detected is due to the DNA recovered from the QPX cells added in the "spiked" sample:

$$\#QPX_{\text{recovered}} = \#QPX_{\text{in spiked sample}} - \#QPX_{\text{in unspiked sample}} \text{ (Equation 1)}$$

Then the recovery rate of QPX DNA from the clam sample was determined as:

$$\text{Recovery rate \%} = (\#QPX_{\text{recovered}} / \#QPX_{\text{added}}) \times 100\% \text{ (Equation 2)}$$

DNA extraction from sediment samples

500 to 850 mg (wet wt) of thawed sediment sample was transferred into a lysing matrix E tube from the FastDNA SPIN Kit for Soil (Qbiogene, Carlsbad, CA). DNA was extracted by following the manufacturer's instructions. The column was eluted twice with 75 µl DDS buffer, and the two eluates were combined. To decrease the substantial PCR inhibition in extracted sediment DNA, a 50 µl aliquot was cleaned by StrataPrep PCR purification kit (Stratagene, La Jolla, CA) following the manufacturer's protocol. To assess the level of PCR inhibition, dilutions (1:1, 1:30 and 1:100) of extracted ("precleanup") DNA and dilutions (1:1, 1:10 and 1:100) of StrataPrep-purified ("postcleanup") DNA were made with ddH$_2$O and 1 µl of the diluted DNA was used as template for real-time qPCR analysis.

To estimate QPX DNA recovery rate of this extraction procedure, 2.0×10^5 QPX cells were spiked into replicates of six randomly selected sediment samples. Total DNA of the "spiked" samples was extracted, purified and assayed by qPCR side by side with the "unspiked" samples, and the recovery rate was calculated using Equation 1 and 2.

DNA extraction from seawater samples

For routine sample analysis, DNA was extracted from the particulate matter collected on sterivex filters by thawing filters and adding 1 ml of freshly made Galluzzi's crude lysis buffer (10 mM Tris-HCl [pH 8.3], 50 mM KCl, 0.5% Nonidet P-40, 0.5% Tween 20, 0.1 mg ml^{-1} proteinase K) (Galluzzi *et al.*, 2004). The filters were incubated at 60°C for 3 hours in a rotisserie oven. Then a 500 µl portion of lysis mixture was transferred by a syringe to a lysing matrix E tube from the Qbiogene FastDNA SPIN Kit for Soil, and the sample was processed further by following the manufacturer's instructions. DNA was eluted twice in 75 µl DDS buffer, and the two eluates were combined. This method is referred to as 'method 6'; the five other methods evaluated followed a similar outline, using different lysis buffers and DNA purification kits, and are described below. To decrease the substantial PCR inhibition found in DNA extracted from seawater samples, a 50 µl aliquot of extracted DNA was cleaned by StrataPrep PCR purification kit following the manufacturer's protocol. Dilutions of extracted DNA (1:1, 1:30 and 1:100) and dilutions of StrataPrep-purified DNA (1:1, 1:10 and 1:100) were made with ddH$_2$O and 1 µl of each dilution was used as template for real-time qPCR assay.

To estimate QPX DNA recovery rate for each extraction method, 2.0×10^5 QPX cells were spiked into at least three replicates of randomly selected seawater samples. Total DNA of the "spiked" samples was extracted, purified and assayed by qPCR side by side with the "unspiked" samples, and the recovery rate was calculated using Equation 1 and 2.

Development of QPX-specific primers for real-time quantitative PCR (qPCR) assay

The ITS regions from *Schizochytrium aggregatum* (ATCC28209), *Schizochytrium limacinum* (ATCCMYA-1381), and *Thraustochytrium aureum* (ATCC34304) were PCR amplified with universal 18S and 28S rDNA primers (18S-RR and 28S46Rev; Table 1.1), cloned, and sequenced as described previously (Gene accession number: FJ533155 to FJ533163, Qian *et al.*, 2007). An alignment of QPX, other thraustochytrid, and other

heterokont ITS region sequences was constructed with BioEdit (version 7) and examined manually to locate sequences unique to QPX. Potential primer sequences were also checked for specificity by BLAST against GenBank (http://www.ncbi.nlm.nih.gov/Blast.cgi) and analyzed with Primer Premier 5 software (Premier Biosoft Inc., Palo Alto, CA) for melting temperatures and secondary structure. Primers were synthesized by Integrated DNA Technologies (IDT, Coralville, IA). For the initial tests of potential qPCR primer pairs under standard PCR conditions, each PCR reaction had a total volume of 25 μl and contained 10 μl of 2.5× PCR MasterMix (Eppendorf Inc., Westbury, NY), 5 μl of 1 μM stock of each primer, 1 μl of template DNA and 4 μl of ddH$_2$O. Standard PCR conditions were denaturation at 95 °C for 30 s, annealing at 55 °C for 1 min, and extension at 72 °C for 2 min for 35 cycles, followed by a final extension step at 72 °C for 10 min. An 8 μl aliquot of each reaction product was examined by 1.5% agarose gel electrophoresis.

Real-time quantitative PCR (qPCR) conditions

All qPCR assays were done on a Stratagene (La Jolla, CA) MX3000P thermal cycler, and all data were analyzed using Stratagene MX3000P software version 2.0. For routine analyses, each reaction mixture contained 2.5 μl 10× Core PCR buffer, 2 mM MgCl$_2$, 0.8 mM dNTP mix, 4 μl of 50% glycerol solution, 1.5 μl DMSO, 30 nM reference dye, 0.167× SYBR Green I dye and 2.5 U SureStart *Taq* DNA polymerase from the Stratagene Brilliant SYBR Green QPCR Core reagent kit, primers at final concentrations of 100 nM each, and 1 μl DNA template. The total volume of the reaction mixture was adjusted to 25 μl using nuclease-free water. The real-time PCR program was: 10 min at 95 °C to activate the *Taq* DNA polymerase, then 40 cycles of 30 s at 95 °C, 1 min at 55 °C and 1 min at 72 °C. Individual well fluorescence data was collected at the end of each thermal cycle, and determination of the fluorescence detection threshold was performed automatically by the instrument. At the end of each run, dissociation curve analysis was performed to check the specificity of the amplified products.

Construction of standard curves

A primary standard curve showing the relationship between initial QPX ITS region copy number and C_T value (the cycle number at which SYBR fluorescence crossed the detection threshold) was generated by 10-fold serial dilution, ranging from 10 to 10^6 copies, of pGEM-T Easy plasmids containing the QPX ITS region amplified by primers QPX-F and 28S46Rev (Table 1.1). Plasmid DNA was purified by using the Wizard Plus SV Minipreps DNA purification system (Promega, Madison, WI) according to the manufacturer's instructions. The plasmid standard was a mixture of sequenced clones from three QPX isolates (MA0505311C5, MA0505116C4, and MA0505325C1; GenBank accession numbers DQ641187, DQ641192, and DQ641195, respectively) (Qian *et al.*, 2007). The concentration of plasmid DNA was measured fluorometrically with a PicoGreen dsDNA quantification kit (Molecular Probes, Eugene, OR) and a TBS-380 Mini-Fluorometer (Turner Biosystems, Sunnyvale, CA) following the manufacturer's instructions.

A secondary standard curve was constructed by 10-fold serial dilution of QPX genomic DNA. It was not possible to use DNA purified from known numbers of QPX cells because DNA loss was ineluctable during the BD Nucleospin tissue kit extraction procedure. Instead, the number of QPX cells represented by each point in this standard curve was calculated by dividing the amount of QPX genomic DNA template in each reaction (measured by PicoGreen dsDNA quantification kit) by the DNA content per QPX cell estimated by the method of Galluzzi *et al.* (2004). Comparing this value against the number of ITS region

copies in each reaction (determined from its C_T value and the primary standard curve) provided an estimate of the ITS region copy number per QPX cell.

qPCR assays of field samples

The number of QPX ITS region copies in the field samples (clam DNA, seawater DNA and sediment DNA) was determined from C_T values by comparison with a plasmid standard curve run in the same plate. To correct for PCR inhibition in the extracted DNA templates, additional "inhibition control" reactions for each sample were also run by adding 1.0×10^3 plasmid copies.

Thus in the qPCR reaction of an assayed clam, seawater, or sediment DNA template

$$\#QPX_{initial} \times (100\%\text{-inhibition}) = \#\,QPX_{measured.1} \text{ (Equation 3)}$$

And in the "inhibition control" reaction of the assayed DNA sample,

$$(\#QPX_{initial} + \#QPX_{additional}) \times (100\% - inhibition) = \#\,QPX_{measured.2} \text{ (Equation 4)}$$

The assumptions of this approach are that the amplification of the additional plasmids is inhibited in the same way as the amplification of the target gene purified from the field sample, and that the inhibitors extracted from the field sample interfere with PCR amplification to the same degree in the parallel assay and "inhibition control" reactions. The value of $\#QPX_{additional}$ is known (1.0×10^3 copies of plasmid), and the values of $\#QPX_{measured.1}$ and $\#QPX_{measured.2}$ are determined by qPCR from the assayed and "inhibition control" reactions, respectively. By integrating the two equations, the two unknown values, inhibition effect (%) and $\#QPX_{initial}$ (the initial number of QPX ITS copies in the reaction), are solved as:

$$\text{Inhibition} = (1 - \frac{\#QPX_{measured.2} - \#QPX_{measured.1}}{\#QPX_{additional}}) \times 100\% \text{ (Equation 5)}$$

$$\#QPX_{initial} = \frac{\#QPX_{measured.1}}{100\% - \text{inhibition}} \text{ (Equation 6)}$$

In each real-time qPCR run, the primary plasmid standards, a negative control without DNA template, the assayed field DNA samples and their inhibition controls were run in duplicate or triplicate in a 96-well plate, and the average value of the two or three measurements was used for data analysis. Replicate reactions generally agreed very well, typically with less than 0.2 standard deviation among their C_T values.

Finally, the original abundance of QPX cells in each field sample was computed as follows:

$$\textit{Original QPX abundance} = (\#QPX_{initial} \times a \times b)/(c \times d \times e) \text{ (Equation 7)}$$

where $\#QPX_{initial}$ is the initial number of QPX ITS copies in the assayed field DNA sample (1 µl) reaction after correction for PCR inhibition; a is the dilution factor of DNA stock for the PCR reaction; b is the volume into which the DNA stock was resuspended (µl); c is the estimated copy number of ITS region per QPX cell (cell^{-1}); d is the estimated average QPX DNA recovery rate of the extraction method; and e is the volume of seawater (ml) or the weight of sediment (mg) or the weight of clam tissue (mg) from which DNA was extracted.

Results

Design and testing of QPX-specific primers for real-time qPCR

   Because the QPX ITS region sequences (GenBank accession numbers DQ641197 to DQ641141) (Qian *et al.*, 2007) were the only ones available for thraustochytrids (members of the family Thraustochytriidae in the order Labyrinthulida of the Heterokonta, or stramenopiles), we sequenced three cloned ITS region amplicons each from the thraustochytrids *Schizochytrium aggregatum* (ATCC28209), *Schizochytrium limacinum* (ATCCMYA-1381), and *Thraustochytrium aureum* (ATCC34304). ITS region sequences from three *Aplanochytrium* strains (labyrinthulids more distantly related to QPX) are now available, as well (accession numbers EU872090, EU872091, and EU872092). The 5.8S rRNA genes from the other labyrinthulids were 92.5%, 91%, 93.3%, and 88.7% identical to the QPX 5.8S rDNA sequence, respectively. In contrast to the 5.8S rDNA, the ITS1 and ITS2 region sequences of the other labyrinthulids were so different from QPX that they could not be aligned (data not shown). The ITS1 region from the other thraustochytrids was similar in size, ranging from 75 to 89 bp, but not similar in sequence, to the QPX ITS1 region, while the aplanochytrid ITS1 sequences were approximately 60 bp longer. The ITS2 region varied widely in size, from 151 bp in *S. limacinum* (most similar to the 130 bp ITS2 in QPX), to 172 bp in *Aplanochytrium*, to between 260 and 272 bp in *T. aureum*, to a high of 820 bp in *S. aggregatum*. The ITS1 and ITS2 regions from QPX and the other labyrinthulids returned no significant hits in BLAST searches of GenBank.

   The thraustochytrid ITS region sequences were aligned in the 5.8S rRNA gene, and where possible in ITS1 and ITS2, with ITS region sequences available in GenBank from more than 30 species representing 12 major groups of heterokonts. Three primers (5.8S24For, 5.8S127For and 5.8S127Rev; Table 1.1) were designed to two sites in the 5.8S rDNA. The 5.8S24For primer mismatched the other thraustochytrids at one or two bases, while the 5.8S127 primer was in a more variable region and mismatched the other thraustochytrids at four or more bases. The *Aplanochytrium* 5.8S rDNA, which was not available at the time the primers were designed, matched 5.8S24For perfectly but mismatched 5.8S127 at six bases. In addition to the previously designed primer QPX-ITS2-R (Qian *et al.*, 2007), two other primers (QPX-ITS2-F2 and QPX-ITS2-R2; Table 1.1) were designed to match another site in the QPX ITS2 region, with one degenerate base to match all known variants of the QPX ITS2 sequence (Qian *et al.*, 2007). The ITS2 primers did not match any other sequences in the alignment at more than a few bases.

   The newly designed QPX 5.8S rDNA and ITS2 primers were paired with each other and with several previously reported primers (Table 1.1) to create nine pairs of primers producing amplicons in the desired size range for a SYBR Green real-time qPCR assay (Table 1.2). The performance of these primer pairs was first tested by standard PCR against QPX-positive templates. All nine amplified the expected band from QPX genomic DNA, but the four that included an 18S rDNA or 28S rDNA primer produced artifacts (nonspecific amplification products or primer dimers) when tested against DNA isolated from QPX-infected clams, and so were excluded from further testing (Table 1.2). The remaining five primer pairs were next tested by standard PCR against QPX-negative templates. The two using primer 5.8S127For produced artifacts (primer dimers) when tested against DNA isolated from QPX-free clams, and so were excluded from further testing. The three remaining primer pairs also produced no amplification products in reactions with DNA isolated from three other thraustochytrids. Additionally, these primer pairs produced no amplification products using template DNA

from QPX-free seawater samples, even though the more general labyrinthulid 18S rDNA primers Laby-A and Laby-Y (Stokes *et al.*, 2002) produced strong PCR products, confirming that labyrinthulids other than QPX were present in the samples but were not amplified by the QPX-specific primers.

These three primer pairs were further tested in the SYBR Green real-time qPCR format. The dissociation (melting) curves of the products from all three primer pairs with positive templates (the plasmid standard curve, QPX culture DNA and DNA from QPX-positive clams) contained only a single peak at 80 to 81°C, which indicated there was a single, specific amplification product in the qPCR format (as in the standard PCR format), with no unspecific amplicons or primer dimers (data not shown). The negative templates (no DNA control, DNA of three other thraustochytrids, DNA from QPX-free clam tissue) did not produce signals crossing C_T within 40 cycles. As expected, all three primer pairs produced a linear relationship between C_T and the log of the initial plasmid copy number over several orders of magnitude. However, the three primer pairs differed from each other in important ways. The 5.8S24For+5.8S127Rev primer set had a poor detection limit of 1000 to 10000 copies per reaction, and the 5.8S24For+QPX-ITS2-R primer set had a low PCR efficiency and poor coefficient of variation between replicates in the standard curve (data not shown). In contrast, the 5.8S24For+QPX-ITS2-R2 primer set gave a strong linear (R^2=0.99) inverse relationship between C_T and the $\log_{10}$ number of plasmid ITS region copies (Fig. 1.1) with a slope of -3.84 ± 0.21 (Mean ± SD, n=35), and was capable of detecting as few as 10 ITS copies per reaction, which corresponded to a mean C_T value of 36.96 ± 1.68. Overall, the primer set 5.8S24For+QPX-ITS2-R2 was the best choice for a QPX qPCR assay in terms of efficiency, sensitivity and reproducibility, and had a reliable detection range of 10 to 10^8 target gene copies.

Quantification of DNA content and ITS region copy number in QPX cells

The DNA content of QPX cells was determined essentially as described by Galluzzi *et al.* (2004), by resuspending frozen pellets of 1.0×10^6 QPX cells in 1 ml of crude lysis buffer, sonicating briefly, and incubating the lysate at 60 °C for 3 h with vortexing every 30 min. After precipitating cell debris by incubation on ice for 30 min and centrifugation at 12,000 × *g* for 10 min, DNA contained in the supernatant was immediately quantified by PicoGreen. The grand mean for three independent sets of counted QPX cells, with triplicate subsamples of each set, was 257.1 ± 37.4 fg DNA cell^{-1}. Based on this DNA content, the secondary qPCR standard curve was constructed with reactions containing template DNA (extracted with the BD Nucleospin tissue kit) equivalent to 0.5, 1, 5, 50, 500 and 5000 QPX cells. The number of ITS copies in each of these reactions was calculated by plotting the C_T values on the plasmid standard curve, providing an estimate of 181 ± 68 ITS copies in each QPX cell (the grand mean of ten different determinations from three independent sets of counted QPX cells).

PCR inhibition in clam, sediment, and seawater DNA templates

PCR inhibition in each DNA template was determined from the parallel "inhibition control" reactions described above. For templates with less than 50% inhibition, the qPCR assays were accepted as effective PCR amplifications, and the value of the PCR inhibition effect was used to correct the initial target gene abundance in the sample. When a template had more than 50% inhibition, it was further diluted and assayed again until effective amplification was achieved. For clam tissue samples extracted with the BD Nucleospin tissue kit, inhibition was a relatively minor problem. 56 of 74 DNA templates had less than 50%

PCR inhibition when assayed without any dilution (average inhibition for those 56 was 13.4 ± 20%), and 10-fold dilution was enough to reduce PCR inhibition to less than 50% in 14 of the 18 remaining clam DNA samples (average inhibition for those 14 after 1:10 dilution was 4.5 ± 23.7%).

PCR inhibition was much greater for sediment and seawater samples. In preliminary experiments for sediment samples, only 1 of 4 assayed without dilution and 2 of 11 assayed with 1:30 dilution had less than 50% inhibition (data not shown). For seawater samples, no matter what DNA extraction method was used (see below), none of the 17 samples assayed without dilution and only 4 of 17 assayed with 1:30 dilution had less than 50% inhibition (data not shown). 1:100 dilution reduced inhibition to less than 50% in all sediment samples tested but only in 11 of 16 seawater samples. Cleanup of the extracted DNA with a StrataPrep PCR purification kit was tested as an additional method to reduce PCR inhibition. For sediment, the reduction of PCR inhibition by the cleanup kit was enough that nearly half of postcleanup sediment samples assayed without dilution (5 of 11) and most assayed with 1:10 dilution (38 of 49) had less than 50% inhibition (average inhibition for those 38 samples was 3.3 ± 24.7%). Although all 11 postcleanup seawater templates assayed without dilution were still more than 50% inhibited, 1:10 dilution was enough to reduce inhibition to less than 50% in most assayed samples (48 of 56; 3.9 ± 28.4% average inhibition). 1:100 dilution reduced inhibition to less than 50% in most of the remaining postcleanup sediment (8 of 11; 21.7 ± 15.7% average inhibition) and seawater samples (6 of 8; 4.8 ± 25.1% average inhibition).

In our final application of the qPCR assay, the StrataPrep PCR purification kit was used routinely to remove inhibitors from DNA extracted from sediment and seawater samples, and postcleanup DNA was diluted 1:10 in an initial qPCR assay. The detection limit of our qPCR assay in clam and environmental samples varied among samples of each type depending on the template dilution required to minimize PCR inhibition and sample size (*a* and *e* in equation 7, respectively) and the PCR inhibition after dilution (equation 5). Assuming 100% recovery of QPX DNA from any QPX cells present, typical detection limits calculated by taking 10 QPX ITS region copies per reaction as the lowest reliable detection limit (#QPX$_{measured.1}$) were 0.1 ± 0.07 QPX cells mg^{-1} clam tissue, 0.3 ± 0.1 QPX cells mg^{-1} sediment and 0.4 ± 0.2 QPX cells ml^{-1} seawater.

Recovery of QPX DNA from pure culture, clam, sediment and seawater samples

The recovery of QPX DNA from pure cultures and QPX-spiked clam tissue samples using the BD Nucleospin tissue kit generally ranged from 20% to 40% (Table 1.3), except during the experiments in October, 2006, when the recovery rates from both pure culture and clam tissue were approximately 10-fold lower (p<0.05, ANOVA with post-hoc Tukey test). Differences in recovery rates were linked to switching between the three BD Nucleospin tissue kits used during this study. Using less tissue homogenate (25 mg compared to 100 mg, Table 1.3) may have improved the recovery of QPX DNA from clam tissue, although the difference was not statistically significant. The recovery of QPX DNA from QPX-spiked sediment samples by the FastDNA SPIN kit for soil followed by StrataPrep PCR purification kit was lower than the recovery from clam tissue, averaging 5.38% and ranging from 3.48% to 9.36%. The recovery of QPX DNA from QPX-spiked seawater samples was tested by six different methods. Among the three commercial tissue kits tested (methods 1-3 in Table 1.3), the BD Nucleospin plant kit had the highest QPX DNA recovery rate (though the differences were not statistically significant). Recovery was improved significantly when the Qiagen

DNeasy tissue kit lysis buffer was replaced by Galluzzi's crude lysis buffer (p<0.05, Table 1.3). Combining Galluzzi's crude lysis buffer with the physical lysis (bead beating) method of the FastDNA SPIN kit for soil provided still higher recovery of QPX DNA (though not statistically significant because of the variability; method 6, Table 1.3). The poor recovery of QPX DNA substantially increased the practical detection limits of the qPCR assay.

Quantification of QPX in clam, sediment and seawater samples (described in Chapter 2 in detail)

The qPCR assay was used to test samples collected from several enzootic sites in Raritan Bay, NY, and from a site in the Peconic estuary. QPX was detected, at abundance between 34 and 215 cells mg^{-1}, in four of the 43 sediment samples but not in any of the 40 seawater samples. All sediment samples that tested positive originated from Raritan Bay. Among all clams assayed, the qPCR assay found QPX abundance above the detection limit in 74 clams (all from Raritan Bay), while only 18 of those were also diagnosed as QPX positive by histology.

Discussion

Specificity and sensitivity of the QPX ITS region real-time qPCR assay

When real-time qPCR is applied to field samples, there is a risk of amplifying unknown QPX-related species that have sequences similar to the primer sites. The few ITS1 and ITS2 region sequences now available from other thraustochytrids and from aplanochytrids are highly divergent from QPX and from each other. Additionally, *in silico* analysis by BLAST against GenBank revealed that while each of the 5.8S24For and QPX-ITS2-R2 primers does match (or mismatches at only one or two bases) sequences from a variety of other organisms, only the QPX ITS region sequences match both primers. The 5.8S24For and QPX-ITS2-R2 primer pair never produced a signal from any *in vitro* labyrinthulomycete cultures other than QPX, QPX-free clam or QPX-free environmental sample in either standard or real-time PCR, even when amplification with the more general primer pair Laby-A and Laby-Y indicated that other labyrinthulids were present. Additionally, thermal dissociation curves of real-time PCR products did not reveal any heterogeneity. DNA extracted from two QPX-positive sediment samples (RB18 in May and RB12+17 in September, see Table 2.1 in Chapter 2) was also amplified by standard PCR with the qPCR primers 5.8S24For and QPX-ITS2-R2 for a total of 65 cycles to generate enough products for cloning, and the sequences of four cloned amplicons matched the QPX ITS region sequence (data not shown). This provided additional confirmation of the specificity of these QPX ITS region primers.

Lyons *et al.* (2006) developed a QPX qPCR assay based on a protein-coding gene. Compared with that approach, the ITS region assay developed here offers higher sensitivity due to the multi-copy nature of the target gene. In most eukaryotes, the rRNA operon is repeated in a tandem array. The number of rDNA copies per cell varies over a wide range, from a few copies for microalgae (Zhu *et al.*, 2005), to around 1000 copies for a nanoplanktonic dinoflagellate (Galluzzi *et al.*, 2004), to between 50 and 10,000 copies in mammals (Prokopowich *et al.*, 2003). We estimated that there are 181 ± 68 rDNA operon copies per QPX cell, and under the assumption that the rDNA copy number in QPX cultures is the same as in QPX cells present in the natural environment, this value was used to convert the detected number of target genes in a clam or environmental sample to cell counts. The conservative detection limit for our qPCR assay was 10 ITS region copies per reaction, which translates to approximately 0.05 QPX cells per reaction, substantially lower than the 1 cell per reaction detection limit of the Lyons et al. assay (Lyons *et al.*, 2006). Gast *et al.*

(2006) developed a DGGE assay for QPX based on the 18S rDNA primers QPX-F and QPX-R2, and were able to detect as few as 0.05 QPX cells ml^{-1} seawater, 0.01 QPX cells mg^{-1} sediment, and 0.1 QPX cells mg^{-1} clam tissue. However, this assay is not quantitative and is very sensitive because it is a nested method that uses over 90 PCR cycles to generate the final product.

A potential complication in estimating the abundance of QPX cells by any molecular genetic method arises from the life history of QPX, which involves three stages: thalli are independent single-nucleate cells which mature to form sporangia that contain many vegetative endospores, and endospores that are released from sporangia in turn mature to form thalli (Kleinschuster *et al.*, 1998). A single thallus in the process of becoming a sporangium could have dozens of nuclei, and dozens of copies of the genome, but be counted microscopically as a single cell. Because the proportion of thalli and sporangia varies with the growth phase of a culture (Liu, unpublished data), the genomic DNA content (and the average number of rRNA operon copies per cell) would be expected to vary accordingly; this fact would make *in vitro* cultured QPX cells a less reproducible DNA source for qPCR standard curves than the plasmid-based primary standard curve used here. Our estimated genomic DNA content of 257.1 ± 37.4 fg cell^{-1} would indicate a genome size of approximately 251 Mbp for QPX, which is 20- to 25-fold greater than the genome sizes recently estimated by PFGE for four other thraustochytrids (Anbu *et al.*, 2007). Further work will be required to determine whether the apparently high DNA content of QPX reflects the contribution of numerous genome-equivalents by sporangia, or whether QPX really has a much larger genome than other thraustochytrids or is polyploid. Despite these uncertainties, the life stages of QPX in cultures and in infected clams appear very similar (Kleinschuster *et al.*, 1998), so estimates of QPX cell number based on cultured cells should be reasonable for at least clam tissue samples.

PCR inhibition in clam and environmental DNA templates

One main problem with examining environmental samples by PCR is the possibility of false negative results caused by PCR inhibitors that are co-extracted with target DNA. Phenolic compounds, clay particles, humic acids, and heavy metals that are potentially contained by seawater and sediment DNA extracts have been identified as PCR inhibitors (Frostegard *et al.*, 1999; Watson and Blackwell, 2000). In clams, complex polysaccharides and collagen co-extracted from tissue could also inhibit PCR reactions (Gu and Levin, 2006). Compared with standard PCR, inhibition is a particularly serious problem in real-time qPCR, because the results are affected not only by the qualitative presence or absence of inhibitors, but also by the quantitative level of inhibition, which varies among different types of samples (e.g., tissue, seawater or sediment), as well as among samples of the same type. Approaches to detect and/or minimize PCR inhibition include the use of additional PCR reactions for each DNA template with different primers (Zhang and Lin, 2005) and serial dilutions of extracted DNA (Galluzzi *et al.*, 2004; Skovhus *et al.*, 2004; Cook and Britt, 2007). However, these approaches do not provide a quantitative calibration of the inhibition effect. Another approach is to extract and quantify environmental samples spiked with a known number of target cells side-by-side with target cells in a medium free of PCR inhibitors (Audemard *et al.*, 2006). In this study, we used an "inhibition control reaction" approach by adding a known amount of target DNA carried by plasmids to parallel PCR reactions to both detect and quantify PCR inhibition for each sample. We found that inhibition in clam tissue samples was often low, and could be overcome by 10-fold dilution of the template when necessary.

For sediment and seawater samples, an extra DNA purification step with the StrataPrep PCR purification kit (or the Wizard DNA clean-up system, which both had approximately 85% DNA recovery; Liu, unpublished data) was always necessary after DNA extraction, and even after that purification 10-fold dilution was still usually required to reduce PCR inhibition to less than 50%. The calculated inhibition effect value, which is inversely related to the detection of the added plasmid DNA (equation 5), was the basis for us to ensure that lack of amplification was not a false negative result due to PCR inhibition, and also to correct the estimates of QPX abundance in samples that gave positive results.

Recovery of QPX DNA from cultures, clam tissues, and environmental samples

Quality and quantity of the DNA prepared by extraction and purification methods are interrelated, because some efforts at removing inhibitors, such as additional column binding and washing steps, will ineluctably result in reduction of DNA yield. For example, Audemard *et al*. (2004) found a tradeoff between PCR inhibition and DNA recovery in comparing two extraction kits for quantification of *Perkinsus marinus* in seawater samples. Although optimization of DNA extraction procedures has been included in previous reports of qPCR assay development (Haugland *et al.*, 2002; Cook and Britt, 2007), little quantitative evaluation has been done of the recovery rate of target DNA from environmental samples. Recovery may vary not only with the type of samples being processed but also with the organism being targeted; an extraction method that is efficient for one group of microorganisms is not necessarily suitable for another group. Therefore, one aim of this study was to use samples spiked with known numbers of QPX cells to provide quantitative estimates of QPX DNA recovery rate from clam and environmental samples.

The efficiency of QPX cell lysis may have been a major factor limiting the recovery of QPX DNA; for example, both the T1 lysis buffer from the Nucleospin tissue kit and an SDS-based lysis buffer (1% SDS, 25 mM EDTA, 0.1 mg ml-1 proteinase K), even when combined with sonication, yielded less than 10% as much DNA from counted samples of QPX cells than the Galluzzi *et al.* (2004) lysis buffer, which contains Tween 20 and Nonidet P-40 instead of SDS (Q. Liu, unpublished data).

Using the BD Nucleospin tissue kit, QPX DNA recovery rates from clam tissue and pure culture generally ranged from 20 to 40% (Table 1.3).Since we used the same extraction protocols, instruments and personnel throughout, the low recovery of QPX DNA by the BD Nucleospin tissue kit in October 2006 was most likely due to differences in the reagents or columns among the three different lots of the kit we used. We suggest that the recovery rates of extraction procedures should be estimated frequently, especially when any element involved in the extraction procedure is changed, such as repurchasing a kit or changing reagents or personnel.

The Qbiogene FastDNA SPIN kit for soil has been widely used for DNA extraction from soil and sediment samples (Skovhus *et al.*, 2004; Selesi *et al.*, 2007). Cook and Britt (2007) found that this kit gave the highest yield of community DNA from soil samples and the highest copy number of the targeted *Mycobacterium* IS900 sequences in comparison with two other commercial kits, probably because it combines chemical lysis buffer and mechanical cell lysis by bead-beating so that soil samples get homogenized and cells in the interior of aggregates are more readily accessible. A wide range of methods have been used for the preparation of DNA from seawater samples, including traditional SDS-phenol-chloroform methods (Schwalbach and Fuhrman, 2005; Zhang and Lin, 2005) and commercial extraction kits like the Qiagen DNeasy tissue kit (Audemard *et al.*, 2004; Park *et*

al., 2007). We found that the choice of lysis buffer and inclusion of a physical lysis step affected recovery (and perhaps also the variability of recovery) of QPX DNA from seawater samples (Table 1.3).

In summary, a specific and sensitive real-time qPCR assay for QPX with primers targeting the ITS regions of the rRNA operon was developed in this study. With the optimized sample processing and DNA extraction and purification methods, the qPCR assay offers a promising tool for describing the distribution and dynamics of QPX in the marine environment and in clams, and for investigating the relationship between QPX in the environment and the development of QPX disease within affected clam populations.

$$y = -3.84x + 40.9$$
$$R^2 = 0.99$$
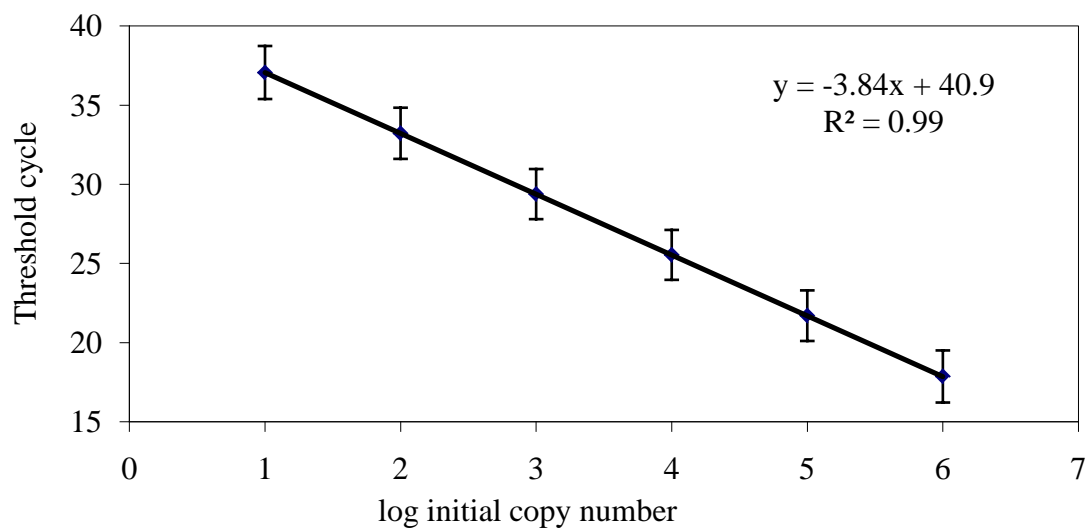
Figure 1. 1. Real-time quantitative PCR plasmid standard curve for primer pair 5.8S24For and QPX-ITS2-R2 averaged over 35 independent qPCR assays.

Table 1. 1. Primers used in this study

Primer Name	Sequence (5'→3')	Target	Application(s)	Reference
QPX-F	ATCCTCGGCCTGCTTTTAGTAG	QPX (18S rDNA)	PCR and cloning	(Stokes *et al.*, 2002)
QPX-R2	GAAGTCTCTACCTTTCTTGCGA	QPX (18S rDNA)	PCR	(Stokes *et al.*, 2002)
QPX-R2-For	TCGCAAGAAAGGTAGAGACTTC	QPX (18S rDNA)	PCR	(Stokes *et al.*, 2002)
Laby-A	GGGATCGAAGATGATTAG	labyrinthulid (18S rDNA)	PCR	(Stokes *et al.*, 2002)
Laby-Y	CWCRAACTTCCTTCCGGT	labyrinthulid (18S rDNA)	PCR	(Stokes *et al.*, 2002)
18S-R	TGATCCTTCTGCAGGTTCACCTAC	eukaryotes (18S rDNA)	PCR	(Medlin *et al.*, 1988)
18S-RR	GTAGGTGAACCTGCAGAAGGATCA	eukaryotes (18S rDNA)	PCR	(Medlin *et al.*, 1988)
5.8S24For	TTTAGCGATGGATGTCT	QPX (5.8S rDNA)	PCR and qPCR	this study
5.8S127For	CATTGCGCTTTCGGGTGATCC	QPX (5.8S rDNA)	PCR	this study
5.8S127Rev	GGATCACCCGAAAGCGCAATG	QPX (5.8S rDNA)	PCR and qPCR	this study
QPX-ITS2-F2	AWAGAGCAGTTTGTGGGC	QPX (ITS2 region)	PCR	this study
QPX-ITS2-R2	GCCCACAAACTGCTCTWT	QPX (ITS2 region)	PCR and qPCR	this study
QPX-ITS2-R	GCCACCTATTCCCAAAAGAGGA	QPX (ITS2 region)	PCR and qPCR	(Qian *et al.*, 2007)
28S46Rev	ACCCGCTGAARTTAAGCATAT	eukaryotes (28S rDNA)	PCR and cloning	(Van der Auwera *et al.*, 1994)

Table 1. 2. Results of testing nine primer pairs in standard PCR format

Primer pair	Amplicon length[a]	Standard PCR template[b]			
		QPX DNA[c]	QPX-positive clam[d]	QPX-free clam[d]	Three thraustochytrids[e]
QPX-R2-For+18S-R	~450 bp	+	unspecific product	N/T	N/T
18S-RR+5.8S127Rev	~250 bp	+	unspecific product	N/T	N/T
5.8S24For+5.8S127Rev	~150 bp	+	+	-	-
5.8S24For+QPX-ITS2-R2	~200 bp	+	+	-	-
5.8S24For+QPX-ITS2-R	~250 bp	+	+	-	-
5.8S127For+QPX-ITS2-R2	~90 bp	+	+	primer dimer	N/T
5.8S127For+QPX-ITS2-R	~120 bp	+	+	primer dimer	N/T
5.8S24For+28S46Rev	~220 bp	+	unspecific product	N/T	N/T
QPX-ITS2-F2+28S46Rev	~150 bp	+	primer dimer	N/T	N/T

[a] Amplicon lengths were estimated based on QPX 18S rDNA, ITS1, 5.8S rDNA, ITS2, and 28S rDNA sequences and confirmed by electrophoresis of PCR products on 1.5% agarose gel.

[b] '+' indicates that the expected product was produced without artifacts, '-' indicates that no products or artifacts were produced; 'unspecific product' and 'primer dimer' indicates the type of artifact produced, N/T indicates not tested.

[c] 'QPX DNA' is purified genomic DNA of cultured QPX cells.

[d] 'QPX-positive' and 'QPX-free' clams were diagnosed by histology and standard PCR with 18S rDNA QPX-specific primers QPX-F and QPX-R2

[e] 'Three thraustochytrids' indicates purified genomic DNA from ATCC28209 *Schizochytrium aggregatum*, ATCCMYA-1381 *Schizochytrium limacinum*, and ATCC34304 *Thraustochytrium aureum*.

Table 1. 3. Recovery rate of QPX DNA by different DNA extraction methods from QPX cultures as well as clams, sediment, and seawater samples spiked with QPX cells

Sample type	Extraction method		QPX DNA recovery rate
QPX culture[a]	BD Nucleospin tissue kit	May 2006 Oct 2006 Oct 2007	$36.58 \pm 8.89\%$ (n=3) $4.68\% \pm 0.55\%$ (n=3) $26.38 \pm 2.72\%$ (n=5)
Clam tissue[b]	BD Nucleospin tissue kit	Oct 2006 100mg 25mg Oct 2007 100mg 50mg 25mg	$0.92 \pm 0.47\%$ (n=3) $1.77 \pm 0.59\%$ (n=2) $16.31 \pm 12.31\%$ (n=3) $16.31 \pm 1.42\%$ (n=3) $29.65 \pm 7.80\%$ (n=3)
Sediment[b,c]	Qbiogene FastDNA Spin kit for soil		$5.38 \pm 2.11\%$ (n=6)
Seawater[b,c]	Method 1 BD Nucleospin tissue kit[i]		$2.85 \pm 2.41\%$ (n=3)
	Method 2 Qiagen DNeasy tissue kit[ii]		$1.30 \pm 0.05\%$ (n=3)
	Method 3 BD Nucleospin plant kit[iii]		$3.96 \pm 0.44\%$ (n=3)
	Method 4 Galluzzi's crude lysis buffer + Qiagen DNeasy tissue kit[iv]		$4.96 \pm 1.05\%$ (n=3)
	Method 5 C0 lysis buffer (BD Nucleospin plant kit) + FastDNA SPIN kit for soil[v]		$4.65 \pm 1.44\%$ (n=3)
	Method 6 Galluzzi's crude lysis buffer + FastDNA SPIN kit for soil[vi]		$9.51 \pm 8.18\%$ (n=9)

[a] Calculated by PicoGreen measurement of total DNA compared to Galluzzi *et al*. (2004) method estimate of 257.1 fg DNA cell^{-1}.

[b] Calculated by real-time qPCR.

[c] After purification of extracted DNA with the StrataPrep PCR purification kit.

[i] 1 ml of buffer T1 with 25 µl proteinase K (20 mg/ml); 56-58 °C for 3 hours.

[ii] 1 ml of ATL buffer with 25 µl proteinase K (20 mg/ml); 56-58 °C for 3 hours.

[iii] 1 ml of C0 buffer from BD Nucleospin plant kit; 56-58 °C for 3 hours.

[iv] 1 ml of fresh made Galluzzi's crude lysis buffer; 60 °C for 3 hours.

[v] 1 ml of C0 buffer from BD Nucleospin plant kit; 56-58 °C for 3 hours.

[vi] 1 ml of fresh made Galluzzi's crude lysis buffer; 60 °C for 3 hours

Chapter 2: Dynamics of QPX in a wild clam population and in the environment

(Some content of this chapter has been published as Liu *et al*. (2009))

Introduction

QPX belongs to the protistan phylum labyrinthulomycota, and is a member of the group known as thraustochytrids (Maas *et al*. 1999; Ragon *et al*. 2000; Stokes *et al*. 2002). Thraustochytrids are common and abundant in coastal and oceanic benthic habitats (Raghukumar, 2002), and their ecological importance may currently be underappreciated (Santangelo *et al*., 2000; Raghukumar *et al*., 2001; Mo *et al*., 2002). Some thraustochytrids are associated with diseases in invertebrates, and QPX is thought to be an opportunistic parasite of hard clams (refs). Although QPX has been detected in hard clam pseudofeces, and in environmental samples such as sediment and seawater as well as macrophytes and invertebrates (Lyons *et al.*, 2005; 2006; Gast *et al*. 2008), a lack of quantitative information about the abundance of QPX in environmental samples hinders understanding of the dynamics of this protist in relationship to environmental factors or to the occurrence and severity of QPX disease in clams.

Management of hard clam populations affected by QPX disease is hampered by the lack of information relative to factors controlling the occurrence and severity of QPX infection. Environmental factors such as salinity and temperature appear to be important, with QPX infections most prevalent at high salinities (Ragone Calvo *et al*. 1998) and in early summer, at least in New York (Fig. 1). High clam population density and the planting of seed from non-local sources might also increase the susceptibility of clam populations to QPX (Ford *et al.* 2002). More quantitative information about the occurrence and progression of QPX disease in relation to these and other variables would support better prediction and response to QPX outbreaks.

In New York State, severe clam mortalities were observed in summer 2002 in the wild clam population in Raritan Bay. Histological analysis of moribund clams revealed QPX disease as the cause of these mortalities. A survey of the bay in the fall of 2002 showed a widespread presence of QPX infected clams (Dove *et al*. 2004), leading to the suspension of the Raritan Bay transplant fishery. Since then, a monitoring program was established by the NYSDEC and MADL to examine QPX prevalence in the clam population in Raritan Bay. The 2002-2005 surveys revealed that, although QPX prevalence determined by histological analysis reached 23-33% in some survey sites (site 8 and 21), the prevalence was relatively low, generally below 10% of infected clams, in most surveyed sites during most sampling dates (Fig. 1). In addition, a cyclic pattern of QPX infection was noticed, with prevalence peaking during summer, then declining until the following spring. Thus the infection appears to be related to the increase in seawater temperature. It is interesting to note that the highest QPX prevalence during the survey was measured at sites 8 and 21, which have a relatively high clam density compared to other sites. These findings suggested a positive correlation between clam densities and QPX prevalence (Allam and Pawagi, 2004), in agreement with observation made by Ford *et al*. (2002) in aquacultured clams, although the biological and ecological bases for this relationship are unknown.

Although the survey in Raritan Bay provides very important information about the distribution and severity of QPX disease in wild clams, the prevalence data determined by

histological methods need to be cautiously interpreted because of the potential for false negative results generated by the sampling and diagnosis techniques. The sensitivity of the new qPCR assay described in Chapter 1 allows us to detect a relatively low QPX abundance in clam tissue, and so may reveal more detail about the dynamics of QPX disease. One of the aims of this study is to field validate the newly developed qPCR assay for QPX diagnosis relative to the standard histological method, and to utilize this molecular tool to examine the dynamics of QPX abundance in clams, seawater and sediments.

Materials and methods

Environmental sample collection

Seawater and sediment samples were collected from between seven and eleven sites in Raritan Bay along with one site in Hashamomuck Pond in Peconic Bay (both in New York, USA; Fig. 2.1) at 6-week intervals from April to September 2006. The sampling at the Peconic Bay site was usually performed during the same or following week of each Raritan Bay sampling. At each sampling site, 4 liters of seawater from one meter below surface was collected with a 2 liter General Oceanics (Miami, FL) Niskin bottle and 400 to 500 ml was filtered through replicate 0.22 µm Sterivex-GV filter units (Millipore, Billerica, MA) with a peristaltic pump. Sediment samples were collected from the patent tong which was also used to collect clam samples by pooling and mixing the intact surface layer (0.5 to 1 cm deep) in a sterile container, then transferring subsamples to 2 ml cryovials. The filters and sediment samples were stored immediately on dry ice and transferred to a -80°C freezer until DNA extraction. For each site, the physical-chemical characteristics of bottom seawater (temperature, salinity and dissolved oxygen concentration) were measured and bottom sediment types were visually assessed and recorded.

Quantification of QPX in environmental samples by real-time qPCR assay

DNA was extracted and purified from Raritan Bay and Peconic Bay seawater samples using Method 6 described in Chapter 1 (Table 1.3). For sediment samples, DNA was extracted by a Qbiogene FastDNA Spin kit for soil and purified using a StrataPrep PCR purification kit following the protocol describe in Chapter 1. 1 µl DNA was used as template in qPCR assay. The original abundance of QPX cells in each sediment and seawater sample was calculated by $(\#QPX_{initial} \times a \times b)/(c \times d \times e)$ as described in Chapter 1 (equation 7), where $\#QPX_{initial}$ is the number of QPX ITS copies in the 1 µl assayed environmental DNA template (copy μl^{-1}) after correction for PCR inhibition, a typically equals to 10 or 100, b equals to 150 µl, c equals to 181 copies $cell^{-1}$, d is the estimated DNA recovery rate of the extraction method (5.38% for sediment samples and 9.51% for seawater samples), and e varied among samples from 500 to 850 mg for sediment samples and from 400 to 550 ml for seawater samples.

Clam sample collection and processing

The clam sampling in Raritan Bay in 2006 was part of the monitoring program of the wild hard clam population, operated by NYSDEC. In this study, clams analyzed by both histological and qPCR methods were collected from three Raritan Bay sites (sites 8, 18 and 21) during the 5 sampling dates and site 20 in Raritan Bay in May and August in 2006, giving a total of 17 groups of clams (~30 clams per group). At each sample site, clams bedding in sediment were collected by a patent tong (total area 1 m^2 per grab). The clam density was estimated by dividing the total number of collected clams by the number of grabs. From all clams collected, 30 clams were randomly selected; multiple grabs were performed to collect 30 live clams when clam density was lower than 30 m^{-2}. The numbers of live and

recent dead (articulated intact empty valves) clams within grabs were counted for the estimation of mortality values. After clam samples were collected in the field, they were immediately placed on ice, transported to the laboratory and usually processed in 6-48 hours.

Gross, histological and molecular examinations of clams were conducted in a standardized, systematic procedure. Shell size (length and width), external shell characteristics (e.g. gaping, chips etc.) were noted for each animal. The clams were then shucked and examined for gross abnormal signs in tissue such as nodules or swelling, which could be signs of QPX infection. Each clam was further dissected and diagnosed for QPX using both standard histological techniques and qPCR assay.

Histopathological analysis

For histopathology, a thin cross section (3-5 mm in thickness) of meat, containing mantle, gills and visceral organs (e.g. digestive glands, stomach, gonad, pericardium and kidney), was taken. A transverse slice of tissue from the base of the siphon, where QPX infections have been suggested to be initiated (Smolowitz *et al.*, 1998), was taken as well. The tissues were transferred to a histo-cassette, fixed in 10% buffered formalin, embedded in paraffin, sectioned at 5 to 6 µm and mounted on slides (performed by a contracted histology facility). The histological slides were stained (Harris's hematoxylin for 2 min and Eosin Y for 1 min) and examined with a light microscope. The presence and distribution of QPX was examined for each of the four tissue types within an individual section (siphon, mantle, gill and visceral mass), and characterized as focal, multifocal, or diffuse. Signs of old lesions or "healing" were also recorded when observed. The QPX load was scored based on the total number of QPX organisms in all tissue types per slide section, as described in Ragone Calvo *et al.* (1998) as rare (1-10), light (11-100), moderate (101-1000) or heavy (>1001). The histological analyses reported here were done by MADL permanent staff (Sujata Pawagi and Bassem Allam) and submitted as a report to the NYSDEC (Allam and Pawagi, 2006).

Quantification of QPX in clam samples by qPCR assay

For qPCR assay, the mantle and siphon tissue remaining after histological sampling was drained on a clean paper towel, weighed and preserved in 100% ethanol at -80 °C. To recover DNA, ethanol-preserved clam tissue was washed twice using phosphate-buffered saline (PBS) and mechanically homogenized in 10 volumes of PBS (e.g., 1 g tissue in 10 ml PBS). A 1 ml aliquot of homogenate of each clam, containing 100 mg clam tissue, was transferred to a 1.5 ml centrifuge tube for DNA extraction. DNA was extracted by following the protocol described in Chapter 1. 1 µl DNA was used as template for qPCR assay, and the original abundance of QPX cells in each clam sample was determined by ($\#QPX_{initial} \times a \times b)/(c \times d \times e)$ as described in Chapter 1 (equation 7). In Raritan Bay clams examined in this study, *a* typically equals to 1 or 10; *b* equals to 150 or 300 µl; *c* equals to 181 copy cell^{-1}; *d* is 16.31% according to previous estimation (Table 1.3); and *e* equals to 100 mg.

QPX prevalence and weighted prevalence in clams

QPX prevalence in each group of clams was calculated as percentage of QPX-positive clams in all sampled animals. QPX prevalence determined by histological method is based on the individuals containing QPX cells in any tissue included in the tissue section examined by microscopy. QPX prevalence determined by qPCR is the proportion of clams displaying positive QPX signals (above detection limit).

To quantitatively describe the average QPX load determined by qPCR in each group of clams, QPX load in each individual clam was rated based on the estimated number of QPX cells in each milligram mantle tissue, from 0 (below detection limit of qPCR assay), 1 (rare

infection, detection limit to 10), 2 (light infection, 11-100), 3 (moderate infection, 101-1000), to 4 (heavy infection, >1001). QPX weighted prevalence was then calculated by dividing the sum of individual QPX loads by the total number of clams examined.

Statistical analysis

     Prior to the analysis, percentage prevalence and mortality values were arcsine transformed, and weighted prevalence was log-transformed. Paired t-test was performed to determine if there was a significant difference between prevalence data determined by histological and qPCR methods for each site. A Spearman Rank correlation test was performed to examine the correlation between the prevalence data generated by these two diagnosis methods. Regression analysis was performed between weighted prevalence determined by qPCR as dependent variable and temperature, dissolved oxygen concentration and estimated mortality as independent variables. Water temperature (Fig. 2.2) measured by a nearby USGS weather station (USGS 01407081 Raritan Bay at Keansburg, New Jersey) up to 150 days before the sampling date was also tested for correlation with weighted prevalence. The other parameters (dissolved oxygen and mortality) were not tested for time-offset correlations due to insufficient data. All differences were considered statistically significant at $p < 0.05$.

Results

Environmental variables

     In 2006, mean bottom seawater temperature across Raritan Bay, excluding site 20, ranged from 9.7 °C to 22.7 °C (Fig. 2.3A) during the study period. At site 20, which is located inside Great Kills Harbor, the temperature was up to 3.4 °C higher than the other sites in Raritan Bay. At the sampling site in Peconic Bay, the temperature was also usually greater than the mean temperature of Raritan Bay sites. The salinities of Raritan Bay sites ranged from 20.7 to 26, and the salinity of site 20 was not significantly different from other sites in Raritan Bay. The salinity of the sampling site in Peconic Bay remained 27.2 ± 0.1 through the year and was about 3 higher than the average of Raritan Bay sites (data not shown). The average dissolved oxygen concentrations of bottom water in Raritan Bay sites, excluding site 20, ranged from 12.1 ± 0.6 mg L^{-1} in April to 4.9 ± 0.5 mg L^{-1} in late June (Fig. 2.3B). At site 20, dissolved oxygen concentrations were generally 2 mg L^{-1} to 3.5 mg L^{-1} less than the other Raritan bay sites. The concentration of dissolved oxygen at the sampling site in Peconic Bay was similar to Raritan Bay (excluding site 20), except in April, when it was 6.4 mg L^{-1} lower.

QPX abundance in environmental samples

     In 2006, 43 sediment samples and 40 seawater samples were collected from clam harvesting areas in Raritan Bay and from Hashamomuck Pond in the Peconic estuary (Fig. 2.1) and assayed by qPCR. QPX was below the detection limit of 10 ITS copies per reaction (4.2 ± 1.7 cells ml^{-1}) in all seawater samples. QPX was also below the detection limit of 5.6 ± 2.1 cells mg^{-1} sediment in 39 of 43 sediment samples, but it was detected at Raritan Bay site 8 and 18 in May and at site 12+17 and site 21 in September with abundance between 34 and 215 cells mg^{-1} sediment (Table 2.1).

QPX prevalence in Raritan Bay clams

     15 groups of clams (~30 clams per group) collected on 5 sampling dates in 2006 from three Raritan Bay sites (sites 8, 18 and 21) were analyzed by both histological and qPCR methods. The typical detection limit of the qPCR assay was estimated to be 0.5 cells mg^{-1} tissue based on all clam samples assayed. Prevalence determined by qPCR assay was

significantly higher than prevalence determined by histology at all three surveyed sites through all sampling times (Student's t-test, p<0.01) (Fig. 2.4). At sites 8 and 18, no QPX was detected by histology in clams sampled in April. Clams began to exhibit low but histologically detectable QPX infection in May and June. The highest histological prevalence for both sites was observed in August (6.6% at site 8 and 13.3% at site 18), then decreased again in the early fall. QPX prevalence determined by qPCR assay was significantly correlated with histological prevalence (Spearman Rank correlation test p<0.05), revealing a similar temporal pattern but with a substantially greater prevalence: QPX infection was detected in April, with a relatively low prevalence (3.3% at site 8 and 10% at site 18). The prevalence then increased to around 13% in May and reached a peak in August (20% at site 8 and 40% at site 18). A significant decrease in prevalence occurred in September, to a slightly higher level than May. Although prevalence at these two sites generally showed a similar temporal pattern, prevalence dropped to 0 by histology and 3.4% by qPCR at site 8 in June, while QPX prevalence increased at site 18 during the same time.

Compared to site 8 and 18, QPX prevalence determined by histology showed a different temporal pattern at site 21 (Fig. 2.4), with the highest prevalence (13.6%) in April and the lowest in August. These results were opposite to the patterns at sites 8 and 18. As at sites 8 and 18, qPCR assay detected a significantly higher prevalence (Student's test, p=0.012) than histology at site 21, but qPCR prevalence was not correlated with that determined by histology. Relatively high (20.7%-23.3%) prevalence was detected in both April and June, followed by 13.3% in both May and August, and 10% in September. Overall, the QPX prevalence determined by qPCR in all site 21 samples was between 10% and 26.7%, showing less variation over time than sites 8 and 18.

Clams collected from site 20 in May and August (30 clams per group) were also examined by both histological and qPCR assays. No QPX infection was detected in these clams by either assay.

QPX loads determined by qPCR in Raritan Bay clams

Like prevalence, the average QPX loads determined by qPCR, quantitatively evaluated by weighted prevalence, showed a temporal pattern at sites 8 and 18 (Fig. 2.4). At site 18, weighted prevalence progressed distinctly with the season. The weighted prevalence was lowest (0.1) in April when only rare QPX loads were detected in QPX-positive clams, and increased to 0.2 in May, due to the appearance of clams with moderate infection. Weighted prevalence reached 0.52 in June when more QPX-positive clams were detected, including some with heavy infection intensities. In August, more clams had light and moderate infections, which gave the highest QPX weighted prevalence (0.77). From August to September, weighted prevalence significantly declined to 0.23 (Student's t-test, p<0.05) as no moderately or heavily infected individuals were detected and rare and light infections were also detected in fewer clams.

At site 8, QPX loads in clams showed a similar progression pattern to that at site 18, with the exception of June (Fig. 2.4). Although the increase in weighted prevalence from April to August was interrupted by the decline of QPX prevalence (only one clam with moderate infection was found in 29 sampled) in June, weighted prevalence still reached its peak (0.47) in August, and then decreased to 0.23 in September samples. It should be noted that weighted prevalence dropped to the same level in September at both sites, but clams at site 8 exhibited a lower prevalence, but with heavier infections than clams at site 18.

The pattern of QPX loads in clams at site 21 looked different from site 8 or 18 (Fig. 2.4). Weighted prevalence was highest in April (0.41), and did not change much through May (0.28) and June (0.41). From June to August, opposite to the increasing prevalence and weighted prevalence observed at site 8 and 18, clams at site 21 exhibited a decrease in QPX load, due to the absence of moderately infected clams.

QPX infection characterization determined by histology or qPCR

Histological method characterized the intensity of QPX infection based on the distribution of QPX cells and the estimated number of live parasites for each tissue type within a cross section of host tissue. Among the 19 clams from sites 8, 18, and 21 in 2006 that were diagnosed QPX positive by histology, 3 clams had rare infections (1-10 cells), 11 individuals exhibited light intensity (11~100 cells) and 5 clams were moderately infected (101-1000 cells). The most frequently observed infection (13 of 19 clams) was diffuse in various combinations of tissues, involving siphon, mantle, gill and visceral mass. Four clams exhibited focal infections that were restricted to one type of tissue, and 2 clams had multifocal infections. Infection intensity and distribution determined by histopathology showed no obvious temporal or spatial pattern (Fig. 2.4).

Among the 17 groups of clams (total 510 clams) assayed, the qPCR assay found QPX abundance above the detection limit (0.5 cells per mg tissue assuming 0% inhibition in the qPCR reaction) in 74 clams (Fig. 2.5, 'qPCR positive' column), including 18 of the 19 clams that were diagnosed as QPX positive by histology. There was one clam assayed by qPCR as negative but histologically diagnosed to have a focal and light infection in siphon tissue. Comparison of QPX abundance in those 18 clams with the 56 clams which were qPCR-positive but histologically negative (Fig. 2.5, 'histology positive' and 'histology negative' columns, respectively) showed that the histologically positive clams included all clams with heavy loads, most clams with moderate infections, and a few clams with light infections detected by the qPCR assay (estimated number of QPX cells ranging from 13 to 2613 mg^{-1} tissue). A Spearman Rank correlation test showed that QPX prevalence determined by histology was correlated to the prevalence of moderate and heavy infections (>101 cells mg^{-1}) detected by qPCR (p<0.001, 15 groups regardless of site). On the other hand, a majority of QPX positive clams determined by qPCR assay to have lighter QPX loads, including all 41 clams with rare infections, most clams with light infections, and some clams with moderate infections, were diagnosed as "negative" by histology. The localization of the parasites within host tissue was also reflected in the intensity of QPX infection determined by qPCR assay (p<0.01, ANOVA). The qPCR estimated number of QPX cells in each milligram mantle tissue was higher in clams with multifocal infection than in the clams with focal or diffuse infection (Fig. 2.6).

Relationship of QPX disease to environmental conditions

At site 18, regression analysis showed a significant correlation between the weighted prevalence determined by qPCR and water temperature on the sampling date (R^2=0.888) while the weighted prevalence at site 21 was found to be significantly correlated with the water temperature recorded 90 to 105 days prior to the sampling date (R^2=0.805 to 0.811, Table 2.2). For site 8, however, the weighted prevalence was never significantly related to water temperature recorded 0 to 120 days prior to the sampling date. Dissolved oxygen concentration and mortality recorded on the sampling date were not significantly correlated with weighted QPX prevalence at any site.

The correlation analysis also showed different lag times between water temperature and weighted prevalence at each site (Fig. 2.7). The best fit (maximum R^2) at site 18 ($R^2=0.961$) had no time lag, while QPX weighted prevalence at site 21 was best correlated with the temperature 120 days before the clam sampling date ($R^2=0.986$).

Discussion

QPX abundance in environmental samples

In this study, no QPX was detected in any of the 40 seawater samples from Raritan Bay and Peconic Bay. This could reflect a low abundance of QPX in seawater combined with the limitations of recovering QPX DNA from seawater samples. Better detection of QPX might be achieved by collecting particulate matter on filters with a larger pore size than the 0.22 µm used here; for example, a 1 µm pore size filter would still capture QPX cells (which typically range from 2 to 20 µm in diameter; Kleinschuster *et al.*, 1998), while allowing larger volumes of water to be filtered and reducing the contribution of bacteria to the extracted DNA. Alternatively, if QPX is associated mainly with marine aggregates, where it has previously been detected (Lyons *et al.*, 2005; Lyons *et al.*, 2006), much larger particles might need to be collected from larger volumes of seawater in order to routinely detect QPX.

QPX was detected in 4 sediment samples collected from Raritan Bay in 2006 (Table 2.1). This is the first report of quantitative detection of QPX in sediment, although thraustochytrids in general are common and abundant in coastal and oceanic benthic habitats (Raghukumar, 2002) and QPX has been detected in hard clam pseudofeces, environmental samples and other invertebrates (Lyons *et al.*, 2005; Lyons *et al.*, 2006, Gast *et al.* 2008). The natural transmission mechanism of QPX disease is not yet known, but sediment, as the habitat of clams and a potential environmental reservoir for QPX, could play a role in disease transmission. The QPX-positive sediment samples were collected from four different sites where QPX disease has been occurring in clams since 2002 (Table 2.1; Allam, unpublished data), suggesting that the presence of QPX in the sediment may be related to QPX disease in local clams. However, due to the limited number of positive sediment samples, any relationship between QPX abundance in sediment and QPX disease prevalence in clams remains to be revealed. One of the limitations of the methods that we employed is related to the small amount of sediment material processed (500 to 850 mg). In small samples from heterogeneous environments such as sediments, estimates of abundance could be much greater than the average in some places but much lower in others. Increasing the amount of sediment processed for each DNA extraction is likely to overload the binding column during DNA extraction and purification and increase PCR inhibition. However, homogenizing a much larger sample prior to removing sub-samples, as for the clam tissue analysis, or analyzing several replicate samples from one field site may help to overcome these limitations.

Detection of QPX in clam samples

The sensitivity of the qPCR assay for diagnosis of QPX disease was tested by comparing it to the standard histological method in wild clams. As a result of an inflammatory reaction of the host, nodules in mantle and siphon tissue can provide a macroscopic indication of QPX infection. However, QPX infections are typically microscopic and focal, multifocal, or diffuse without the presence of visible nodules (Dove *et al.*, 2004; Ragone Calvo *et al.*, 1998; Smolowitz *et al.*, 1998). Focal and multifocal infections can be missed by histological diagnosis because only a thin section of tissue is examined. To minimize the risk of false negatives occurring because a focal infection site was not included in assayed tissue, the

whole mantle and siphon (excluding the thin section used for histology) was homogenized and a subsample of the homogenate was used for DNA extraction and subsequent qPCR assays. Making a weight-based tissue homogenate also standardized the digestion of tissue during DNA extraction and allowed quantitative measurement of QPX abundance in the clam tissue. QPX prevalence detected by qPCR assay was significantly higher than that detected by histology in the clams analyzed here (Fig. 2.4). Among all 510 clams assayed, QPX infection was detected in 74 clams by qPCR assay. Although most (13 of 18) of the clams containing the greatest numbers of QPX cells (moderate to heavy infections) were also QPX-positive by histology, all 41 clams with rare QPX loads as well as two thirds of lightly infected clams were histologically QPX negative (Fig. 2.5), suggesting that the qPCR assay, like the standard PCR assay using the rDNA primers QPX-F and QPX-R2 (Stokes *et al.*, 2002), is a more sensitive diagnostic tool for QPX especially when relatively few QPX cells are present.

Ford *et al.* (2002) reported that in their histological analysis, lower-intensity infections tended to be focal, whereas multifocal and diffuse infections were more likely to be higher intensity. However, our qPCR results showed that clams with multifocal infections in histological analysis had the highest QPX abundance, while QPX abundance in the clams with diffuse infections was not significantly different from that in the clams with focal infections (Fig. 2.6). This contradiction may be related to the limited number of histology-positive clams in our study, particularly those with focal or multifocal infections. Also because the histological and qPCR assays used different tissue for DNA and slide preparation, sampling error is likely to be greater in the case of focal infection. For example, the only clam assayed by qPCR as negative but diagnosed positively by histology appeared to have a focal and light infection in siphon. Because of the different strategies used in sample processing and in classification of infection intensity by histological and qPCR methods, it is understandable that QPX prevalence and infection intensity determined by histology was not always correlated with the prevalence and weighted prevalence determined by qPCR assay (significant Spearman rank correlations ($p<0.05$) existed in samples from site 8 and 18, but not in samples from site 21).

Progression of QPX disease in Raritan Bay clams

QPX infection at Raritan Bay site 18 based on the results of both histology and qPCR assay showed a clear seasonal pattern (Fig.2.4): QPX was detected with a relatively low prevalence and weighted prevalence (averaged QPX loads) in April. The prevalence and weighted prevalence then increased synchronously in May and June and reached a peak in August, before declining in September. This trend was consistent with the cyclic pattern in QPX prevalence determined by histological analysis from the same site from 2002 to 2005 (Fig.1). Although the transmission mechanism of QPX in clams is unclear, analyzing the seasonal change of QPX prevalence and weighted prevalence allowed us to estimate host-pathogen dynamics including infection acquisition, infection progression and associated host death and healing at this site. Generally, the acquisition of new infections and the development of established infections are the two major processes contributing to the increases in both QPX prevalence and weighted prevalence, while the decreases in both QPX prevalence and weighted prevalence are likely due to the mortality of those clams having advanced infections and/or clam healing. In April, all QPX-positive clams had rare infections, indicating that these clams acquired new infections prior to April or carried non-lethal infection from the previous year. Through spring and summer, when the average QPX load

increased, total prevalence also increased, suggesting that lighter infections (rare and light intensity) gradually progressed into more severe infections (moderate to heavy) in the clams which were already infected, while more clams in the population were acquiring new infections. After QPX prevalence and weighted prevalence reached the highest level in August, a statistically significant drop of weighted prevalence was observed in September. The absence of clams with moderate to heavy infections in the September sample could be related to the mortality of the most severely infected clams; meanwhile the concurring decrease in rare and light infections in the fall could be due to more healing than acquisition of new infections in the clam population.

Like other host-parasite models, such as *Perkinsus marinus* in the oyster *Crassostrea virginica*, environmental factors can influence the host-parasite dynamics between clam and QPX. In temperate coastal environments such as Raritan Bay, temperature is a major environmental factor that shows strong seasonality (Fig.2.2 and 2.3). In this study, QPX weighted prevalence at site 18 showed a significant correlation with temperature at the time of sampling (Table 2.2, Fig. 2.7), suggesting that temperature may be an important environmental factor regulating the seasonal transmission and development pattern of QPX disease at this site (Fig. 2.4). However, gaining an understanding of the complex interactions between hosts, parasites and their environment is often a great challenge. For example, the gradual progression of QPX infection was a major process during April to June, when temperature was below 20 °C, suggesting a positive impact of a colder environment on the ability of QPX to establish infection and proliferate in clams. In contrast, clam healing seemed to mainly occur during August and September when temperature was near 25 C, suggesting a positive impact of a warmer environment on the ability of the clams to eliminate the parasite. However, as a chronic infectious disease, the abundance of QPX within the host requires time to respond to changing environmental conditions. Thus, the mortality of clams with relatively heavier infections resulting from the continued development of QPX infection might occur at the same time that clams with lighter infections are healing. As it is difficult to interpret the effect of temperature on different aspects in QPX transmission and host-parasite dynamics in the natural environment only based on the data of QPX prevalence and infection intensity in clams, laboratory experiments under controlled conditions were conducted in further studies as described in Chapter 3 and 4 to specifically investigate the impact of temperature on QPX development in infected clams and on parasite transfer between infected and susceptible clams.

Seasonal infection patterns of marine bivalve diseases are not uncommon. For example, a pathogen of oyster, *Perkinsus marinus*, has been well documented to exhibit a distinct seasonal cycle, with minimum prevalence and intensity in early spring, and maximum prevalence and intensity in late summer (Brousseau, 1996; Burreson and Ragone Calvo, 1996; Oliver *et al.*, 1998). Such a seasonal pattern is similar to the pattern of QPX infection observed at Raritan Bay site 18 in 2006. However, in contrast to our findings in QPX disease, *P. marinus* infection acquisition was limited to the summer months (July, August and September) with relatively higher temperature, and high summer temperatures enhance *P. marinus* multiplication within host oysters (Ragone Calvo *et al.*, 2003; Audemard *et al.*, 2006). Carnegie *et al.* (2008) also highlighted the importance of warm temperature on seasonal infection cycling of the oyster pathogen *Bonamia sp.*, and demonstrated that temperatures >20-25 °C favored the parasite to overcome oyster defenses, which contrasts

with the disadvantageous effect of high temperature in August and September on QPX in the host-pathogen interaction observed in Raritan Bay clams.

At site 8 in Raritan Bay, the general pattern of QPX prevalence and weighted prevalence through the year was similar to that at site 18, except for a decline in June which probably prevented the weighted prevalence at site 8 from showing a significant relationship with water temperature in the regression analysis, although the general trend of R^2 values suggested that the weighted prevalence at this site had a similar pattern as that at site 18 (Fig. 2.7). Interestingly, a sudden decline of QPX prevalence was also observed in June, 2005 (Fig.1) based on histological results. The lower prevalence in June was associated with the absence of rare and light infections and seems unlikely to have been caused by mortality from developing QPX disease (the observed mortality in June was not higher than that in other months), or by quick healing combined with lack of transmission, given the existence of rare infections in the previous and following clam sample groups. Instead, the June data seems more likely a result of sampling error. Site 8 also had relatively fewer clams with rare QPX loads compared to site 18. However, the information from this study was not sufficient to determine if the difference was related to a lower infection acquisition rate or more rapid disease progression at this site.

Clams had a different temporal pattern of QPX disease at site 21 in Raritan Bay. In 2006, unusually (compared to the other sites) high QPX prevalence and infection intensity determined by histology and qPCR were observed in April at this site. In 2005, histological method also detected maximal QPX prevalence in April and 0% prevalence in August (Fig. 1). The relationship between weighted prevalence in 2006 and temperature was also different at site 21 as compared to site 18, with the best correspondence found with a 105 day lag by regression analysis (Table 2.2) or 120 day lag by correlation (Fig. 2.7). It is unclear what might cause two different seasonal patterns in the three sampling sites which were basically experiencing the same environmental conditions. The only factor that displays a major difference between sites 8 and 18 compared to site 21 is clam density, which was estimated as high as 90 clams m^{-2} at site 21 but less than 30 clams m^{-2} at the other two sites (Table 2.1). At site 21, infection acquisition and progression may start earlier because the higher clam density increases the chances of QPX spreading from one clam to another. The greater prevalence and weighted prevalence at site 21 in April may reflect the result of QPX progression under lower temperatures. Stresses associated with high clam density may also result in more rapid disease progression. Positive correlations between clam density and QPX prevalence have been reported in wild (Allam and Pawagi, 2004) and cultured (Ford *et al.*, 2002) clam populations. The analysis in Lyons *et al.* (2007) also supported the previous observations that clam density could be important in the transmission of QPX pathogen once it is established in a clam bed. The more heavily infected clams (light and moderate) found in April samples may have been over-winter survivors which maintained rare or light infections acquired during the previous year. Perrigault *et al.* (2010) found that *in vitro* cultured QPX was able to survive at 3 °C up to a week, suggesting that QPX probably could overcome short periods of cold temperature in winter. When water temperature increases in spring, parasites in these stressed clams may quickly proliferate, causing a more severe infection. Because this study did not encompass the late winter/early spring months, it is not possible from the available information to differentiate between these two possibilities, and both may contribute to the infection pattern observed at site 21. For instance, if lower temperature

favors disease transmission by facilitating parasite acquisition in the hosts, it may also promote disease development in those infected clams surviving from the previous year.

Clam density may also be an important factor that contributes to the difference in QPX infection pattern between wild clams and aquaculture clam stocks deployed in natural environments. Ragone Calvo *et al*. (2007) investigated QPX disease in five clam stocks (MA, NJ, VA, SC and FL) deployed at a density of 538 clams m^{-2} at two QPX enzootic sites, in New Jersey and Virginia. These densities were similar to those used by commercial operations, but were 6-20 times higher than the natural clam densities at three Raritan Bay sites in our study. In their 2.5 year study, no seasonal pattern in QPX prevalence and infection intensity determined by histology was found. Rather, the prevalence and intensity in the susceptible clams showed a generally increasing trend over time. At both sites, the most severe infections were observed in clams from the FL and SC stocks. This study did not include any clam strains from New York. In a recent field experiment, Dahl *et al*. (2010) compared the performance of a FL clam stock and two New York local clam seeds deployed in grow-up cages at a density of 1000 clams m^{-2} in the QPX enzootic Raritan Bay area. Similar to the Ragone Calvo *et al*. (2007) study, the southern clam stock (FL clams) showed higher susceptibility toward QPX compared to the two New York strains: FL clams acquired new infections during the first summer of deployment and exhibited increased prevalence and QPX loads in the second summer up through autumn. In contrast, QPX was not observed in the cultured New York *notata* strain until the second summer, when prevalence remained minimal, while the first generation New York "wild type" strain did not acquire QPX at all during the 16 months of study. These studies were in agreement with laboratory transmission experiments (Dahl *et al*. 2008), supporting that host genetic origin is an important determinant in susceptibility to QPX disease, and may influence disease dynamics in the field.

In this study, clam mortality was also estimated during sample collection. In 2006, this estimated mortality data was not correlated with QPX prevalence or weighted prevalence at any site in the Spearman Rank correlation test. Moreover, there was no significant correlation between mortality and any environmental parameter, including temperature, dissolved oxygen or even lagged water temperature (data not shown). Previous field investigations in the Raritan Bay area (Allam, unpublished data) reported that clam deaths caused by QPX were typically highest in summer. However, the estimated clam mortality in this study in August was actually lower than spring or early summer at two sampling sites, 8 and 21, and the estimated clam mortality in September was the lowest (0-1.5%) at all three sites (Table 2.3). The result that relatively higher prevalence and weighted prevalence were not necessarily accompanied or followed by higher mortality, may reflect in part the difficulty in field estimation of hard clam mortality: moribund hard clams tend to rise to the sediment surface, but the time required for this process is hard to estimate, and may be seasonal; also, the fragile shells of some small dead clams may disintegrate quickly and be lost from mortality counts by the time of sampling. Significant mortalities from epizootics of QPX disease have been observed in hard clam aquaculture plantings in parts of Atlantic Canada, Massachusetts, New Jersey and Virginia (Smolowitz *et al.*, 1998; Ragone Calvo *et al.*, 1998; Ragone Calvo *et al.*, 2007; Lyons *et al.*, 2007), however few studies have sampled QPX-infected wild clam populations frequently enough to demonstrate a relationship between prevalence and disease-associated mortality.

Besides the three sampling sites that are enzootic for QPX disease, one site in the Raritan Bay area that is particularly interesting is site 20. It is located in Great Kill Harbor in

Staten Island and has a very high clam density (~370 clams m^{-2}), but no QPX disease has yet been found there. In this study, when qPCR was applied on clam samples from site 20 collected in May and August, the results still showed 0% prevalence, consistent with histological results. In three other groups of samples (April, June and September), the histological method did not detect any QPX infection either. It is likely that this site is still free of QPX disease. During the sampling in 2006, water temperature at site 20 was always higher, and dissolved oxygen concentration was always lower, compared to other sampling sites in Raritan Bay (Fig. 2.2). These environmental parameters, together with a very high clam density, do not make a less stressful environment for clams. The factors that impede transmission of QPX or strengthen the resistances of clams at this site are worth further study.

It is impossible, from the available data in this study, to determine the general pattern of QPX infection in the Raritan Bay clam population. Few studies have seasonally surveyed QPX-infected clam populations to adequately characterize the infection pattern in other wild clam populations. To date, it seems that the pattern of QPX infection varies from situation to situation. Further experiments focusing on the environmental factors or other factors such as clam density will be important to differentiate the effects of different factors on the transmission and development of QPX disease in clams. More detailed data on prevalence and infection intensity along with mortality from Raritan Bay clams is needed to assess and address the seasonality of QPX disease in this region.
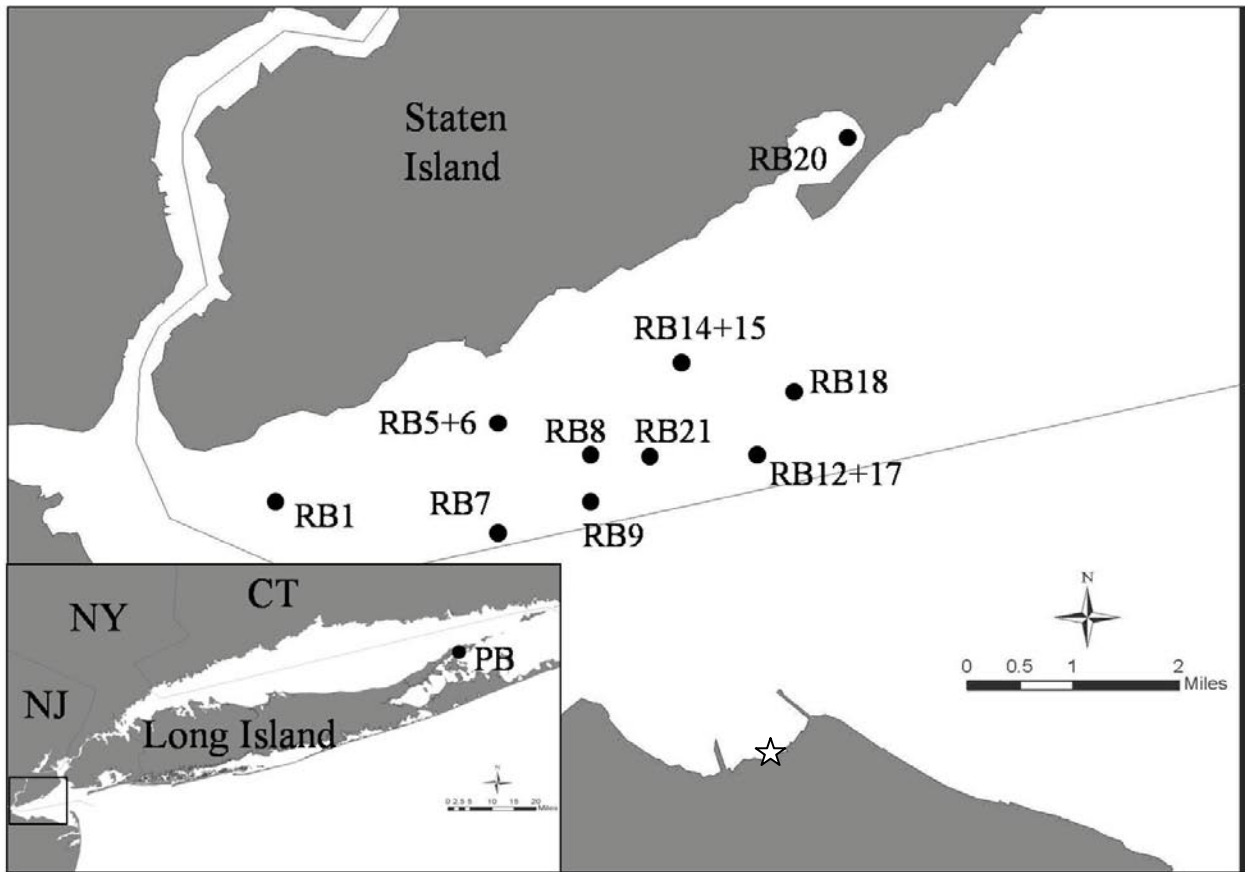
Figure 2. 1. Locations of the Hashamomuck Pond (Peconic Bay, PB) and Raritan Bay (RB) sampling sites at the east end of Long Island and south of Staten Island (NY), respectively. Sites as RB 5+6, RB 12+17 and RB 14+15 represent sampling sites at the intersection between two areas. The star indicates the location of USGS weather station at Keansburg, New Jersey, where the annual water temperature (Fig.2.2) was measured.
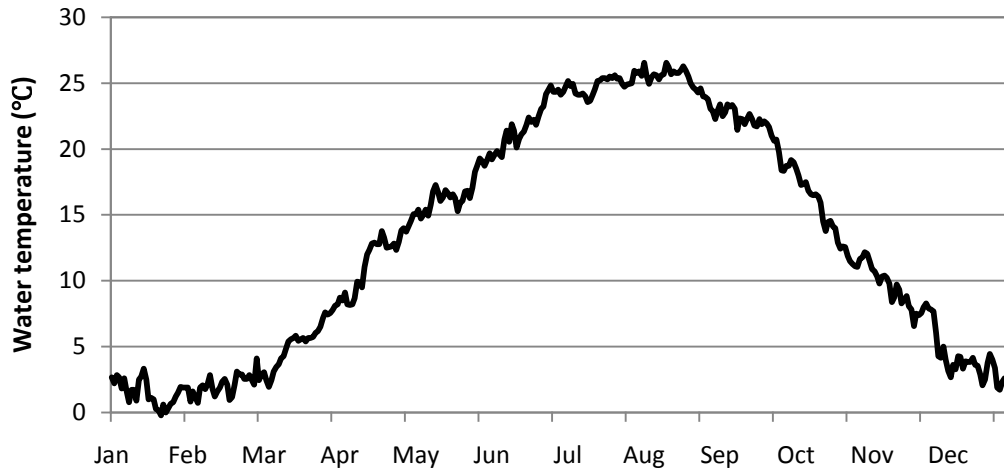
Figure 2. 2. Daily mean water temperature (calculated from period 2000-10-01 to 2006-09-30) recorded at USGS weather station 01407081 in Raritan Bay at Keansburg, New Jersey.
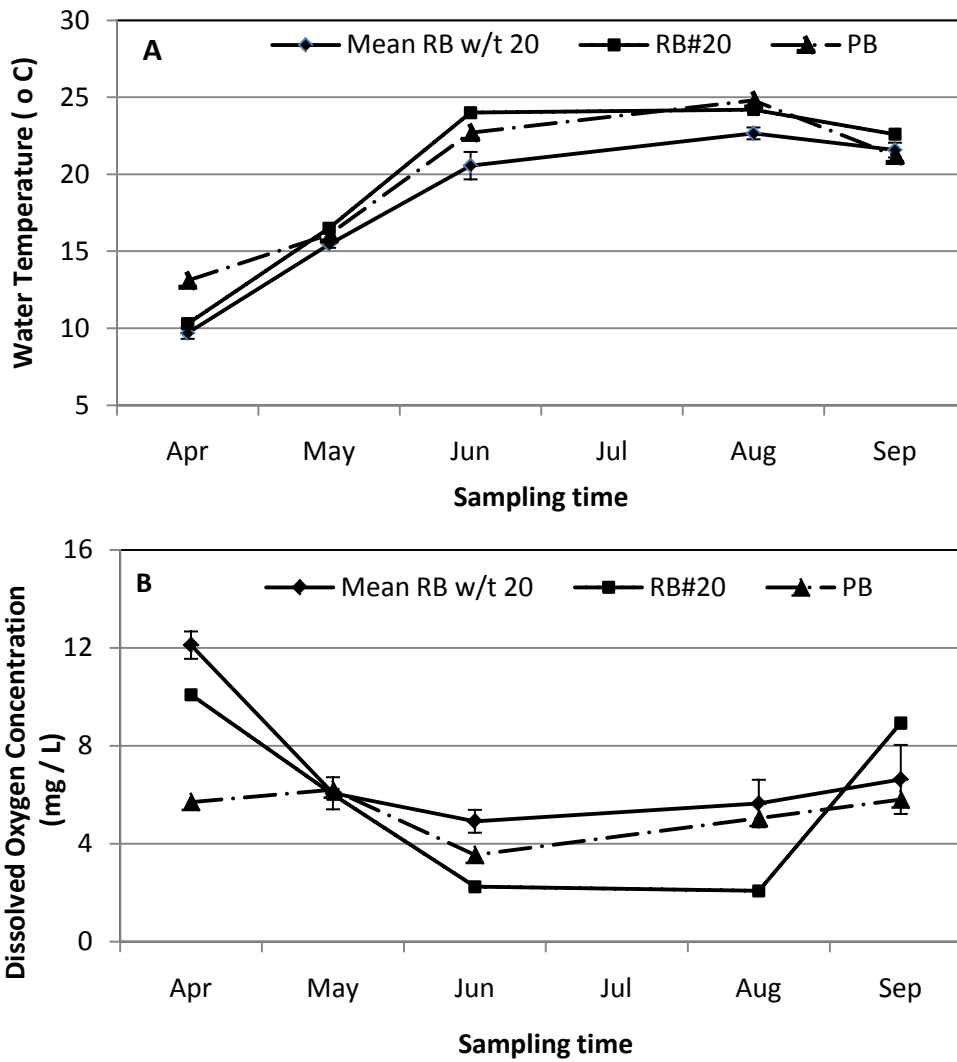
Figure 2. 3. (A) Temperature and (B) dissolved oxygen concentration of bottom water at sampling sites in Raritan Bay and Peconic Bay in 2006. "Mean RB without site 20" indicates the average of all available values of temperature or dissolved oxygen concentration in Raritan Bay sampling sites except site 20.

Table 2. 1. QPX abundance in sediment samples estimated using qPCR assay, and characteristics of sampling sites in Raritan Bay (RB) and Peconic Bay (PB), New York, in 2006

Sampling site	QPX abundance (ITS copies per reaction/ cells mg^{-1})					Clam density (clams/m^2)	Historical QPX prevalence (%)	Bottom type
	April	May	June	August	September			
RB 1	0[b]/0[c]	0/0	0/0	0/0	0/0	10 ± 6[d]	0.4 ± 1.2[e]	sandy
RB 5+6[a]	0/0	0/0	0/0	0/0	0/0	12 ± 6	1.4 ± 1.8	sand/mud/shell
RB 7	0/0	0/0	-	0/0	-	14 ± 7	7.4 ± 6.9	mud/hash
RB 8	0/0	23/34	0/0	0/0	0/0	30 ± 14	9.2 ± 6.6	mud/shell
RB 9	-[f]	-	-	0/0	-	18.7	-	mud/shell
RB 12+17[a]	0/0	-	-	0/0	337/215	33 ± 11	4.5 ± 5.3	mud
RB 14+15[a]	-	-	-	-	-	26.5	-	sand/mud
RB 18	0/0	474/169	0/0	0/0	0/0	14 ± 4	4.2 ± 4.4	mud/shell
RB 20	0/0	0/0	0/0	0/0	0/0	369 ± 152	0	mud
RB 21	0/0	0/0	0/0	0/0	84/52	93 ± 21	6.7 ± 7.1	mud/shell
PB	0/0	0/0	0/0	0/0	0/0	-	0	mud

[a] A sampling site at the intersection between two areas.

[b] QPX ITS copies per reaction; 0 indicates below the detection limit of 10 copies.

[c] QPX cells mg^{-1} sediment calculated by equation 7 where a=10, b=150 µl, c=181 copies per cell, d=5.38% and e varied among samples from 500 to 850 mg. 0 indicates below the detection limit of 5.6 ± 2.1 cells mg^{-1} sediment.

[d] Average estimated density (Mean ± STD) over all sampling dates in 2006. Clam density was estimated as (# clams $_{live}$ + #clam $_{newly\ dead}$)/# grab.

[e] Averaged histological QPX prevalence (Mean ± STD) over all samplings from 2002 to 2006; data from Allam and Pawagi (2006).

[f] No data available
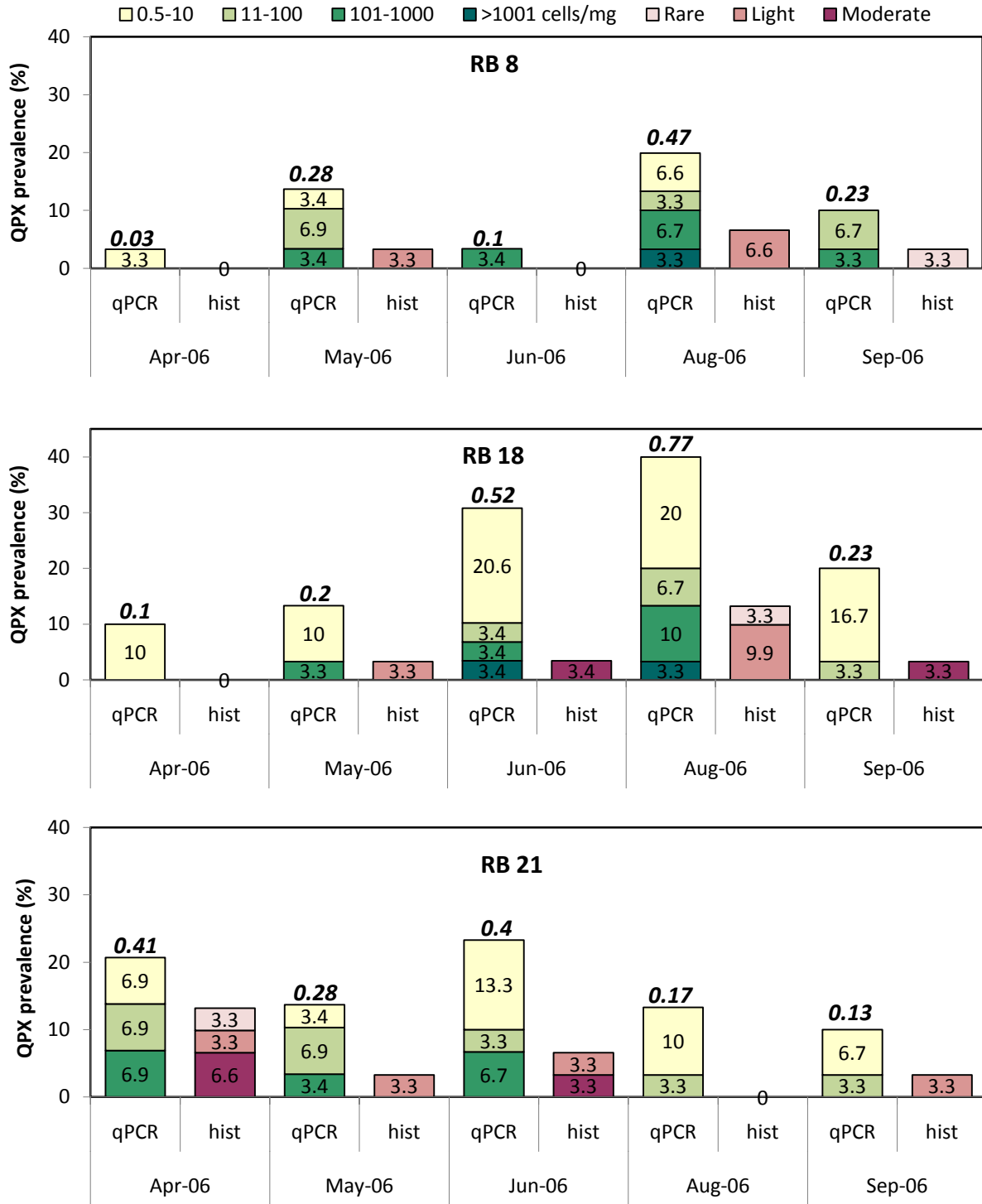
Figure 2. 4. QPX prevalence at site 8, 18 and 21 in Raritan Bay in 2006. Numbers in stacked columns represent the percentage of clams with different infection intensity determined by qPCR assay or histological method. The total prevalence determined by each method is the sum of all numbers in the column. The number on the top of each qPCR column indicates the weighted prevalence.
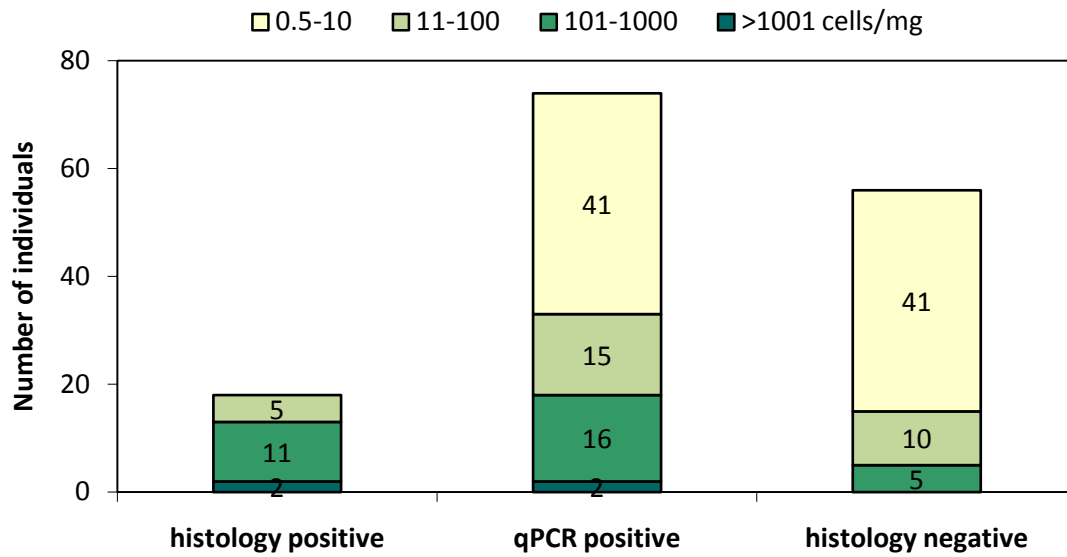
Figure 2. 5. Number of clams with each level of QPX loads determined by qPCR assay. Each number in the stacked column indicates the number of infected clams with a certain level of QPX load. "Histology positive" includes the 18 clams diagnosed as QPX positive by both histological and qPCR methods. "Histology negative" includes the 56 clams diagnosed as QPX negative by histology, but as QPX positive by qPCR. "qPCR positive" includes all 74 QPX positive clams diagnosed by qPCR.
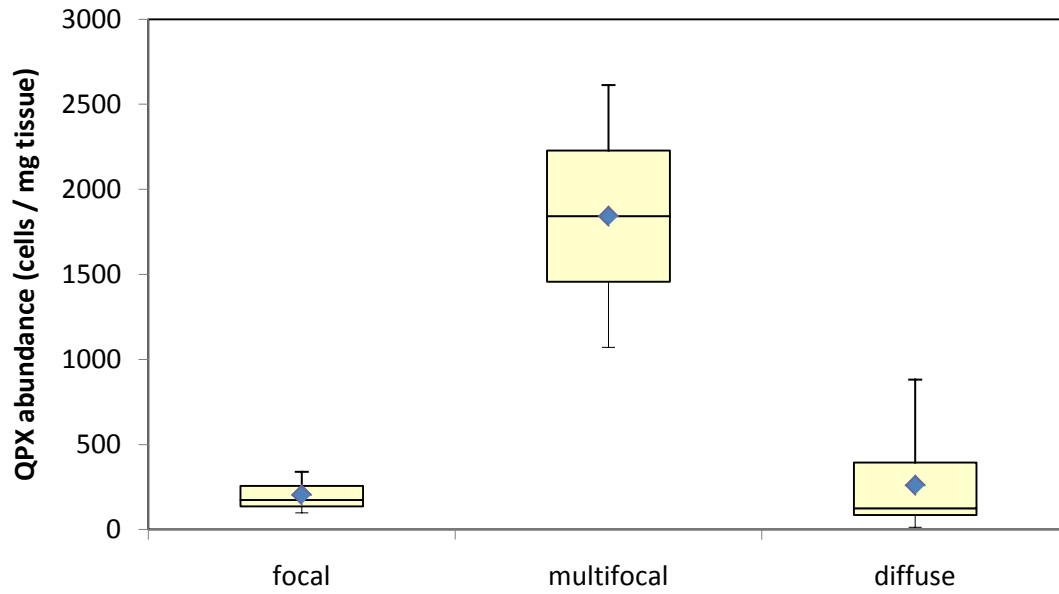
Figure 2. 6. QPX abundance determined by qPCR in clams with different localization of infection in histological examination: focal infection (N=3), multifocal infection (N=2) and diffuse infection (N=13).

Table 2. 2. Regression analysis of QPX weighted prevalence (determined by qPCR) and environmental variables in Raritan Bay (RB) in 2006

Time Lag (Days)	Independent variable	RB 8		RB 18		RB 21	
		R^2	P-value	R^2	P-value	R^2	P-value
	Temperature[a]		0.193	**0.888** [b]	**0.016**		0.399
0	Dissolved oxygen		0.129		0.143		0.649
	Mortality		0.844		0.909	0.667	0.091
-15	Temperature		0.129	0.768	0.051		0.206
-30	Temperature		0.135		0.158	0.655	0.097
-45	Temperature		0.199		0.210	0.691	0.081
-60	Temperature		0.256		0.254	0.695	0.079
-75	Temperature		0.339		0.365	0.659	0.095
-90	Temperature		0.273		0.384	**0.805**	**0.039**
-105	Temperature		0.368		0.572	**0.811**	**0.037**
-120	Temperature		0.521		0.82	0.648	0.1

[a] Temperature used is daily mean value for each day for the previous 6 years (calculated from 10/01/2000to 09/30/2006) measured at USGS 01407081 Raritan Bay weather station at Keansburg NJ (Fig.2.2). Time lag indicates the relationship between QPX weighted prevalence and average temperature 15 to 120 days earlier.

[b] Coefficients of determination were only presented for linear regression results with p<0.1, and in bold only for significant linear regression (p<0.05)
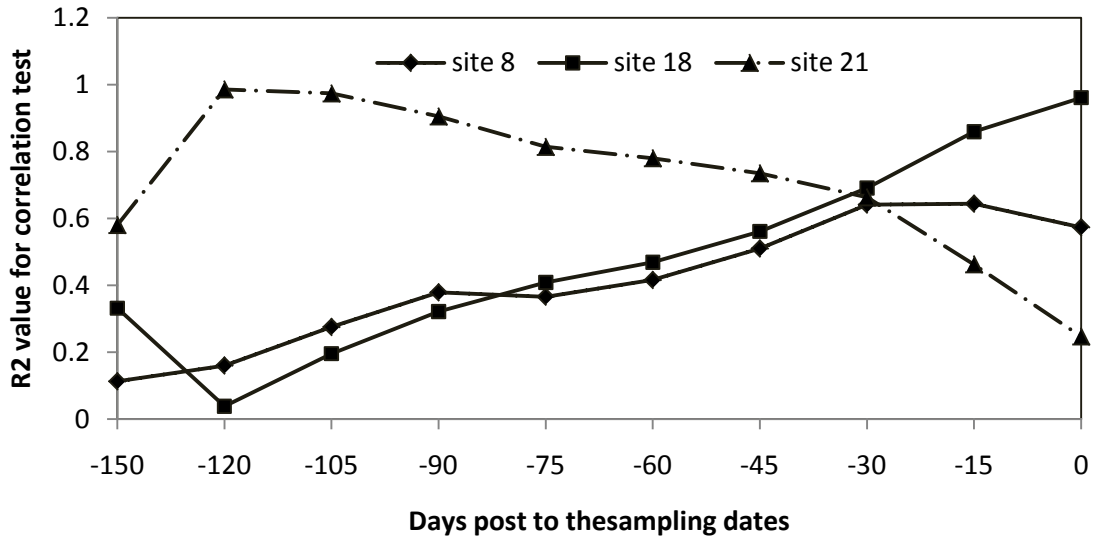
Figure 2. 7. R^2 values for correlation between daily water temperature and QPX weighted prevalence determined by qPCR assay at three sampling locations in Raritan Bay

Table 2. 3. Estimated clam mortality in three sites in Raritan Bay (RB) in 2006

Sampling site	Clam mortality (%)				
	April	May	June	August	September
RB 8	6	11.3	10.3	9.8	1.5
RB 18	4.9	2.4	0	10	0
RB 21	23.3	13.2	10.2	9.2	1.1

Chapter 3: Effect of temperature on QPX dynamics in clams

Introduction

In the field study described in Chapter 2, a seasonal pattern of QPX prevalence and weighted prevalence determined by qPCR was demonstrated in two of three Raritan Bay sites studied: QPX infection was relatively low in spring, increased through late spring/early summer, and peaked in summer before declining in early fall. This pattern generally agrees with the results of the monitoring program in Raritan Bay from 2002 to 2005 based on the histological diagnostic method. In temperate coastal environments such as Raritan Bay, temperature is a major environmental factor that shows strong seasonality. Since a hard clam is a poikilothermic organism whose internal temperature varies along with the ambient temperature, temperature may affect the prevalence and severity of QPX infection through a direct impact on the parasite itself, on the host or on the balance of the host-pathogen interaction that favors the parasite (or the host) leading to disease (or parasite elimination).

Hard clams tolerate a wide range of temperatures. Ansell (1968), in a review of hard clam growth and activity throughout its geographic distribution, concluded that the optimum temperature range for shell growth was 15-25 °C. Below 6 °C, hard clams cease pumping (Ansell, 1964). Temperatures outside a range of 9 °C to 31 °C also cause cessation of growth of juveniles and adults and detrimental effects on eggs and larvae (Ansell, 1968; Bardach *et al.*, 1972). It has been documented that temperature strongly influences the immune system of marine mollusks and their ability to resist infectious diseases (Paillard *et al.*, 2004; Travers *et al.*, 2009). Audemard *et al.* (2006) also demonstrated a significant correlation between the weighted prevalence of *Perkinsus marinus* in the eastern oyster *Crassostrea virginica* and the water temperature. On the other hand, the effect of temperature on QPX growth *in vitro* was investigated using QPX isolates from different geographical locations by Perrigault *et al.* (2010). Their study showed an optimal proliferation of *in vitro* cultured QPX between 20 and 23 °C (depending on isolate), and temperatures below or above these optima reduced the proliferation of QPX to about 6 % and 9 % at 3 °C and 32 °C, respectively. Although there is some data regarding the impact of temperature on hard clams and on QPX growth *in vitro*, little is known about the effect of the same factor on the clam host-QPX pathogen interaction. Dahl and Allam (2007) reported a transmission trial using cohabited QPX infected adult clams, collected from the field, with naïve seed clams maintained at room temperature (21 °C). No susceptible clams obtained detectable QPX infection by the end of the cohabitation trial. Moreover, the post-trial histological analysis showed a significant amount of dead and degrading QPX cells in the tissue of those presumptively infected adult clams, suggesting that laboratory conditions, including room temperature, may favor the resistance of the clams to QPX and promote healing of the previously infected hosts even though the temperature is optimal for QPX growth. In this study, based on the recent information described above, laboratory experiments under controlled conditions were conducted to investigate the effect of temperature on QPX dynamics in experimentally and naturally infected clams.

Materials and methods

Clams

Naïve seed clams were acquired from a commercial hatchery in Florida. They were originally free of QPX, and used for the challenge experiments. The naturally infected clams used in this study were collected from Cape Cod, Massachusetts, where clams have been experiencing severe QPX disease since 1995. After clams arrived at the lab, they were randomly distributed in recirculating tanks filled with filtered seawater and allowed to acclimate at different temperatures corresponding to the treatments (27 °C, 21 °C and 13 °C).

QPX

FL clams were experimentally exposed to QPX by injecting *in vitro* cultured QPX cells into the pericardial cavity as previously described (Dahl and Allam, 2007). An exponentially growing culture of New York isolate NY0313808BC7, which was initially isolated from an infected clam collected from Raritan Bay, NY in 2003, was maintained in clam muscle homogenate medium according to methods described by Perrigault *et al*. (2009).

QPX clearance experiment

A total of 78 FL clams were individually inoculated with 100 μl of QPX at a concentration of 3.9×10^6 cells ml^{-1}, and subdivided into 2 replicate groups (39 clams per group) in separate 35 liter tanks. A total of 120 FL clams were injected with 100 μl sterile culture medium, and subdivided into 6 replicate tanks. The QPX-challenged clams and medium-injected control clams were incubated at room temperature (21 °C) and 30 psu. Seawater was filtered using biological filter cartridges containing activated carbon and was continuously oxygenated to saturation. Clams were fed with a ration of commercial algae concentrate (DT's Live Marine Phytoplankton, Sycamore, IL) on a daily basis (10^7 algae cells clam^{-1} day^{-1}). Clam mortality was monitored daily.

QPX-challenged clams were sampled at Day 3, Day 7 (Week 1), Month 1, Month 2, Month 3 and Month 4 following the initial challenge. After the sampling at Month 4, the remaining clams were combined and maintained in one tank until the final sampling at Month 12. At each sampling date (except the final sampling), 10 clams (5 from each replicate) were collected and immediately processed for qPCR assay. The entire mantle and siphon tissue was taken, briefly drained on a clean paper towel, and mechanically homogenized in 20 volumes of PBS based on its weight (e.g. 0.1 g tissue in 2 ml PBS). The tools were sterilized by flame between samples to avoid cross contamination. 2 ml aliquot of homogenate of each clam, containing 100 mg clam tissue, was used for further DNA extraction. Control clams were sampled at Month 2 and Month 4 (10 clams per sampling date and 5 from each replicate) following the initial injection. After the sampling at Month 4, the remaining control clams were combined into two replicate tanks until the final sampling at Month 9. The mantle and siphon tissue for all control clams were taken and preserved as the rest of the experimental and control clams in the temperature experiments described below.

Effect of temperature on experimentally and naturally infected clams

For the high (27 °C), room (21 °C) and low (13 °C) temperature treatments, 40 pre-acclimated FL clams were separately injected with 100 μl of QPX at a concentration of 5×10^5 cells ml^{-1}, and subdivided into 2 replicate groups of experimentally QPX-challenged clams (20 clams per group). 40 FL clams (per treatment) were also injected with 100 μl sterile culture medium and maintained in 2 replicate tanks as controls. Similarly, 40 presumably infected MA clams were submitted to each of the 3 temperature treatments in two replicate tanks (20 clams per tank). Other than the experimental temperature treatment,

all clams were kept under the standard laboratory conditions (30 psu, water filtration and oxygen saturation, and daily feeding). Mortality was monitored twice a day and dead and moribund clams were removed.

Experimentally-challenged and control FL clams and presumably infected MA clams were sampled 2 and 4 months after the beginning of the experiment. At each sampling date, 10 clams (5 from each replicate) were collected and immediately dissected. The mantle and siphon tissue were taken and preserved at -80 °C. On the day of DNA extraction, the tissues were homogenized in 20 volumes of PBS based on tissue weight. A 2-ml aliquot of homogenate from each clam, containing 100 mg clam tissue, was used for DNA extraction.

DNA extraction and qPCR assay

For qPCR assay, DNA was extracted and purified from clam tissue following the protocol described above (Chapter 1) and 1 µl DNA was used as template in qPCR assay. In the experiments described in this chapter, the original abundance of QPX cells in each clam sample was determined as follows (see Chapter 1 for details): $(\#QPX_{initial} \times a \times b)/(c \times e)$ where $\#QPX_{initial}$ is the number of QPX ITS copies in the 1 µl assayed clam DNA template (copy µl^{-1}) after correction for PCR inhibition; a typically equals to 1 or 10; b equals to 300 µl; c equals to 181 copy cell^{-1}; and e equals to 100 mg. Because no estimation of QPX DNA recovery rate associated with the extraction protocol for either fresh tissue (in the QPX clearance experiment) or freshly frozen preserved tissue (in the temperature experiments) was available, the estimates of QPX abundance in clam tissue obtained in these experiments did not account for DNA recovery rate (the value was 16.31% for clam tissue in Chapter 2 and 4). This change would not affect the comparison of QPX prevalence and weighted prevalence within or among different treatments within the same experiment, because all clam samples in those experiments were processed the same way, thus were assumed to have the same DNA recovery rate.

Prevalence and weighted prevalence

QPX prevalence in each group of clams was determined as described in Chapter 2. Based on the estimated number of QPX cells in each milligram mantle tissue, the QPX load was ranked as rare (detection limit to 1), light (1-10), moderate (10-100), heavy (101-1000) and very heavy (>1001). The typical detection limit of qPCR assay was estimated to be 0.1 cell mg^{-1} tissue based on all assayed clam samples described in this chapter. Weighted prevalence in each group was calculated as described in Chapter 2, except the very heavy category was counted as rate 5 in the calculation.

Statistical analysis

In the QPX clearance experiment, due to the small number of QPX challenged clams and multiple times of sampling, only 5 clams were taken from each of the two replicate tanks at each sampling. Because the clams from replicate tanks were combined into the same tank after the sampling at Month 4, clam mortality and QPX prevalence data are reported by pooling all clams, regardless of replicate. Kaplan-Meier survival analysis was used to compare the cumulative mortality (survival) distribution function of experimental versus control clams and of clams in the different temperature treatments. Mortality data, consisting of time of death (i.e. day of experiment) for individual clams and censored data, reflecting the removal of clams at a set of time points for qPCR assay, were included in the test. A student's t-test (unpaired, two tailed and assuming unequal population variance) was used to compare the QPX loads between two independent sample groups. A one-way analysis of variance (ANOVA) was used to compare the QPX loads obtained from different treatments

at the same sampling time in the temperature experiment. Control clams injected with sterile culture medium were not assayed by qPCR for QPX diagnosis because there was no evidence that QPX infection ever occurred, based on a limited number of control clams (N=6) sampled at Day 3 post-challenge which were all QPX-negative by qPCR.

Results

Mortality and parasite load in clams after experimental QPX injection

Kaplan Meier survival analysis showed that the cumulative mortality of the FL clams challenged with QPX was significantly higher than that of the control clams (Log-Rank test, p<0.05, Fig.3.1). All deaths of QPX-challenged clams occurred between the third and sixth month following the initial injection, while the deaths of control clams were observed either within the first two months or after the sixth month.

During the first week following the challenge by injection with QPX, QPX prevalence was 100% and weighted prevalence was approximately 3 (Table 3.1). Most clams (70% to 80%) had moderate QPX loads (Fig 3.2). In the clam samples collected after 1 month, total prevalence remained 100%, but weighted prevalence decreased significantly compared to Week 1 (Table 3.1, p=0.016). Clams with heavy QPX loads became absent and the proportion of clams with moderate QPX loads decreased while light QPX loads increased. Clams collected after 2 months and 3 months showed no significant change in prevalence or weighted prevalence (Table 3.1, p>0.05), but showed a more even distribution among the QPX load categories. After 4 months, QPX prevalence dropped to 60%, with only moderate and rare QPX loads detected, although the difference in QPX loads was not statistically significant (Table 3.1, p=0.103) between Month 4 and Month 3 samples. No QPX was detected in any clam in the final (Month 12) samples. Although the 13.9% mortality observed between Months 3 and 6 (Figure 3.1) could have impacted both the prevalence and QPX load distribution data, it cannot account for the disappearance of QPX from all experimental clams. Overall, the data suggested that QPX was cleared from these clams sometime between 90 and 360 days after exposure.

Effect of temperature on mortality and QPX load in naturally and experimentally infected clams

Minor mortality occurred in experimentally infected and control FL clams for all three temperature treatments (13 °C, 21 °C and 27 °C) during 4 months of incubation: no mortality occurred in QPX-challenged clams, and only one control clam of the 27 °C treatment died during the experiment (Dahl *et al.* unpublished data). Since all experimentally infected clams in the three temperature treatments were injected with the same strain of QPX at the same time by the same person, they presumably had the same initial prevalence (100%) and weighted prevalence. After two months, 70% of challenged clams in the 13 °C treatment had detectable QPX loads, as did 90% at 21 °C and 60% at 27 °C (Fig.3.3). Clams in the high temperature treatment (27 °C) appeared to have lower weighted prevalence (1.1) than those in the 21 °C and 13 °C treatments (1.7-1.8), although the difference was not statistically significant (Table 3.2a; ANOVA, p>0.05). During the next two months, temperature showed a distinct effect on QPX prevalence and parasite loads in the challenged clams. At 13 °C, QPX was detectable in more clams (90%) than it had been at two months, and weighted prevalence increased from 1.8 to 2.2, suggesting QPX abundance in the clams had slightly increased although the change was not statistically significant (Table 3.2a, p>0.05). In contrast, there was a 70% decrease in QPX prevalence in challenged clams at 21 °C and a 30% decrease at 27 °C. QPX loads declined significantly in these two groups (Table 3.2a, p<0.05),

and QPX-positive clams in these two treatments had only rare or light QPX loads (Fig.3.3). Therefore, by Month 4, clams held at 13 °C exhibited a significantly higher weighted prevalence compared to those incubated at 21 °C or 27 °C (ANOVA, p<0.001), suggesting a substantial impact of temperature on QPX persistence or clearance in challenged clams.

For naturally infected MA clams, the clams incubated at 13 °C exhibited a significantly greater cumulative mortality compared to the clams incubated at 21 °C and 27 °C (Log-Rank test, p<0.05, pairwise, Fig. 3.4A). There was no significant difference between the mortalities of clams in the 21 °C and 27 °C groups. All deaths in the 21 °C and 27 °C treatments (2 and 3, respectively) and most of the deaths (8 of 10) in the 13 °C treatment occurred before the first sampling at Month 2 (74th day). The initial MA samples, assayed about a week before temperature treatments began, had a high QPX prevalence (63.3%, N=30) and about half of the QPX-positive clams (33%) had very high parasite loads (>1001 QPX cells mg^{-1} tissue) (Fig. 3.4B). After two months, clams in all three temperature treatments displayed lower QPX prevalence and significantly or almost significantly decreased QPX loads (Table 3.2b, Student's t-test, p≤0.05). Clams kept at 13 °C had the highest prevalence and weighted prevalence, although the difference was not statistically significant (Table 3.2b, ANOVA, p>0.05). After 4 months, a further decline in prevalence and weighted prevalence was only observed in the 21 °C treatment (Table 3.2b).

Discussion

QPX clearance from challenged clams under standard laboratory conditions

Experimental transmission of QPX was performed by injecting *in vitro* cultured QPX cells into the pericardial cavity of naïve FL clams. This technique, directly delivering a large abundance of log-phase parasites to the host's circulatory system, is the only effective method known to induce high QPX prevalence over a matter of a few months (Dahl and Allam, 2007) under laboratory conditions. All experimentally infected clams in this study were challenged by the same *in vitro* cultured NY QPX isolate (NY0313808BC8), which has been demonstrated by Dahl *et al.* (2008) to have a relatively high virulence and successfully induced relatively high QPX disease-associated mortality in clams originating from Florida compared to the other QPX isolates they used.

A preliminary experiment was conducted to evaluate the persistence of QPX cells in experimentally infected clams incubated under the standard laboratory conditions of 21 °C, 30 psu and oxygen saturation. QPX prevalence remained at effectively 100% for the first three months after injection, then began to decline, reaching zero sometime between 4 and 12 months (Fig.3.2). Immediately after injection (Day 3 to Week 1), a moderate QPX load (11 to 100 cells/mg tissue) was detected in most clams. This is comparable to the theoretical QPX load, which was estimated to be 40 to 80 cells per milligram tissue, assuming 10% -20% DNA recovery rate for the 3.9×10^5 QPX cells injected into each clam and 1 gram as the typical tissue weight at the time of injection. The QPX cells detected in the challenged clams during this period reflected the newly injected parasites, many of which were probably not representing in an established infection, but simply adhering to the tissues or trapped in the circulatory system.

The average QPX loads were generally lighter after 4 weeks, suggesting many of the injected parasites were actively eliminated, probably by the defense response of the host or simply because they could not survive in the new environment. Clam mortality occurring during the early phase of the post-challenge period (0-2 months) was possibly associated with wounding during the injection procedure, such as the mortality of control clams

(Fig.3.1). However, since no QPX-challenged clam died during this period although the QPX loads in clams were relatively high, the observed mortality later in the experiment (Month 3 to 5) probably was not directly caused by tissue trauma. Through the third month after injection, the QPX loads did not change significantly, but clam mortality began to occur, and may have removed some infected clams from the population. During the fourth month both prevalence and weighted prevalence declined significantly. The QPX abundance in most clams became lower, even below the detectable level in some individuals, suggesting that the host effectively eliminated the parasites. Some mortality occurred during months 3 and 4, but even if the clams that died had the heaviest QPX loads, the mortality was not enough to account for the decrease in weighted prevalence. After 12 months, no clams showed any detectable QPX, suggesting that the long-term clearance process continued and that QPX was likely eliminated from the clams.

Clam mortality can be affected by many factors other than QPX disease, such as physical insult from the injection or husbandry practices. A Kaplan Meier survival analysis showed significantly higher cumulative mortality in QPX-challenged clams compared to control clams injected with sterile medium over 9 months (Fig. 3.1). The difference in the mortality of experimental and control clams, especially most deaths of QPX-challenged clams (5 of 6 deaths) during the period of Month 2 to 4 following challenge, may reflect death of clams from the development of QPX infection, or at least the contribution of the infection as a stressor that could affect the ability of the host to survive under our laboratory conditions. In this trial, most mortality was likely associated with the development of QPX infection, even if QPX might not be the sole lethal factor. At the same time, external environmental factors may also affect the outcome (mortality or survival rate) of the interactions between a host and its pathogen, through a direct impact on the virulence of the parasite, or on the immune factors of the host or on both. The standard laboratory conditions (room temperature, 30 psu and oxygen saturation) used in this study seemed to make a favorable environment for the host, because all sampled challenged clams were able to eliminate the pathogen and heal by the end of one-year incubation.

The effect of temperature on the clam/QPX interaction

Temperature had a prominent effect on the interaction between clams and QPX. Both experimentally and naturally infected clams kept at 13 °C systematically showed higher prevalence and QPX loads compared to those at 21 °C and 27 °C after 2 or 4 months incubation (Fig 3.3 and 3.4B). Between Month 2 and Month 4, QPX prevalence and weighted prevalence in experimental clams at 13 °C did not change much, in contrast to the evident recovery process in clams at 21 °C and 27 °C. In the naturally infected MA clams, 10 of 30 clams in the 13 °C treatment died, while only 2 or 3 clams died in the other two treatment groups. These mortalities were likely among clams with heavy and very heavy parasite loads, which accounted for half of the initial clam sample. Even though the significantly higher mortality at 13 °C might have removed the most heavily infected clams from this sample, the remaining clams at 13 °C still showed the highest QPX prevalence and weighted prevalence throughout the experiment, while the clams at 21 °C and 27 °C were experiencing a healing process. These results suggested that a low temperature environment might be more advantageous for QPX in the host-pathogen interaction, while higher temperature favors the clams and facilitates the clearance of QPX from infected clams.

It is noteworthy that the mortality and parasite loads in the QPX-challenged clams might be affected by the amount of parasites initially injected into the host's tissue. When more

cells are injected, there is a better chance for parasites to overwhelm and successfully survive the host's cellular and humoral defense mechanisms. For example, clams in the preliminary clearance experiment displayed a slower recovery process and about 15 % higher cumulative mortality (or 85% survival distribution function) during the 4-month incubation (Fig. 3.1) than clams in the 21 °C treatment in the temperature experiment; all of these clams were held under the same laboratory conditions, but those in the first experiment were injected with approximate 8 fold more parasite cells.

The results of these laboratory-controlled temperature experiments could help interpret the seasonal pattern in QPX infection observed in our field study of Raritan Bay clams described in Chapter 2 (Fig. 2. 4). During spring and early summer (April to June) when water temperature was ≤ 20 °C (Fig. 2.3), increases in QPX prevalence and weighted prevalence were evident. Although it is unknown how a relatively low temperature (≤ 20 °C) would affect the QPX acquisition process, the gradual progression of QPX infection during this period was likely to be associated with lower temperature, probably resulting from the positive impact of a colder environment on QPX to proliferate in clams. At site 18 and 8, QPX prevalence and weighted prevalence reached maxima in August, and started to decline in early fall (September) when temperature was high (>22 °C). At site 21, the decline started in June when temperature became higher than 20 °C. A warmer temperature seemed to promote clam healing in many infected clams and contribute to the decrease in QPX prevalence and weighted prevalence, although part of the disappearance of heavily infected clams might also be due to mortality.

QPX disease is usually chronic, which means that QPX within the host requires time to proliferate and establish an infection or to be eliminated by the host defense system in response to changing environmental conditions such as temperature fluctuations. Even under standard laboratory conditions with a favorable temperature (21°C or 27 °C), experimentally and naturally infected clams usually needed at least four months to completely eliminate QPX parasites. In the natural environment, a time lag between the change of temperature and response of QPX prevalence and weighted prevalence would be expected, and was shown in our field study. For example, the continuing increases in QPX prevalence and QPX loads between June and August at site 18 when water temperature was already above 21°C, a favorable temperature for clams to eliminate QPX in lab experiments, was likely to reflect such a time lag. Ford and Smolowitz (2007) investigated the potential time lags between temperature and infection prevalence of *Perkinsus marinus* in the oyster *Crassostrea virginica*, and found lag times were site-specific: there was 4- to 5- month lag at the four Massachusetts sites and 3 month lag at the other 3 sites in New York and New Jersey. For Raritan Bay clams, our available data in this study was not sufficient to estimate the general time lag between water temperature and QPX infection prevalence. A multiple-year study will be needed for a better understanding of the relationship between environmental factors, particularly temperature, and the infection dynamics of QPX in clams.

A study of *in vitro* cultured QPX has shown that New York QPX isolates achieved maximum growth around 23 °C in standard culture medium, and lower or higher temperature reduced *in vitro* growth of QPX (Perrigault *et al.*, 2010). Interestingly, that study also found a better QPX survival in seawater at 15 °C compared to 23 °C, suggesting that the effect of temperature on the parasite itself may vary under different nutrient conditions. This study considered the parasite inside its host and thus investigated the effects of temperature on host-pathogen relationships. In our *in vivo* experiments, both experimentally infected clams

(FL clam-NY QPX) and naturally infected clams (MA clam and MA QPX) incubated at 21 °C and 27 °C under laboratory conditions experienced continuous recovery. These results suggest that both northern and southern-originated hosts are able to effectively eliminate QPX in a warmer environment, even under an optimal temperature for parasite growth. On the other hand, elimination of parasites from infected clams was inhibited in the low temperature (13 °C) treatment, accompanied with higher mortality and more intense parasite loads. This new information suggests that a low temperature environment may be required for QPX to proliferate and defeat the defensive system of the host. At present, it is uncertain whether this unbalanced host-pathogen interaction results from a poorer defense system of the hosts due to low temperature-associated stress or an elevated virulence of the parasites or both.
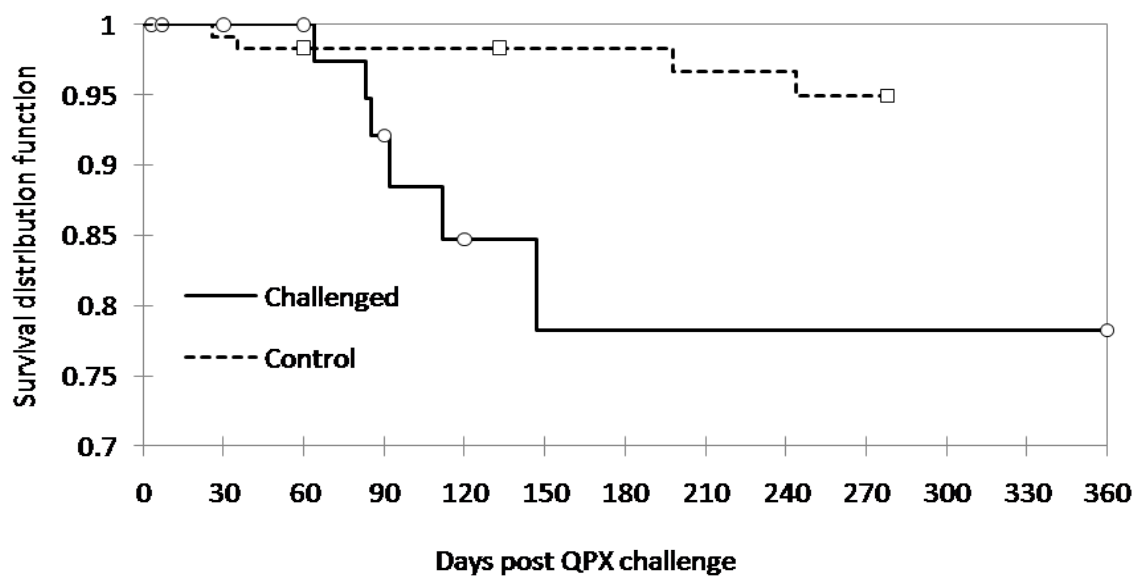
Figure 3. 1. Kaplan Meier cumulative survival rate of experimental and control clams in the QPX clearance experiment.
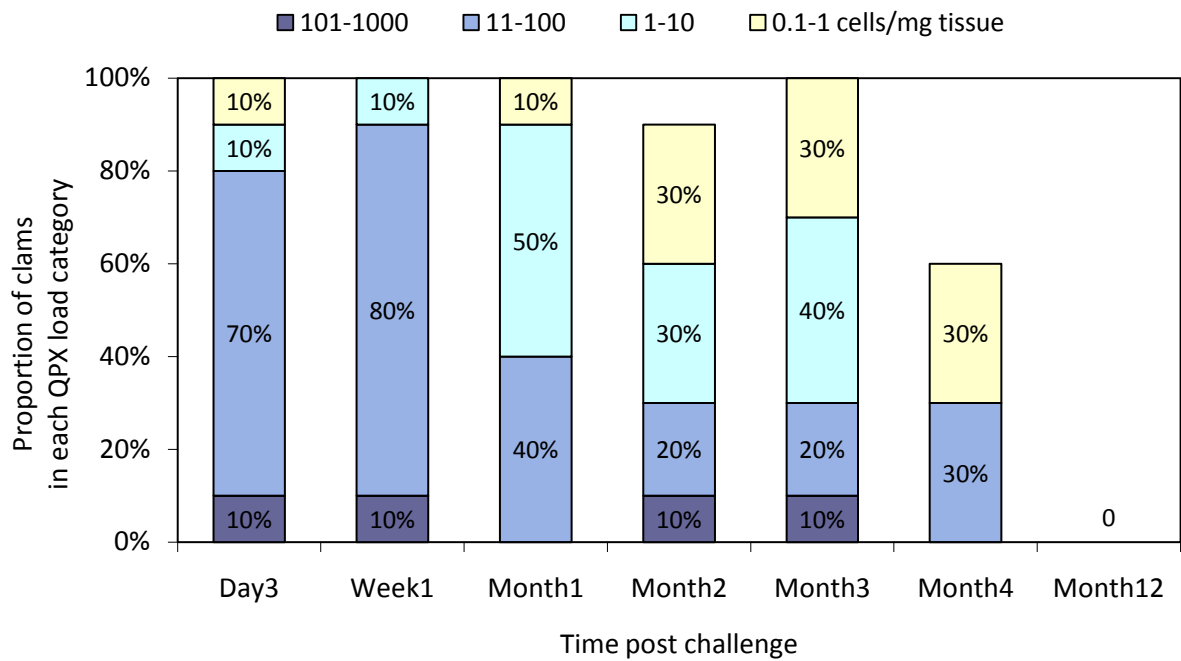
Figure 3. 2. Proportion of clams in each QPX load category in samples (N=10 for Day 3 to Month 4, N=12 at Month 12) from the QPX clearance experiment (21 °C, 30 psu, and oxygen saturation).

Table 3. 1. Prevalence and weighted prevalence of QPX in QPX clearance experiment

Time	Prevalence	Weighted prevalence	P value (Student's test)*
Day 3	100%	2.8	
Week 1	100%	3.0	0.502
Month 1	100%	2.3	0.016
Month 2	90%	1.9	0.373
Month 3	100%	2.1	0.689
Month 4	60%	1.2	0.103
Month 12	0%	0	0.018

* p value of student's t-test (unpaired, two tailed, unequal variance) in the comparison of average QPX loads between this and previous sampling, e.g. Day 3 verse Week 1
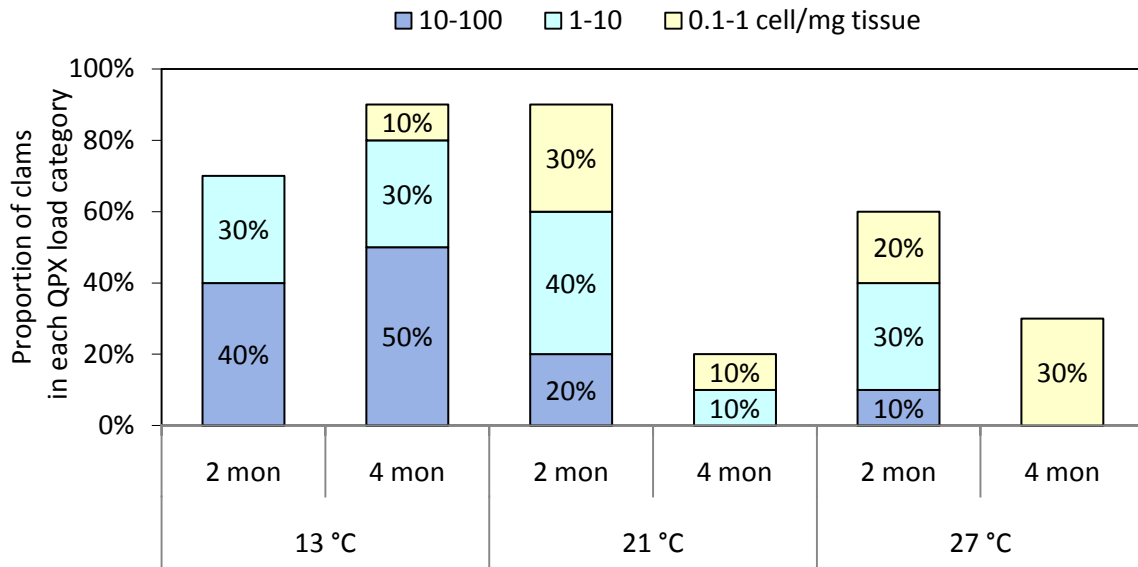
Figure 3. 3. Proportion of experimentally infected FL clams in each QPX load category determined by qPCR assay in the temperature experiment (N=10 at each sampling for each temperature treatment).
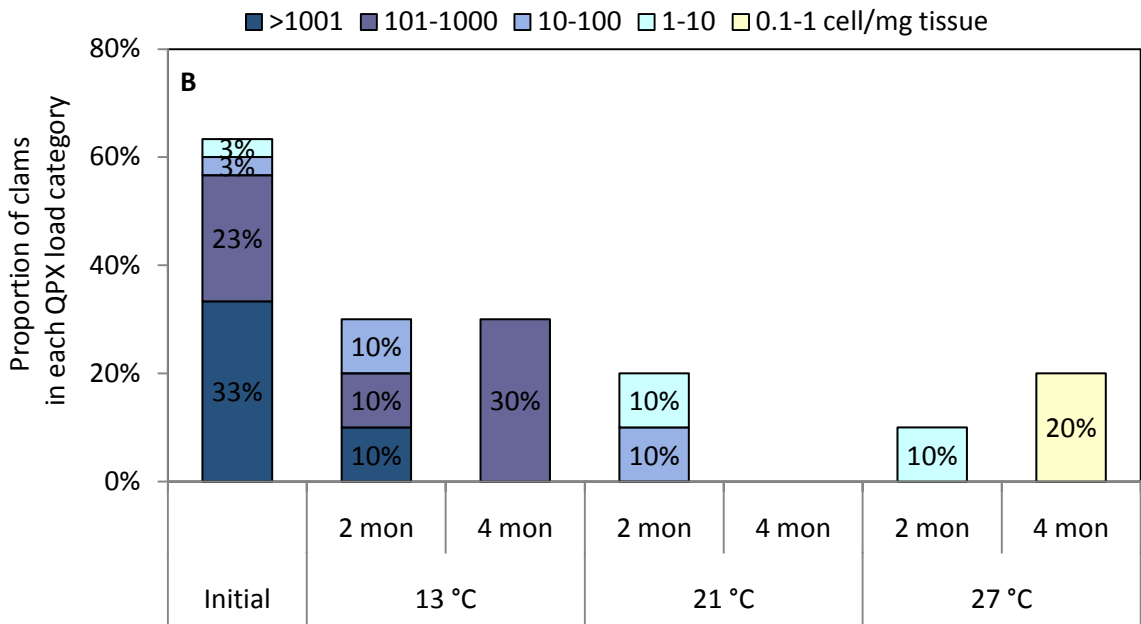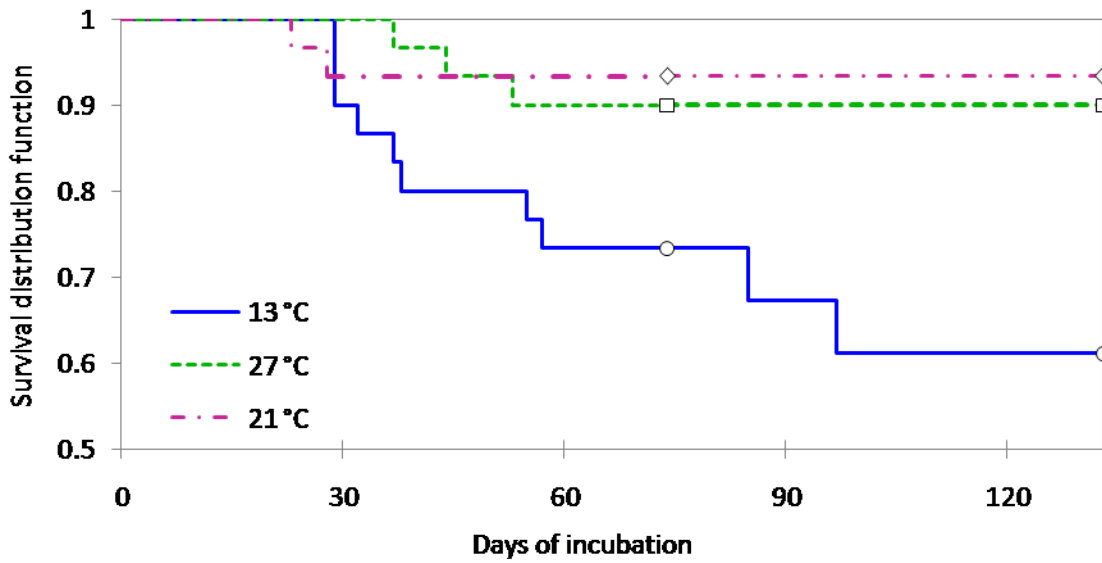
Figure 3. 4. (A) Kaplan Meier cumulative survival rate of naturally infected MA clams incubated at 13 °C, 21 °C and 27 °C in the temperature experiment (40 clams for each treatment). 10 censored clams (removal of live clams for qPCR assay) were sampled on the 74th (Month 2) and 145th day (Month 4). (B) Proportion of naturally infected clams in each QPX load category determined by qPCR assay. Initially 30 clams were sampled for qPCR before clams were distributed randomly for temperature treatment.

60

Table 3. 2. (a). Prevalence and weighted prevalence of QPX in experimentally infected clams in the temperature experiment.

Time	Treatment	Prevalence (N=10)	Weighted prevalence	P value ANOVA	P value Student's test*
2 month	13 °C	70%	1.8		-
	21 °C	90%	1.7	0.341	-
	27 °C	60%	1.1		-
4 month	13 °C	90%	2.2		0.160
	21 °C	20%	0.3	<0.001	0.002
	27 °C	30%	0.3		0.056

Table 3.2 (b) Prevalence and weighted prevalence of QPX in naturally infected clams in the temperature experiment.

Time	Treatment	Prevalence (N=10)	Weighted prevalence	P value ANOVA	P value Student's test*
Initial		63%	2.8	-	-
2 month	13 °C	30%	1.2		0.05
	21 °C	20%	0.5	0.257	<0.001
	27 °C	10%	0.2		<0.001
4 month	13 °C	30%	1.2		1
	21 °C	0	0	0.058	0.177
	27 °C	20%	0.2		1

* the p value of student's t-test (unpaired, two tailed, unequal variance) in the comparison of average QPX loads between each sample and previous sampling within the same treatment, e.g. 2 month verse 4 month in 13 °C treatment

Chapter 4: Investigation of QPX transmission between cohabitated infected and naive clams

Introduction

QPX is thought be an opportunistic pathogen, capable of growing outside its host. QPX has been detected in seawater, sediment, marine aggregates, and associated with macrophytes and other invertebrates (Lyons *et al.* 2005, 2006, Gast *et al.* 2008), suggesting the QPX organism is a common component of coastal marine environments. However, although it is widely distributed, QPX probably does not normally occur at high numbers in the natural environment, because our field study in Chapter 2 only detected QPX at abundances above the detection limit of the qPCR assay in a few sediment samples, and all these samples were collected from the areas where QPX disease has been occurring in local clams. As a facultative endoparasite, QPX must breach barriers of a host to establish an infection and survive the host's internal defenses to proliferate. Histopathology results show that typical QPX infection primarily occurs in pallial organs (e.g. mantle, gill and siphon) (Smolowitz *et al.*, 1998; Ford *et al.*, 2002; Dove *et al.*, 2004) indicating a direct transmission from the environment because these organs are directly exposed to seawater and may be the portals of entry for QPX from the environment. However, it is unclear whether the abundance of QPX cells in their environment is related to the severity of QPX disease in clams, due to the limited knowledge of the release and uptake processes of QPX from clams.

In the natural environment, the transmission mechanism of QPX disease is still not clear. Descriptions of QPX dynamics in the field (e.g., Chapter 2) have been, for the most part, based on data concerning patterns of prevalence and infection intensity in clams, and are difficult to interpret in terms of acquisition of new infections because other processes, such as healing and mortality, are difficult to measure. Under laboratory conditions, attempts to transmit QPX parasite by adding QPX cells to water in tanks with clams or by cohabitating infected adult clams with naïve seed clams did not induce detectable infections (Dahl and Allam, 2007). The reasons behind these failures may be the lack of environmental reservoir(s) required to facilitate the transmission or because the laboratory conditions are not conducive to establishment of new QPX infections.

Results from our field study (Chapter 2) and other studies (Gast *et al.* 2008) showed that sediment is a natural environmental reservoir for QPX outside clam hosts, and may play an important role in QPX transmission among clams living in this habitat. The temperature experiment presented in Chapter 3 suggested a low temperature environment (13 °C) is more advantageous for QPX during host-pathogen interactions than higher temperatures (21 °C and 27 °C). Based on these findings, we conducted laboratory-based QPX transmission experiments by cohabitating infected and susceptible clams with the incorporation of sediment as a potential QPX reservoir, and tested the impact of low temperature on disease transmission.

Materials and methods

Persistence of QPX in sediment

A small scale experiment was conducted to test the persistence of QPX in sediment. Surface sediment (1-5 cm in depth) was collected in November 2007 from the intertidal area in Flax Pond, NY. The sediment was pre-screened by 1 mm mesh to remove litter and larger benthic animals. 1 ml sieved sediment subsample was examined by qPCR assay for QPX

presence and found to be QPX-negative before the sediment was used for the experiments. A subsample of screened sediments was autoclaved in a 50 ml falcon tube at 121 °C for 15 min to kill potential QPX predators, such as dinoflagellates and ciliates. QPX cells which had been grown in modified MEM medium (Kleinschuster *et al.*, 1998) were collected by centrifugation, resuspended in artificial seawater, and mixed with either sieved sediment or autoclaved sieved sediment. These samples were placed in 100 mm Petri-plates (1 cm in depth) and incubated in separate tanks filled with approximately 10 liters of seawater. The air bubbling was adjusted to maintain the saturation of oxygen without disturbing the sediment. Sediments were sampled after 1 hour, 3 hours, 24 hours and 72 hours. During each sampling, approximately 1 ml of sediments from non-autoclaved and autoclaved treatments was collected in a 1.5 ml eppendorf tube. DNA was extracted and purified and QPX abundance in each sample was determined by the qPCR assay as described in Chapter 1.

Transmission experiment at 21 °C

Naturally infected adult clams (MA clams) and susceptible, naïve clams (FL clams) used in this experiment were from the same batches as those used in the temperature experiments described in Chapter 3. MA clams were acclimated in the laboratory as described for those used in the 21 °C treatment for a week before being used in this experiment, while FL clams were maintained in the lab at 21 °C for 6 months until the start of the experiment.

The sediment used in this experiment was obtained and pre-treated as for the non-autoclaved sediment used in the experiment described above. Sediment was placed into two 35 liter tanks, covering the bottom approximately 3 cm in depth. Each tank was filled with approximately 28-30 liters of seawater, and allowed to sit for 2 days before adding clams. Each experimental tank was cohabitated by 7 MA clams and 11 FL clams at Day 0. The tanks were covered with plastic film to minimize evaporation. Salinity was maintained constant at 28 psu, and oxygen saturation was ensured by continuous air bubbling. Unlike the experimental tanks described in chapter 3, no water filtration systems were used in this experiment to avoid the elimination of infective QPX cells from seawater. Clams were fed with a ration of commercial algae concentrate (DT's Live Marine Phytoplankton, Sycamore, IL, 1 ml per day) and mortality was monitored daily.

When MA clams were found dead, the mortality was recorded and the tissue was left in the tank to allow possible QPX release during decomposition. Live FL clams were sampled from each tank at Day 25 (1 month) (N=3), Day 56 (2 months) (N=4) and Day 123 (4 months) (N=4). The final sampling at Day 123 (4 months) also included the remaining live MA clam(s). The clams were dissected, and the entire mantle and siphon tissue was sampled. The tools were sterilized between samples to avoid cross contamination. The tissues were drained on a clean paper towel, and mechanically homogenized in 20 volumes of PBS based on their wet weights (e.g. 0.1 g tissue in 2 ml PBS). A 2 ml aliquot of homogenate of each clam, containing 100 mg clam tissue, was taken for DNA extraction. Seawater and sediment samples were collected at Day 0, Day 8 (1 week), Day 25 (1 month), and Day 56 (2 months). At each sampling time, for each tank, 500 ml water was filtered through a Sterivex-GV filter and 1 ml sediment was collected in an eppendorf tube. The environmental samples were stored at -80 °C until DNA extraction.

Transmission experiment at low temperature

For this experiment, naturally infected adult clams (MA clams) were collected from Cape Cod, Massachusetts and acclimated at room temperature in the laboratory for a week prior to the experiment. The susceptible, naïve clams (FL clams) were obtained from a

commercial nursery operating in Florida and maintained in the lab at room temperature for approximately 7 months until the experiment began. The sediment was collected in late September, 2008 from eastern Long Island Sound by an Ekman Grab, and was maintained at 4 °C until used in this experiment. The intact surface layer of sediment was pooled and screened as described above. The experimental tanks were set up as described above, and allowed to sit in a cold room at 13 °C for 2 days before clams were added. The experimental tanks were run in duplicate, and each tank was cohabitated by 10 MA clams and 20 FL clams. The tanks were maintained as those in the transmission experiment at room temperature, except water temperature was maintained at 13 °C in this experiment.

Compared with the transmission experiment conducted at room temperature, a different strategy to collect environmental and clam samples was applied in this experiment due to the occurrence of unexpected early mortalities. For MA clams, when a clam was found dead, one side of the mantle (including siphon) tissue was collected. The remaining clam tissue (with shells) was placed back into the tank, to provide a potential source for infective QPX cells. For FL clams, when a dead or dying (gaping) clam was observed, the clam was removed from the tank and tissues, including mantle, gill and visceral mass, were collected to examine the possible QPX acquisition in the tissue. For each (MA or FL) clam, the sampled tissue was drained on a paper towel, weighed and preserved in a 15 ml falcon tube containing 100% ethanol. Prior to DNA extraction, the tissue was removed from ethanol, washed and mechanically homogenized in 20 volumes of PBS based on its weight (e.g. 0.1 g tissue in 2 ml PBS). A 2 ml aliquot of homogenate of each clam, containing 100 mg clam tissue, was used for further DNA extraction.

Seawater was sampled at Day 5, Day 9 (1 week) and Day 29 (1 month). At each sampling time, 500 ml seawater from each tank was filtered with a Sterivex-GV filter. Sediment was sampled more frequently through the entire experiment: except at Day 0 and Day 8, sediment was usually collected on the same or the following day when a new moribund MA clam was observed. At each sampling time, approximately 1 ml sediment sample (single or duplicate) was collected in an eppendorf tube. The environmental samples were stored at -80 °C until DNA extraction.

DNA extraction and qPCR assay

For the two transmission experiments, DNA was extracted and purified from clam tissue and environmental samples following the protocols described in Chapter 1. Purified environmental DNA was quantified with a PicoGreen dsDNA quantification kit and diluted (usually 10-50 fold) to produce template DNA with a concentration of 1 ng/µl. Finally, 1 ng DNA was used as template in qPCR assay. The original abundance of QPX cells in each sediment and seawater sample was determined as follows: $(\#QPX_{initial} \times a*)/(c \times d \times e)$ where $\#QPX_{initial}$ is the number of QPX ITS copies in the 1 ng assayed environmental DNA template (copy ng^{-1}) after correction for PCR inhibition; $a*$ is the total DNA content of each purified environmental DNA sample (ng); c is the estimated copy number of ITS region in each QPX cell (181 copies $cell^{-1}$); d is the estimated DNA recovery rate of the extraction method (5.38% for sediment samples and 9.51% for seawater samples); and e is the volume of seawater (ml) or weight of sediment (mg) from which DNA was extracted. The original abundance of QPX cells in each clam sample was determined as described in Chapter 2. It needs to be noted that in the two transmission experiments, clam tissues were preserved and processed in different ways, but because the DNA recovery rate of the fresh tissue extraction protocol used in the room temperature transmission experiment was not estimated, we used

the same DNA recovery rate (16.31% for ethanol preserved tissue) for the estimation of QPX abundance in all clam samples.

Statistical analysis

A Student's t-test was used to compare the estimated QPX abundance in the environmental samples between replicates in the low temperature transmission experiment. A Log Rank test after Kaplan Meier cumulative survival rate analysis was performed to determine whether there was a significant difference between the cumulative mortality in replicate tanks. All differences were considered statistically significant at $p < 0.05$.

Results

Persistence of QPX in sediment

In the initial sediment sample, QPX abundance was below the qPCR assay detection limit (6.4 ± 0.6 cells mg^{-1}). After the addition of lab-cultured QPX cells, QPX was detected in both the non-autoclaved sediment and autoclaved sediment samples collected up to 24 hours (Fig. 4.1), but was below the detection limit at day 3. In both types of sediment, QPX abundance experienced exponential decay, with at most a 4 hour half-life. There was no significant difference in the decay rate of QPX in the non-autoclaved and autoclaved sediment. The relatively short lifetime of detectable QPX in the sediment suggests QPX cells transferred from *in vitro* culture are not capable of long-term survival in sediment.

Transmission experiment at room temperature

The MA clams used in this study were collected from Cape Cod, where clams have been experiencing severe QPX disease at least since 1995. Their initial QPX prevalence, assessed by qPCR assay a week prior to the beginning of the experiments, was 63.3%, with a large proportion of clams with very heavy infections (>1001 cells mg^{-1} tissue) (Fig. 3.3 in Chapter 3), which made them a good potential source of QPX for transmission experiments. Persistent mortality was observed in the MA clams co-incubated with FL clams in tanks containing Flax Pond sediment (Fig. 4.2). Half of the MA clams died in the second month, and the final cumulative mortality reached 86% (6 deaths out of 7 clams) in both replicates by the end of the experiment at month 4. There was no significant difference in cumulative mortalities between replicate tanks (Log-Rank test, $p > 0.05$). In contrast to the MA clams, during the entire experiment no dead or moribund FL clams were observed. QPX was below the detection limit of qPCR assay (1.3 ± 0.3 cell mg^{-1} tissue) in all FL clams (N=10 for each tank) and in the MA clams alive at the end of the experiment (N=1 for each tank, sampled at month 4).

Low levels of QPX were detected by qPCR in sediment samples collected at Day 8 (before the first death of any MA clam) and Day 25, but were below the detection limit (3.6 ± 1.0 cells mg^{-1} sediment) at Day 56 (Fig. 4.2). As almost no DNA was successfully recovered from any of the collected seawater samples, probably due to the efficient filtration activity of clams (based on the quantification results of Picogreen assay; data not shown), no seawater DNA was examined by qPCR assay.

Transmission experiment at low temperature

The naturally infected MA clams used in this experiment had a 72% initial QPX prevalence, and most of the infected clams had moderate (28%) and heavy (28%) infections a week prior to the beginning of the experiments(data not shown). When these naturally infected MA clams and initially QPX-free FL clams were cohabited in Long Island Sound sediment at 13 °C, the two replicate tanks showed significantly different trends in cumulatively mortality (Log-Rank test, $p < 0.001$) (Fig. 4.3A and 4.4A). For MA clams in

tank 1, the earliest mortality occurred during week 2, and then persistent mortality (1 or 2 deaths in each week) was observed during the rest of the experiment. At day 39, because serious deterioration of water quality was observed, the remaining live clams (4 FL and 1 MA) were transferred into a new tank containing fresh seawater, but no sediment. However, the mortality continued, and all the clams were dead by day 46. The MA clams in tank 2 also exhibited constant mortality, but more gradually over time, so the experiment in tank 2 lasted a longer time (10 weeks) compared to that in tank 1 (7 weeks), until MA and FL clams reached 100% mortality. The association between the deaths of FL clams and cumulative mortality in MA clams looked similar between the two tanks: FL clams had no mortality or very low mortality until the mortality of MA clams reached 60%, when FL clams started to show mass mortalities, experiencing 95% mortality within 10 to 15 days.

From four MA clams in tank 1 and seven in tank 2, one side of the mantle tissue of recently dead animals was sampled for QPX diagnosis by qPCR assay. The results (Fig. 4.3A and 4.4A) showed that two clams in tank1 and five clams in tank 2 were QPX-positive, with 5 to 624 QPX cells mg^{-1} tissue. Due to degradation, tissue samples of some MA clams that died during the first half of the experiment (in both tanks) were not available for qPCR assay. Most moribund or dead FL clams were sampled for qPCR assay before tissue degradation began (Fig. 4.3C and 4.4C). In tank 1, rare to light loads of QPX (1-100 QPX cells mg^{-1}) were detected in 4 sampled clams during week 6 and 7, and 11 FL clams were QPX-negative by qPCR assay in weeks 5 to 7. In tank 2, 6 clams sampled during week 8 and 2 clams sampled during week 9 were found to be QPX positive, when FL clams exhibited 50% and 40% instantaneous mortalities, respectively. Most QPX-positive FL clams in tank 2 contained rare to light QPX abundance, while one clam sampled in week 8 exhibited a moderate level of QPX abundance (>101 cells mg^{-1}).

QPX was consistently detected at relatively high abundance (between 44 and more than 3000 cells mg^{-1}) in sediment samples in both tanks (Fig. 4.3B and 4.4B). QPX abundance in the sediment samples from tank 2 looked relatively higher than that in tank 1, but the difference was not statistically significant (Student's t-test, p>0.05). QPX was also detected in all collected seawater samples during week 1, week 2 and week 5 from both tanks, at between 1.0 and 4.5 cells ml^{-1}, by qPCR assay with a detection limit of 0.2 ± 0.1 cells ml^{-1} (Fig. 4.3B and 4.4B). No clear correlation was observed between QPX abundance in environmental samples and mortalities in MA or FL clams, and QPX was detected in the environment before any clam mortality occurred.

Discussion

QPX survival in the natural environment

Laboratory grown QPX cells did not persist in a qPCR-detectable form in the sediment for very long (Fig. 4.1). The rapid decline of QPX abundance was unlikely caused by predation, since the half-life for QPX (determined from the decay constant) in the non-autoclaved sediment (4.05 hr) was not much different from that in the autoclaved sediment (3.89 hr). Buggé and Allam (2007) reported that cultured QPX cannot grow in natural seawater without medium supplementation. Sediment is potentially nutritionally rich compared to seawater, but it also did not support long-term survival of QPX. In coastal and benthic habitats, the group of labyrinthulomycetes to which QPX belongs, the thraustochytrids, is usually associated with degrading organic detritus from plants or animals (Raghukumar, 2002). Buggé and Allam (2007) found that QPX growth was supported by several macroalgae species when their fresh or decomposed products were used as growth

media, but was also inhibited by products from others. Although a positive relationship between thraustochytrid abundance and sediment organic matter content is generally suggested (Raghukumar, 2002; Bongiorni and Dini, 2002), the survival of QPX in sediment may depend on the specific organic substrates in the sediment, and may be affected by the antimicrobial properties of specific substrates. The sediment used in this QPX survival experiment was originally collected from the intertidal area of Flax Pond, which is not a clam habitat, and determined to be QPX free (below the detection limit) by qPCR assay. It is possible that the sediment used in this experiment could not provide the nutrients that QPX requires for growth, or contained compounds inhibitory to QPX, and thus most QPX cells died quickly. In our field study (Chapter 2), all QPX-positive sediment samples were collected from sites where QPX disease had been occurring in the local clams, suggesting that the presence of QPX in the sediment may be related to the presence of clams (or of clams with QPX disease).

The quick decline of QPX abundance in the sediment in our experiment may be due to the sudden transition of QPX from nutrient-enriched culture medium to nutrient-poor seawater and sediment. Buggé and Allam (2007) reported a microscopical observation of abundant cell debris after QPX cells were transferred from culture medium to seawater maintained at 23°C. These observations, associated with a significant decrease of QPX biovolume (Buggé and Allam, 2007; Perrigault *et al.*, 2010), suggested that the sudden transfer from culture to seawater may alter some physiological characteristics of QPX cells and may even cause severe cellular damage. In our experiment, QPX was collected and resuspended in artificial seawater before being mixed into sediment. This procedure, although very quick (approximately 30 min), may have negatively affected a large fraction of QPX cells before they reached the sediment. It is not known how cultured QPX cells respond to contact with sediment (and the pore seawater in sediment), or whether QPX can maintain viability and infectivity and resume growth when supported by alternative nutrients in the sediments or other substrates. The evidence that QPX abundance significantly decreases after being directly transferred from *in vitro* culture conditions to a more "natural" environment might explain, at least partially, the failure of previous experimental transmission attempts by adding QPX cells into the water column. Apparently, "spiked" QPX cells from cultures do not survive in a large quantity in the "natural" environment under lab conditions (21°C) or become more difficult to detect (perhaps to extract DNA from) due to morphological or physiological changes, which appears to reduce their infectivity. It remains unknown how well QPX cells from other sources, such as from live, infected clams or from dead and disintegrating clam tissue, would persist.

QPX release mechanism

QPX cells were detected in sediment samples collected from both transmission experiments. At room temperature, QPX abundance was barely above the detection limit in the sediment samples collected at Day 8 and Day 25 (Fig. 4.2). At least on Day 8, the sediment QPX cells must have been released from live infected MA clams, because the first clam mortality occurred at Day 20 in tank 1 and at Day 14 in tank 2. At 13 °C, QPX was consistently detected in sediment samples collected during the entire experiment (Fig. 4.3B and 4.4B). In Tank 1, QPX cells were again detected before the first infected clam died on Day 10. These results strongly support the hypothesis that release of QPX from live, infected clams is a source of parasites in the sediment. In the transmission experiment at 13 °C, QPX cells were also detected in all seawater samples (Fig. 4.3B and 4.4B). These are the only

seawater samples in which QPX abundance has been found above the detection limit of our qPCR assay. These results are in agreement with the findings by Perrigault *et al.* (2010) showing significantly better *in vitro* survival of QPX in seawater at 15 °C as compared to 23 °C. It is likely that QPX cells released from live, infected MA clams also contributed to QPX cells detected in the seawater samples as the earliest QPX positive seawater sample was collected at Day 5 in tank 1, before the first death of a MA clam on day 10 (Fig. 4.4A and 4.4B). However, this study could not reveal how stable QPX cells would be in the environment after being released by clams, compared to cultured QPX cells. Our discovery of QPX in seawater and sediment samples in the absence of host mortality suggested that shedding of QPX from live, infected clams may be a principal mode of parasite release prior to mass mortality of infected clams or in the absence of host mortality, as suggested by Bushek *et al*. (2002) for the oyster parasite *Perkinsus marinus*.

For many lethal parasites with a direct life cycle, the death of infected hosts, with consequent release of parasite cells from disintegrating host tissue into the environment, has been considered the main source of infectious forms (Ragone Calvo *et al.*, 2003; Bushek *et al.*, 2002). However, results of our transmission experiments were not able to support (or reject) this mechanism for QPX transmission. In the room temperature transmission experiment, QPX cells were detected in the sediments collected within the first month when mortality of infected MA clams was low, but were not detected in the sediment in the second month (Day 56; Fig. 4.2) when more MA clams died. This may indicate that degradation of infected clam tissue did not facilitate the release of QPX or that QPX cells released in this way had too short a half-life in the environment to be detected. As no tissue of dead MA clams was sampled during this experiment, the disease status of the MA clams that died at various times is not certain, and the absence of QPX in the sediment during the late stage of the experiment may be simply because the clams that died later were not infected. In the low temperature transmission experiment, tissue samples of some dead clams were taken for QPX diagnosis, and sediment was sampled more frequently in an effort to trace the effect of mortality on QPX abundance in the environment. However, no clear correlation was observed between QPX abundance in the environmental samples (seawater and sediment) and the mortalities in MA or FL clams. Due to the limited knowledge about the release mechanism of QPX from infected clams, and about the survival time of QPX released into the environment from infected clams, we could not differentiate the contributions of QPX potentially released from live, infected clams versus dead clams to the detected QPX abundance in the environmental samples.

Interestingly, the abundance of QPX in sediment samples was dramatically different between the two experiments: QPX abundances in the sediment at low temperature were 10- to 1000-fold higher than those in the sediment at room temperature. This difference may simply be due to the fact that more infected MA clams (N=10) were present in the transmission experiment at 13 °C than the experiment at room temperature (N=7). In the transmission experiments, because the tissue of dead infected clams was left to degrade in the tank, temporary water quality deterioration (indicated by signs like cloudy water and floating disintegrated clam tissue) was observed. This period usually last 2 or 3 days in the experiment at room temperature, but longer (3-5 days) in the experiment at 13 °C, especially during the later period of the experiment. It is possible that having more tissue of dead clam floating in the water for a longer time provided more nutrients that are required by QPX for survival and growth, although QPX abundance in the environmental samples (seawater and

sediment) had no clear correlation with clam mortality. Alternatively, as mentioned above, the findings by Perrigault *et al.* (2010) clearly supported a better survival of QPX in seawater maintained at 15 °C as compared to 23 °C, and a similar positive impact of low temperature on QPX survival in sediment is highly probable.

QPX disease transmission

In our transmission experiment at room temperature, QPX was detected in the sediment during the first month, indicating there was an active source of QPX. Naturally infected MA clams from a group with an initial 63.3% QPX prevalence died within less than 4 months after being co-incubated with naïve FL clams. It is not known whether the MA clams in this experiment died of QPX or from other causes, including perhaps the physiological stress of periods of poor water quality due to clam tissue decomposition. However, no FL clams died or acquired detectable loads of QPX. Although lack of histological analysis prevents us knowing whether there were healed infections in FL clams, the negative results for all FL clams in qPCR assay suggested QPX disease transmission did not occur in this cohabitation experiment. Although sediment as an environmental reservoir was incorporated in our experiment, and the more sensitive qPCR detection method was applied, the results were similar to those reported by Dahl and Allam (2007) suggesting that room temperature may not be a conducive environment for parasite acquisition or establishment of infection in the susceptible hosts.

In contrast, during the later period of the 13 °C experiment, light and moderate levels of QPX abundance were detected in some FL clams in both replicate tanks (Fig. 4.3C and 4.4C), indicating the parasites were acquired in some of these susceptible hosts. The colder environment may impair the defense of hosts to QPX parasites and facilitate the parasite's ability to breach host barriers and establish an infection. Also, the relatively greater abundance of QPX cells in the seawater and sediment suggests an increased opportunity for parasites to come into contact with susceptible clams, although no clear correlation between infection acquisition and parasite abundance in the environment was revealed in this experiment.

Although light and moderate QPX loads were found in some FL clams, the mass mortality observed in FL clams at the end of the 13 °C experiment was unlikely caused by QPX disease alone. In both tanks, FL clams started to show mass mortality soon after half of the MA clams died, and most FL clams died within the next 10 to 15 days. Unlike in the transmission experiment at room temperature, water quality seemed to be responsible for the deaths of most FL clams and half of MA clams in the 13 °C transmission experiment. Probably due to a higher clam density (30 clams/tank) and slower biodegradation processes at low temperature, fouled water and sediment covered with disintegrated tissue was more often observed during the transmission experiment at 13 °C. New mortality of MA clams often occurred before the degradation of a prior dead clam was completed. Particularly during the later period of the experiment, filtration activity and gill ventilation of clams may have been seriously impaired by accumulated waste products and local high CO_2 concentration. Fouled water may have led to mass mortality in a very short period of time.

QPX was detected in more FL clams (8 out of 20) at relatively higher intensities (rare to moderate) in tank 2 compared to tank 1, in which 5 FL clams out of 15 showed rare to light QPX loads (Fig. 4.3C and 4.4C). The apparent difference in QPX loads may be related to the length of the two replicate experiments. The experiment in Tank 2 lasted 3 more weeks than that in tank 1, which may have given parasites more opportunity to contact and invade the

hosts, and allowed a longer time for the establishment and progression of infection in the hosts before they died. The relatively higher parasite load may be also associated with parasite abundance in the environment, since a relatively higher abundance of QPX was detected in the sediment samples collected in tank 2, although the difference was not statistically significant.

One of the drawbacks in our transmission experiment is lack of histological proof of QPX infection in susceptible clams. One can argue that some of the QPX detected by qPCR assay came from QPX cells adhering to the surface of sampled tissue after the clam began gaping, rather than real parasite invasion and active infection. Given the relatively high abundance of QPX (40-800 cell mg^{-1}) in the sediment samples, it is possible that some QPX cells attached to sediment particles were collected with clam tissue samples, although every effort was made to avoid this possibility by draining tissue on a paper towel, soaking tissue with ethanol for preservation and washing tissue with PBS before homogenization. Additionally, one FL clam (sampled at Day 45, tank1) still had a light level of QPX abundance after being placed in fresh seawater for 3 days, suggesting that real QPX infection acquisition did exist in some QPX-positive FL clams, if not all of them.

In summary, the results of these transmission experiments suggested that room temperature (21 °C) may not be a conducive environment for parasite transmission, in terms of parasite acquisition and establishment of new infection in hosts, while a colder environment at 13 °C may impair host defense against QPX, and help the parasite breach host barriers to establish an infection. These findings are in agreement with the results of our previous temperature experiments (Chapter 3), which suggested that a low temperature was more favorable to QPX in the host-parasite interaction, likely to facilitate the development of QPX infection in infected clams, while a warmer environment (21 °C and 27 °C) seemed to promote clam healing. The findings of laboratory-based *in vivo* experiments enable us to better interpret and understand the temporal patterns of QPX disease revealed by our field study in Raritan Bay clams (Chapter 2). During April to August, especially from April to June when water temperature was mostly below 20°C, the seasonal patterns at Raritan Bay site 8 and 18 showed increased QPX prevalence and weighted prevalence. At the same time, a large proportion of clams were also found to have rare to light infections, suggesting the concurrence of parasite acquisition from environment, establishment of new infection and development of existing infection was likely related to the effect of relatively low temperature. On the other hand, when temperature remained relatively high, especially during August and September, QPX prevalence and weighted prevalence started to decline. Although some established infections may have continued to develop due to the potential time lag in response of parasite-host interaction to temperature changes, the simultaneous decline in the proportion of clams with lighter QPX loads suggested that new parasite acquisition was reduced or hindered and clam healing was promoted, probably because of the advantageous effect of higher temperature on hosts in the host-pathogen interaction.
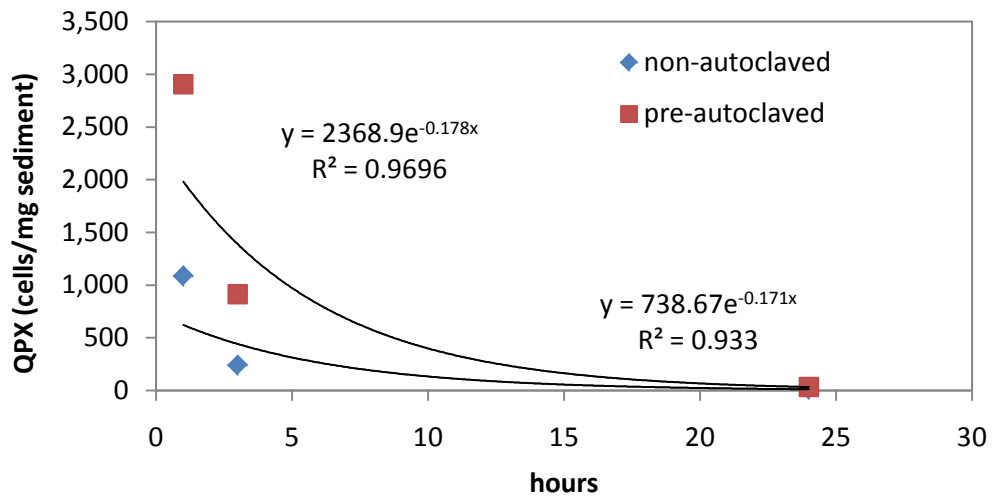
Figure 4. 1. QPX abundance (as measured by qPCR assay) after being suspended in sediment. Half-life of QPX was at most 4.05 hours (=ln2/0.171) in non-autoclaved sediment and 3.89 hours (=ln2/0.178) in autoclaved sediment.
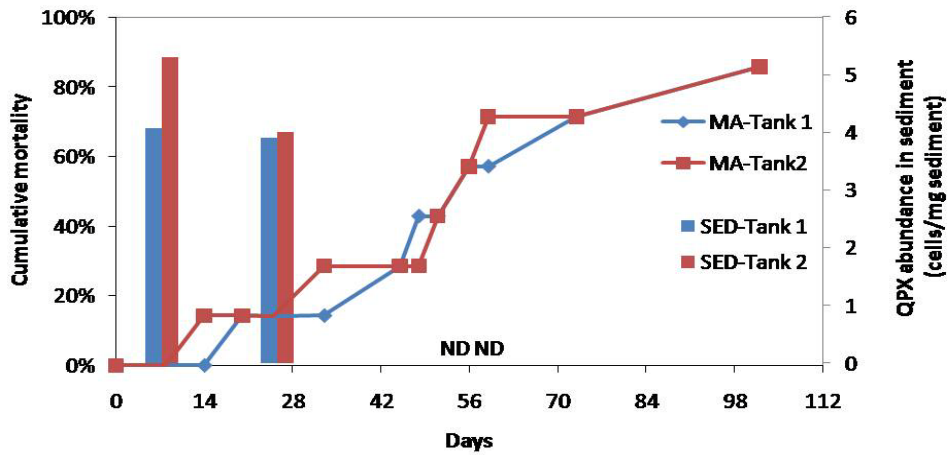
Figure 4. 2. Cumulative mortality plots for MA clams cohabitated with FL clams (lines) and QPX abundance in sediment samples (columns) in the transmission experiment at room temperature. Tank 1 and Tank 2 are replicate treatments. Sediment samples were collected at Day 8, Day 25 and Day 56, but QPX was below the detection limit of qPCR at Day 56, being indicated by "ND".
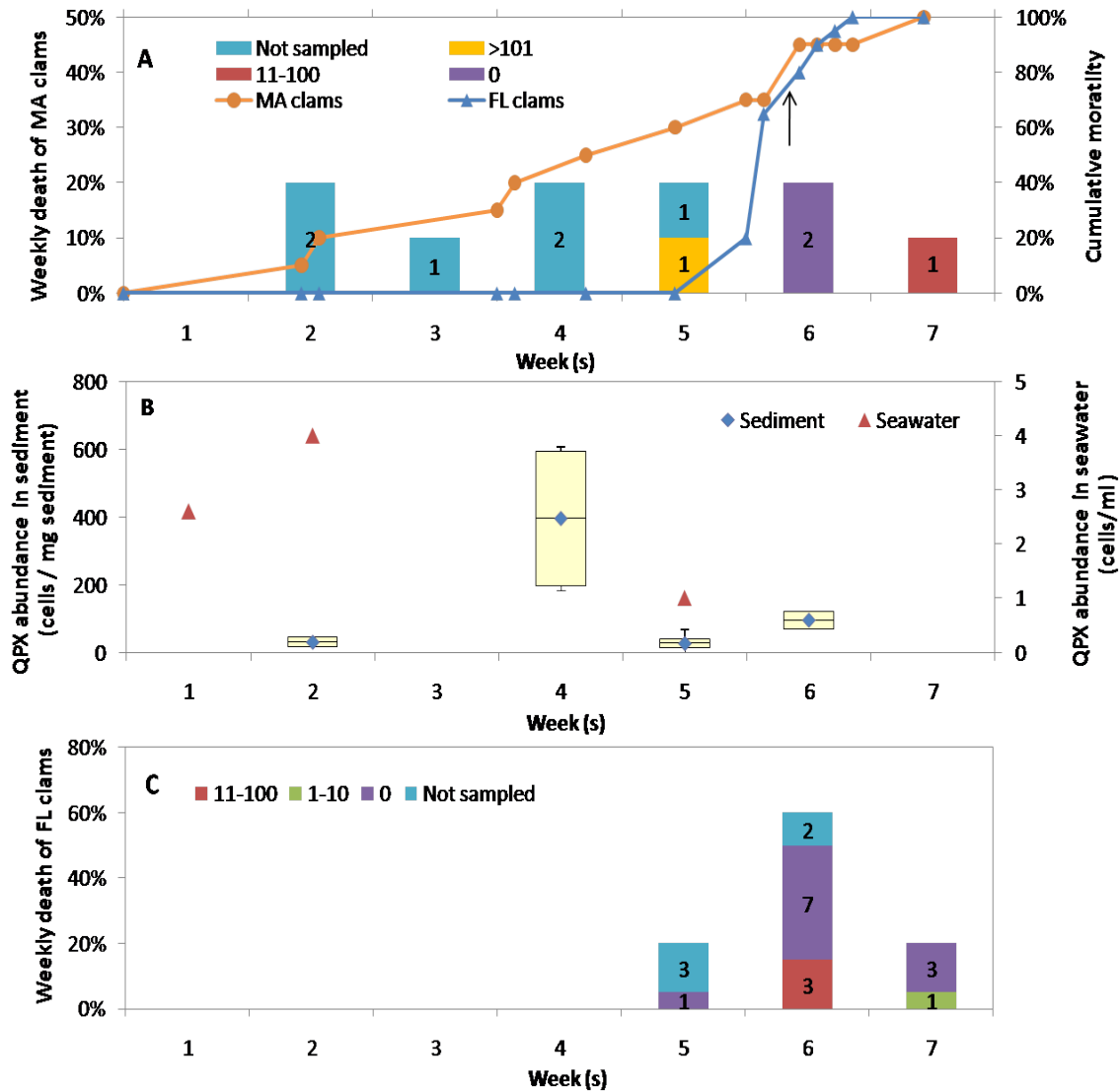
Figure 4. 3. Low temperature transmission experiment Tank 1. (A) Cumulative mortality plots for cohabitated MA and FL clams (lines) and weekly death of MA clams (bars). Numbers in different colored bars represent the number of clams with different levels of QPX abundance (cells/mg tissue) in their tissues. 0 indicates below detection limit of 1.3 ± 0.3 cells mg^{-1} tissue. The arrow indicates the day when remaining live clams (4FL and 1MA) were moved to a new tank. (B) QPX abundance in sediment and seawater samples. In each of Week 2, 4, 5 and 6, two sediment samples were assayed and presented by the box plot. In each of Week 1, 2 and 5, one seawater samples was assayed and presented by the point plot (C) FL clam weekly death and QPX abundance (cells/mg tissue) in sampled FL clams. The samples in week 7 represent the four FL clams moved to a new tank, although the actual deaths occurred during week 6.
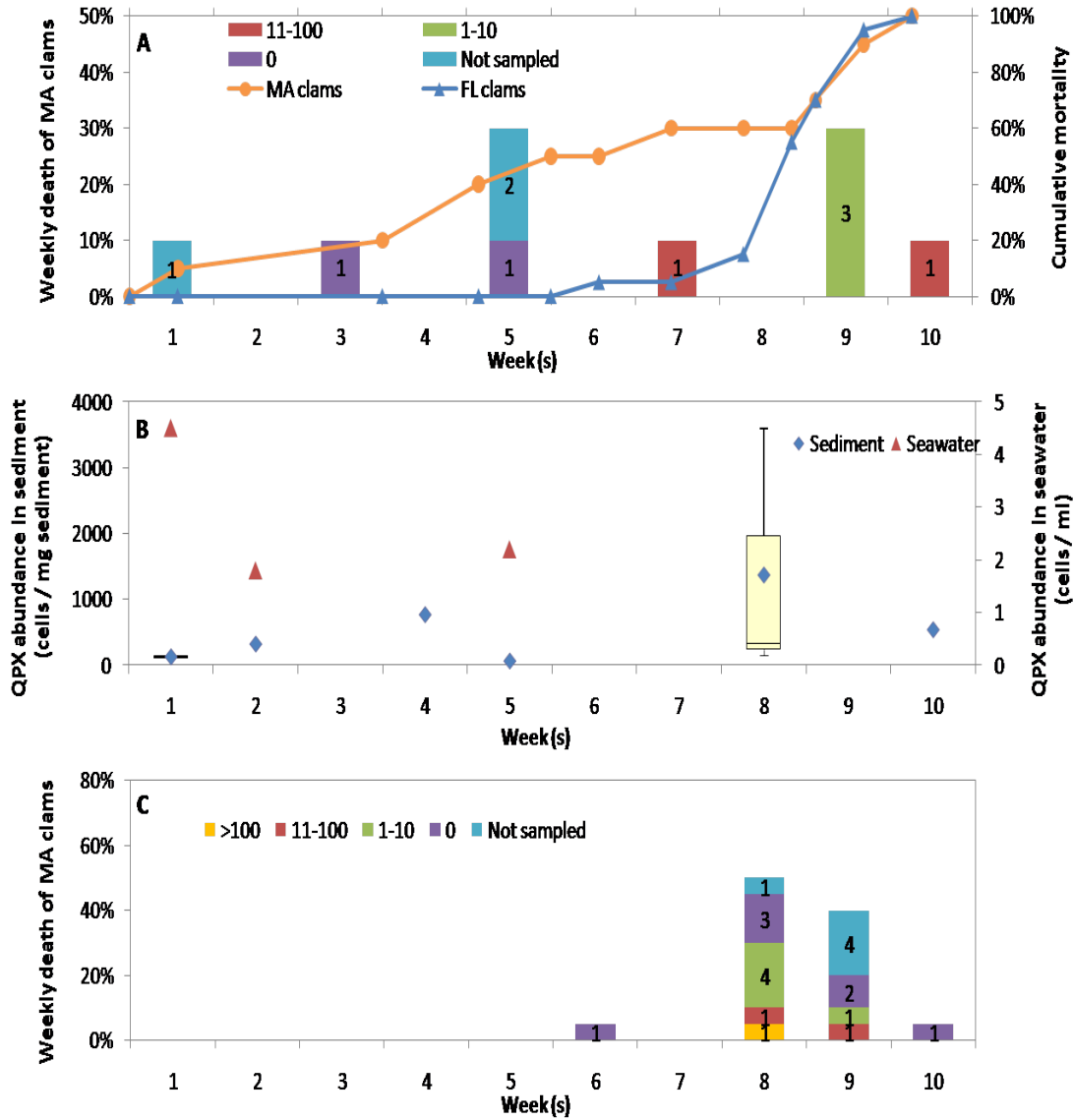
Figure 4. 4. Low temperature transmission experiment Tank 2. (A) Cumulative mortality plots for cohabitated MA and FL clams (lines) and weekly death of MA clams (bars). Numbers in different colored bars represent the number of clams with different levels of QPX abundance (cells/mg tissue) in the clam tissues. 0 indicates below detection limit of 1.3 ± 0.3 cells mg^{-1} tissue. (B) QPX abundance in sediment and seawater samples. In Week 1 and Week 8, two and three sediment samples were assayed and presented by the box plots, respectively. In each of Week 2, 4, 5 and 10, one sediment sample was assayed and presented by the point plot. In each of Week 1, 2 and 5, one seawater samples was assayed and presented by the point plot (C) FL clam weekly death and QPX abundance (cells/mg tissue) in sampled FL clams.

Chapter 5: The abundance and diversity of labyrinthulomycete community in the environment

Introduction

The labyrinthulomycetes (labyrinthulids, thraustochytrids and aplanochytrids) comprise a ubiquitous, diverse, abundant, but poorly understood group of marine protists. They are thought to live mainly as saprobes, obtaining their nutrition from non-living organic matter of plant, algal or animal origin (Raghukumar, 2002). Some labyrinthulomycetes can be parasitic, causing a variety of established and emerging diseases of marine organisms, including QPX disease in hard clams (Whyte *et al.*, 1994; Ragan *et al.*, 2000; Qian *et al.*, 2007). Labyrinthulomycetes play an important role in the decomposition of particulate organic matter (POM) and may be important contributors to the nutrition of marine metazoans by enriching the quality of poor food resources because of their high content of essential polyunsaturated fatty acids (PUFAs) (Lewis *et al.*, 1999; Carmona *et al.*, 2003; Huang *et al.*, 2003; Kumon *et al.*, 2003). However, the significance of labyrinthulomycetes as a component of the marine ecosystem has been underappreciated, mainly due to the limited knowledge of some basic questions such as their abundance and diversity in the environment.

The two available microscopy-based methods (MPN and AfDD) for detection and enumeration of labyrinthulomycetes suffer serious technical problems, and may under- or overestimate labyrinthulomycete abundance (Raghukumar, 2002). In the available quantitative data based on AfDD assay, it is unclear whether what the authors called "thraustochytrids" also included labyrinthulids and aplanochytrids because some genus and species named based on morphological characteristics are not consistent with 18S rRNA sequence-based phylogenetic relationships. Classifying labyrinthulomycetes in environmental samples and cultures is also very difficult because some features used for species identification can change with growth conditions (Leander *et al.*, 2004). Until now, the only available studies describing changes in species composition of labyrinthulomycete communities were based on differences in the size of the thraustochytrids. The development of methods for accurate determination of numbers and diversity is a prerequisite for the investigation of the role of labyrinthulomycetes in the marine ecosystem.

Since its initial development, quantitative real-time PCR (qPCR) has been broadly applied to assess the abundance of specific groups of microorganisms in the marine environment (Zhu *et al.*, 2005). However, to our knowledge, no molecular-based quantification technique (qPCR) has been applied to detect and quantify labyrinthulomycetes in the environment. T-RFLP (Terminal Restriction Fragment Length Polymorphism) is also a PCR-based technique, in which a gene of interest (e.g. 18S rRNA) is amplified from a heterogeneous community using a fluorescently labeled primer. Following digestion with restriction endonucleases, differently sized terminal restriction fragments (TRFs) can be differentiated through use of an automated DNA sequencer, generating "fingerprints" of complex microbial communities (Liu *et al.*, 1997). This technique has been shown to be effective for studying diversity in the microbial assemblages in various marine and terrestrial environments (Baldwin *et al.*, 2005; Morris *et al.*, 2005; Nelson *et al.*, 2008; Vigil *et al.*, 2009; Yi *et al.*, 2009), but not yet on labyrinthulomycete communities.

In this study, using primers Laby-A and Laby-Y (Stokes *et al*. 2002), an 18S rRNA gene-based qPCR assay and T-RFLP analysis were developed to assess the abundance and diversity of labyrinthulomycetes in sediment and seawater samples collected between April

and September, 2006, from several sites in Raritan Bay (New York). The same samples were used to investigate the dynamics of the pathogenic thraustochytrid QPX by qPCR assay targeting the ITS region of the QPX rRNA operon as described in Chapter 1 and 2. To our knowledge, this is the first report using molecular techniques to study the abundance and community structure of labyrinthulomycetes in the environment. In the previous field study, the limited number of QPX-positive environmental samples prevented us from further studying QPX dynamics in the environment or relationship between the abundance of QPX in the environment and QPX prevalence in clams. The dynamics of the whole labyrinthulomycete community would provide a broader context with the potential for a better understanding of how QPX behaves as a natural component of this community in the environment.

Materials and methods

Standard curve for qPCR assay using Laby-A and Laby-Y primers

Using QPX as a representative labyrinthulomycete, the primary and secondary standard curves for quantification of labyrinthulomycetes by qPCR assay were constructed following the protocols described in Chapter 1. Briefly, a primary standard curve was generated by 10-fold serial dilution, ranging from 1 to 10^6 copies, of pGEM-T Easy plasmids containing a QPX 18S rRNA gene amplified by universal eukaryote primers 18S-F (5'-AACCTGGTTGATCCTGCCAGT -3') and 18S-R (Table 1.1) from QPX isolate NY0313808BC8 (Qian *et al.*, 2007). This clone was 99.8% identical to the consensus of 3 published QPX 18S rRNA sequences (excluding the primer sites, it has four C for T or G for A substitutions compared to GenBank accession number DQ641204 and AF261664, and five substitutions compared to AF155209). The secondary standard curve was constructed with the same 10-fold serial dilution of QPX genomic DNA used in qPCR assay for QPX quantification (Chapter 1). The number of cells represented by each point in the secondary standard curve was calculated by dividing the concentration of QPX genomic DNA template in each reaction by the DNA content per QPX cell determined in Chapter 1. Comparing QPX cell number against the number of 18S rRNA gene copies in each reaction (determined from its C_T value based on the primary standard curve) provided an estimate of copy number of 18S rRNA genes per QPX cell.

qPCR assay using Laby-A and Laby-Y primers

DNA was extracted and purified from sediment and seawater samples collected from Raritan Bay and Peconic Bay following the protocol described in Chapter 1. Purified DNA was quantified with a Picogreen dsDNA quantification kit and diluted to produce template DNA with a concentration of 1 ng µl^{-1}. 1 ng DNA was used as template in qPCR assay with Laby-A (Table 1.1, Chapter1) and Laby-Y (5'- CWCRAACTTCCTTCCGGT -3') primers under the same conditions as those used in qPCR assay for QPX described in Chapter 1. The original abundance of labyrinthulomycetes amplified by Laby-A and Laby-Y primers in each sediment and seawater sample was determined as follows:

$$(\#Laby_{initial} \times a*)/(c \times d \times e) \text{ (equation 8)}$$

where *#Laby$_{initial}$* is the number of labyrinthulomycete 18S rRNA gene copies amplified by Laby-A and Laby-Y primers in the 1 ng assayed environmental DNA template (copy ng^{-1}) after correction for PCR inhibition; *a** is the total DNA content of each purified environmental DNA sample (ng); *c* is the estimated copy number of 18S rRNA region in each labyrinthulomycete (QPX) cell (copies cell^{-1}); *d* is the estimated DNA recovery rate of

the extraction method (5.38% for sediment samples and 9.51% for seawater samples based on estimations for QPX); and e is the volume of seawater (ml) or weight of sediment (mg) from which DNA was extracted.

Terminal restriction fragment length polymorphism (T-RFLP)

Part of the 18S rRNA gene was amplified for T-RFLP analysis with primer Laby-A labeled with (6)-carboxyfluorescein (FAM) and the labyrinthulomycete-specific primer Laby-Y labeled with hexachlorofluorescein (HEX). Each 50 µl PCR reaction contained 0.2 µM of each primer, 0.2 mM of each dNTP, 1.5 mM $MgCl_2$, 50 mM KCl, 30 mM Tris-HCl (pH 8.3), 1.25 U Taq DNA Polymerase (Eppendorf Inc., Westbury, NY or Qiagen, Valencia, CA), and 4 to 5 ng purified environmental DNA template. PCR amplifications were performed under the following thermal conditions: initial denaturation at 95 °C for 30 s, annealing at 55 °C for 1 min, and extension at 72 °C for 1 min for 40 cycles, followed by a final extension step at 72 °C for 10 min.

PCR products of 10 to 20 replicate reactions were pooled, purified and concentrated to 10 ng/µl with the Promega Wizard SV gel and PCR clean-up system following the manufacturer's protocol. Of each sample, 100 ng purified PCR product was digested with the restriction endonucleases *HaeIII* (Promega) or *Sau96I* (New England Biolabs) (in duplicate) in a total volume of 20 µl per reaction at 37 °C for 4 hr according to the manufacturer's instructions. Digested DNA was precipitated with 0.1 volumes 3M NaOAc (pH 5.2) and 2.5 volumes of cold 95% ethanol in the presence of glycogen (1 µg/µl) followed by centrifugation at $12,000 \times g$ for 20 min. Pelleted DNA was rinsed with 70% ethanol, air-dried and resuspended in 20 µl sterile water.

Digested DNA (2 µl) was combined with 0.5 µl GeneScan 600 LIZ size standard (Applied Biosystems, Foster City, CA) and 9.5 µl deionized formamide. The samples were analyzed using an ABI 3130XL DNA Sequence Analyzer in GeneScan mode (Applied Biosystems). All TRFLP electropherograms were visually inspected to check their quality. The size of the fragments and corresponding fluorescence intensities (peak height and area) were determined using Genemapper v3.5 (Applied Biosystems), with a baseline threshold of 150 fluorescence units. TRFs less than 70 bases were eliminated from all T-RFLP profiles to minimize the effect of leftover primer and primer dimer peaks.

T-RFLP data analysis

Further T-RFLP data processing was performed using T-REX software (Culman *et al*. 2009; http://trex.biohpc.org/). Firstly, signals were separated from noise based on a statistical theory proposed by Abdo *et al*. (2006). "True peaks" were identified as those with peak areas exceeding the standard deviation (assuming zero mean) computed over all peaks. Then, peaks were aligned automatically across all samples in each data set using T-Align function (Smith *et al.*, 2005). Briefly, the shortest T-RF across all samples was identified and tagged. Peaks within ± 0.5 bp were identified and grouped into a T-RF with that first peak. The next smallest peak across all samples not falling into the first T-RF was identified and tagged, and peaks within ± 0.5 bp were grouped with the second TRF. This process continued until all peaks were grouped into a T-RF. T-RFs labeled with 6-FAM or HEX were aligned separately by T-REX (fragments with the same length but labeled with different fluorescence are not grouped together). The independently produced duplicate T-RFLP profiles for each sample were aligned to create a single derived sample profile and peak areas were averaged over replicates. T-RF peak areas were transformed into relative units by dividing integrated T-RF peak areas by the cumulative peak area of each sample to account for differences in the

quantity of DNA between samples. Rare T-RFs, occurring in fewer than 5% of the samples in each analyzed data set (combined sediment and seawater data set, and separated sediment and seawater data sets for each enzyme), were excluded to reduce noise from inadequately sampled taxa.

Data output from T-REX were prepared for statistical analysis by creating a data matrix of T-RF (peak area) × sample. For non-metric multidimensional scaling (NMS), a T-RF profile matrix including T-RFs labeled with 6-FAM and T-RFs labeled with HEX was used as the main matrix. The second matrix included quantitative characteristics of the environment (temperature, salinity, and dissolved oxygen concentration), clam habitat (clam density and QPX prevalence determined by histology in local clams), and labyrinthulomycete community (T-RF richness and absolute abundance estimated by qPCR assay). All quantitative variables in the second matrix were relativized by dividing each data value by the maximum value of that variable to reduce the effect of extreme values. To enable the MRPP analysis described below, the second matrix also included categorical variables. Some categorical variables were based on the order of sampling time or the site of sample collection. The quantitative variables were ranked by dividing the relativized values into categories (Table 5.1) (McCune and Grace, 2002).

Sorensen distance and autopilot medium options were selected for NMS analyses of T-RFLP data using a random starting configuration and the software package PC-ORD (version 5.10) (McCune and Grace, 2002). Final ordinations were always two-dimensional solutions, and the two ordination axes were rigid-rotated for each analysis in PC-ORD to have Axis 1 express the highest proportion of variation among samples. Pearson correlation coefficients, which express the relationship between ordination scores and variables, were calculated (McCune and Grace, 2002). For all data sets, environmental variables having a Pearson $r \geq$ 0.3 or $r \leq$ -0.3 on at least one ordination axis were considered important contributors to ordination pattern. If $0.5 > r \geq 0.3$, or $-0.5 < r \leq -0.3$, the pattern is described as minor or the variable was considered as weakly correlated with the axis. If $r \geq 0.5$ or $r \leq -0.5$, the pattern is described as major, and the correlation as strong (Will-Wolf *et al.*, 2006).

Multi-Response Permutation Procedure (MRPP; McCune and Grace 2002) is a non-parametric test for multivariate differences between two or more groups of entities and was used for comparison of communities among groups within each categorical variable. The Sorensen distance measure was also used for MRPP analyses. Differences were considered statistically significant where $p < 0.05$.

Results

Quantification of labyrinthulomycetes in environmental samples using qPCR assay with Laby-A and Laby-Y primers

A SYBR Green real-time qPCR assay using Laby-A and Laby-Y primers was developed for quantification of labyrinthulomycete organisms in environmental samples. The primary standard curve constructed by 10-fold serial dilution of plasmid DNA containing a cloned QPX 18S rRNA gene showed a linear inverse relationship between C_T and the $\log_{10}$ number of plasmids described as $C_T = -2.60 \times \log_{10}$ (#initial 18S rRNA gene copy) + 35.43, determined from 6 independent experiment runs. The conservative detection limit of the assay was 100 copies of 18S rRNA gene per reaction, but in some experiment runs, the lowest detection limit was as few as 1 copies of 18S rRNA gene per reaction. The secondary standard curve was generated with reactions containing genomic template DNA equivalent to 0.5, 1, 5, 50, 500 and 5000 QPX cells (the same DNA used for estimating the number of

QPX ITS copies per cell in Chapter 1), and the 18S rRNA gene was estimated to be present at 537 ± 133 (Mean $\pm$ SD, n=4) copies in each QPX cell.

Sediment and seawater samples collected from site 1, 8, 18, 20 and 21 in Raritan Bay and a site in Peconic Bay from April to September in 2006 were assayed by qPCR for quantification of labyrinthulomycetes (Table 5.2). These samples were also used for detection and enumeration of QPX as described in Chapter 2 (Table 2.1). The thermal dissociation curves of products from control reactions with positive labyrinthulomycete templates (the plasmid standards, genomic DNA purified from QPX isolates, *Thraustochytrium aureum* (ATCC34304) and *Schizochytrium aggregatum* (ATCC28209)) contained a single peak at 83.5 to 84.5 °C (Fig. 5.1A), indicating that there was a single and specific amplification product, with no unspecific amplicon or primer dimer. In 20 of 29 sediment samples and 20 of 30 seawater samples, the qPCR assay generated specific amplicons with single peaks (83.4 to 84 °C) in dissociation curve analysis, consistent with the control labyrinthulomycete templates (Fig. 5.1B). The abundance of labyrinthulomycetes in those 20 sediment samples was estimated to range from 83 to 824 18S rRNA copies per ng sediment DNA extract or 2 to 75 (overall average 33 ± 24) cells per mg sediment (Table 5.2). The abundance of labyrinthulomycetes in the 20 seawater samples was estimated to range from 77 to 738 18S rRNA gene copies per ng seawater DNA extract or 3 to 56 (overall average 25 ± 16) cells per ml seawater (Table 5.2). In the other 9 sediment and 10 seawater samples, the dissociation curve analysis showed melting peaks of amplification products at 75 to 76 °C which likely indicated primer dimer or other undesired amplification products (e.g. peak 1 in Fig. 5.1C). Although in some of these samples (1 of 9 sediment and 5 of 10 seawater samples), melting peaks at 83 to 84 °C were also found, consistent with amplification of 18S rRNA gene of labyrinthulomycetes (e.g. peak 2 in Fig. 5.1C), the fluorescence from undesired amplification products could not be distinguished from the intended products. The abundance of labyrinthulomycetes in these 9 sediment and 10 seawater samples was estimated to be below the detection limit of the qPCR assay, which was 7.4 ± 5.9 cells per mg sediment or 7.4 ± 3.3 cells per ml seawater, taking 100 18S rRNA gene copies per reaction (per ng DNA extract) as the lowest reliable detection limit. There was no clear pattern of the estimated labyrinthulomycete abundance with either sampling time or sampling site.

T-RFLP profiles

A total of 116 T-RFLP profiles (after averaging replicate profiles) of the Laby-A to Laby-Y region of 18S rRNA genes of labyrinthulomycetes from sediment (58 profiles from 29 samples) and seawater (58 profiles from 29 samples) collected from Raritan and Peconic Bays in 2006 were obtained using *HaeIII* and *Sau96I* endonucleases. Most T-RFs ranged in size from 70 to 295 bases. After automatic alignment by T-Align (Smith *et al.*, 2005) with a tolerance limit of ± 0.5 base, 70 and 84 T-RFs (operational taxonomic units) were found in sediment and seawater samples, respectively, for the *HaeIII* data set (Table 5.3), with 43 fragments found in both sample types. For the *Sau96I* data set, 58 different T-RFs were identified for the sediment samples and 90 T-RFs for the seawater samples, with 36 fragments in common. Generally, the seawater samples had more T-RFs and higher percentage of unique T-RFs than the sediment samples, regardless of the endonuclease (Table 5.3).

Non-metric Multidimensional Scaling and Multi-Response Permutation Procedure analysis of T-RFLP profiles

Labyrinthulomycete communities in Raritan and Peconic Bay sediment and seawater samples collected in 2006 were compared through NMS analysis of T-RFLP profiles for both restriction enzymes (Fig.5.2A and B). NMS showed a distinct separation between sediment and seawater samples: communities in the sediment were grouped on the left of Axis 1 and communities in the seawater samples were grouped on the right of the Axis 1, except for one sediment sample collected from site RB1 in August, which was grouped with the seawater samples. Axis 1 accounted for 91% of the total variation for the *HaeIII* data set and 89% for the *Sau96I* data set. T-RF richness was positively correlated with Axis 1 with similar magnitudes (0.65 for *HaeIII* and 0.62 for *Sau96I*; Table 5.4) for both enzymes, indicating that the number of T-RFs in the samples was the most important contributor to the distribution pattern of the samples along Axis 1. Symbol sizes in Fig. 5.2A and B indicate the relative temperature of the samples. The increase in symbol size toward the top of Axis 2 in Fig. 5.2B suggested an effect of temperature on community structure (r = 0.44; Table 5.4), but this ordination axis only represented 9% of the total variation in the *Sau96I* data set.

Sediment and seawater data sets were also analyzed separately. For labyrinthulomycete communities in sediment, the NMS ordinations (Fig. 5.2C and D) represented 95% of the variation, with 69% on Axis 1 and 26% on Axis 2 for *HaeIII* and 68% and 27% on the two axes for *Sau96I*, respectively. Although NMS did not clearly separate sediment communities by time of sampling, responses of labyrinthulomycete communities to the seasonal gradient were observed with samples from early Spring (April) on the upper portion of Axis 2 and samples from early fall (September) on the bottom of Axis 2. Temperature and dissolved oxygen concentration were the factors most strongly correlated with Axis 2 (temperature at -0.54 and -0.59, DO at 0.46 and 0.48; Table 5.4). For labyrinthulomycete communities in seawater samples, NMS ordination explained 96% of the total variation in the *HaeIII* data set, with 77% on Axis 1 and 19% on Axis 2. For the *Sau96I* data set, 57% of total variation was explained by Axis 1 and 38% by Axis 2. The NMS diagrams (Fig. 5.2 E and F) clearly showed that labyrinthulomycete communities in April, May and June were grouped separately from those in August and September, with most of the samples from earlier seasons (April to June) arranged on the left and later seasons (August and September) on the right along ordination Axis 1. Pearson correlation coefficients showed temperature (0.55 and 0.61 on Axis 1, Table 5.4) and TRF richness (0.89 for *HaeIII* and 0.71 for *Sau96I* on Axis 2, Table 5.4) as the most important factors influencing the location of samples in ordination space. Salinity and clam density were also weakly correlated with Axis 1 and Axis 2 for both data sets (Table 5.4). For *Sau96I*, a weak positive correlation also existed between the abundance of labyrinthulomycetes and ordination Axis 2 (0.42, Table 5.4).

An MRPP test was applied to identify statistically significant differences among different categories of each variable, based on the results from the NMS ordinations (Table 5.5). When communities in sediment and seawater samples were analyzed together, the composition of labyrinthulomycete communities in sediment samples was significantly different from seawater samples (p<0.0001, Table 5.5). Seasonal differences in the structures of labyrinthulomycete communities were statistically significant when sediment and seawater communities were ordinated separately (but not together, Table 5.5). TRF richness was associated with a statistically significantly difference (p<0.05) in the composition of labyrinthulomycete communities in all data sets except for the sediment data set based on *Sau96I* (Table 5.5). MRPP tests also showed significant differences among communities with different labyrinthulomycete abundance (determined by qPCR assay) in the sediment data

sets and for all samples combined for both enzymes. In contrast, labyrinthulomycete communities did not differ at different sites or with clam density. In addition, the MRPP test showed no significant difference in composition of labyrinthulomycete communities associated with QPX prevalence determined by histology (Table 5.5).

Indicator species analysis

The MRPP test showed a statistically significant difference between labyrinthulomycete communities in sediment and seawater samples (Table 5.5), and the first axis in NMS ordinations (Fig. 5.2A and B) was the most important for these patterns. For the *HaeIII* data set, 39 sediment T-RFs and 56 seawater T-RFs had a Pearson correlation efficient of $r^2 \geq 0.1$ with Axis 1, among which 27 T-RFs were found in both sample types. For the *Sau96I* data set, 40 and 64 T-RFs had a Pearson correlation efficient of $r^2 \geq 0.1$ with Axis 1 in sediment and seawater samples, respectively, with 27 T-RFs found in both sample types. To identify the T-RFs contributing most to the differences between labyrinthulomycete communities in sediment versus seawater, the 20 T-RF peaks with the highest correlation strength (Pearson's r^2) with Axis 1 for each enzyme were examined (Table 5.6a and b). For the *HaeIII* data set, 3 T-RFs labeled by Laby-A (B89, B105, B133; Table 5.6a) and 2 T-RFs labeled by Laby-Y (G86 and G105, Table 5.6a) only occurred in seawater samples, and no T-RFs occurred only in sediment. For the *Sau96I* data set, six T-RFs (B85, B86, B104, B105, G86 and G106 Table 5.6b) were unique to seawater samples while none were unique to sediment samples.

Significant differences were also found among communities from different seasons in both sediment and seawater samples (Table 5.5). For sediment samples, temperature and dissolved oxygen, environmental variables closely associated with seasonal change (Fig. 2.3), were correlated with Axis 2 in NMS ordinations (Fig. 5.2C and D, Table 5.4). 25 and 24 TRFs in *HaeIII* and *Sau96I* data sets, respectively, had Pearson correlation efficient $r^2 \geq 0.1$ with Axis 2 (Table 5.6a and b). For seawater samples, the ordination axis associated with temperature was Axis 1 (Fig. 5.2E and F, Table 5.4). 71 (*HaeIII*) and 55 TRFs (*Sau96I*) had Pearson correlation efficients $r^2 \geq 0.1$ with Axis 1. The 20 T-RF peaks with the strongest correlation with NMS Axis 2 for the sediment data sets and the 20 T-RF peaks with the strongest correlation with NMS Axis 1 for the seawater data sets are also listed in Table 5.6a and b.

Discussion

Ideally, primers chosen for qPCR assay and T-RFLP analysis should be specific to the targeted labyrinthulomycetes yet sufficiently general so that they can amplify all labyrinthulomycete subgroups. Primers Laby-A and Laby-Y were originally designed by Stokes *et al.* (2002) and intended to specifically amplify a ~430 bp fragment of labyrinthulomycete 18S rDNA. Comparison of available 18S rRNA sequences of labyrinthulomycetes and other heterokonts suggested that Laby-A would probably amplify most other heterokonts, and perhaps other eukaryotes, while Laby-Y was specific to labyrinthulomycetes in that it perfectly matched many labyrinthulomycete 18S rDNA sequences but not those of any other eukaryotes (Collado-Mercado *et al.*, 2010). Collado-Mercado *et al*. (2010) found that 75 Laby-A/Laby-Y cloned amplicons from sediment samples collected from Port Jefferson Harbor and Peconic Bay grouped with labyrinthulomycetes in phylogenetic analysis, suggesting that the combination of Laby-A and Laby-Y primers was specific to labyrinthulomycetes. However, the alignments also suggested that Laby-Y did not match all labyrinthulomycetes, and probably could not amplify some subgroups within the thraustochytrid phylogenetic group (TPG) (Collado-

Mercado *et al.*, 2010). In this study, we were actually assessing the abundance and diversity of those labyrinthulomycetes that could be amplified by Laby-A and Laby-Y primers, but probably not all labyrinthulomycetes. Thus, the results may underestimate the abundance and diversity of labyrinthulomycetes in the environment.

Quantification of labyrinthulomycetes in environmental samples using qPCR assay with Laby-A and Laby-Y primers

The development of the qPCR assay with Laby-A and Laby-Y primers for quantification of labyrinthulomycetes followed the same protocol used for development of the qPCR assay for QPX enumeration described in Chapter 1. It used QPX as a representative species to construct primary and secondary standard curves, and also applied the DNA recovery rates estimated for QPX (Chapter 1) to estimate the abundance of labyrinthulomycetes in sediment and seawater samples. The primary standard curves using plasmid DNA containing a cloned QPX 18S rRNA gene showed a relatively high variability among runs compared with the qPCR assay for QPX detection. Although the detection limit could reach as few as 1 copy per reaction in some runs (data not shown), we used 100 18S rRNA gene copies per reaction as the conservative reaction detection limit to estimate the detection limit for labyrinthulomycetes in each environmental sample. It is unknown what caused this run to run variation among standard curves. More experimental runs and optimized PCR conditions will be required to reduce the run to run variation and achieve more reproducible standard curves.

Based on secondary standard curves (N=4) from the same QPX genomic DNA dilutions as used in Chapter 1, the qPCR assay with Laby-A and Laby-Y primers estimated that there were 537 ± 133 18S rRNA gene copies in each QPX cell, while the qPCR assay with 5.8S24For and QPX-ITS2-R2 primers estimated the value to be 181 ± 68 ITS copies per QPX cell. The 18S rRNA gene and ITS region are expected to have the same copy number since they are closely linked in the rRNA gene array. The nearly 3-fold difference in the estimated copy number of rRNA genes between the two qPCR assays was likely to be associated with the high variability of ITS2 region in QPX (Qian *et al.*, 2007). Although some degeneracy was included in primer QPX-ITS2-R2 (Table 1.1), in order to cover as much variation within the primer site as possible (QPX-ITS2-R2 perfectly matches 23 of 26 sequence types presented in Fig. 3 in Qian *et al*. 2007), the fact that qPCR assay with 5.8S24For and QPX-ITS2-R2 primers only amplified around one third of the ITS copies suggests that there may be more ITS2 sequence types in QPX than reported.

A possible complication with using our qPCR assay to estimate cell abundance of labyrinthulomycetes is that the copy number of rRNA genes may vary among different species. The number of rRNA copies per cell varies over a wide range in marine protists, from a few copies for microalgae (Zhu *et al.*, 2005), to around 1000 copies for a nanoplanktonic dinoflagellate (Galluzzi *et al.*, 2004). To our knowledge, besides QPX, there has been no estimate of the number of rRNA gene copies for other labyrinthulomycete species. rRNA copy number does appear to be correlated with genome size (Prokopowich *et al.*, 2003). Our estimated QPX genome size of approximately 251 Mbp (see discussion in Chapter 1) is 20- to 25-fold greater than the genome sizes recently estimated by PFGE for four other thraustochytrids (Anbu *et al.*, 2007), suggesting that our estimated rRNA copy number per QPX cell might also be greater than other labyrinthulomycetes, or at least thraustochytrids. Thus, using the value of rRNA gene copy number in QPX as a representative for labyrinthulomycete communities may underestimate the cell abundance of these diverse protists in the environment. Also, the DNA recovery rates of other

labyrinthulomycetes from sediment and seawater may be different from those for QPX, and vary among different species. Further work will be required to determine the copy number of rRNA gene and DNA recovery rates for more labyrinthulomycete species, particularly for typical species from different genera or subgroups that are most abundant in the environment.

Thermal dissociation curve analysis is often used to examine the specificity of amplification in qPCR assays. In our qPCR assay with Laby-A and Laby-Y primers, the dissociation curves for reactions with positive labyrinthulomycete templates and with most environmental samples contained a single peak at 83.5 to 84.5 °C, indicating specific amplification of labyrinthulomycete 18S rDNA. In some samples, the dissociation curves showed a peak at 75 to 76 °C that was associated with primer dimer or other undesired amplification products. Although primers Laby-A and Laby-Y appear to be strictly specific to labyrinthulomycetes and produce ~430 bp fragments of 18S rRNA for all sequenced labyrinthulomycetes (Stokes *et al.*, 2002; Collado-Mercado *et al.*, 2010), there may be undiscovered organisms in the environment that also have matching sites with this primer pair. Cloning and sequencing the unspecific amplicons would be required to determine whether they were from primer dimer or from DNA of other organisms. If the peak at 75 to 76 °C was the only peak present, these reactions were easily determined to be negative for labyrinthulomycetes. However, in some complicated cases, both peaks were present. As SYBR Green binds to all dsDNA, the quantification results of these reactions were calculated from the fluorescence signals including those associated with the targets (18S rRNA gene of labyrinthulomycetes) and those associated with the non-targets (primer dimer and/or genes of other organisms). Because it is impossible to distinguish the fluorescence associated with the intended products from that associated with the undesired amplification product, in our study, results of these reactions were also counted as negative for labyrinthulomycetes which likely underestimated the abundance of labyrinthulomycetes in these samples.

Despite the likelihood that the qPCR assay with Laby-A and Laby-Y primers may underestimate the abundance of labyrinthulomycetes, the qPCR-based labyrinthulomycete abundance estimates for the labyrinthulomycete-positive sediment samples (overall average 25 ± 16 cells mg^{-1}; Table 5.2) were mostly higher than the reported density of thraustochytrids in Mediterranean Sea benthic habitats (0.7-13.4 cell mg^{-1}) estimated by AfDD method (Bongiorni *et al.*, 2005), and fell in the same range reported in mangrove leaf detritus by MPN method (18- 25 cells mg^{-1} dry wt detritus) (Raghukumar *et al.*, 1995). In seawater, our qPCR assay detected labyrinthulomycetes at an average abundance of 25 ± 16 cells ml^{-1} (ranging from 3 to 56 cells ml^{-1}, Table 5.2). This estimate was comparable to those reported based on AfDD method in the Sea of Japan (average 16 cell ml^{-1}) by Kiruma *et al.* (1999) and coastal Seto Inland Sea (10 cell ml^{-1}) (Naganuma *et al.*, 1998), but lower than those in some samples collected from the Arabian Sea (40-230 cells ml^{-1}) (Raghukumar *et al.*, 2001). There have been very few reports about spatial and temporal patterns in the abundance of labyrinthulomycetes. Bongiorni and Dini (2002) reported that sandy coastal sediment in the Mediterranean sea had the highest thraustochytrid abundance in late spring. They also reported higher thraustochytrid abundance and biomass in a seagrass meadow and nearby unconsolidated sediment due to the input of fish farm wastes, which suggested a positive relationship between thraustochytrid abundance and sediment organic matter content. Raghukumar *et al*. (2001) observed a strong seasonality of thraustochytrid abundance in the water column, with increased abundance toward the end of phytoplankton blooms. However,

in our study, no seasonal or spatial trend was observed in the abundance of labyrinthulomycetes determined by qPCR assay.

Response of labyrinthulomycete community to environmental variables

    T-RFLP analysis is a popular high-throughput fingerprinting method used to monitor changes in the structure and composition of microbial communities. Differences in the sizes of T-RFs reflect differences in the sequences of 18S rRNA genes (i.e., sequence polymorphisms), which are often associated with phylogenetically distinct groups of organisms. Thus the pattern of T-RFs in a sample is a composite of DNA fragments with unique lengths that reflect the composition of the dominant members of the community; in our case, the different phylogenetic subgroups of labyrinthulomycetes.

    NMS is one of the most robust ordination procedures for analyzing T-RFLP data (Culman *et al.*, 2008). It does not make any assumptions about the distribution of the input variables or their relationships to one another, making it more appropriate for T-RFLP community analysis. In Fig 5.2A and B, the first ordination axes captured most of the variation in T-RFLP, and showed a positive correlation with the T-RF richness, an index of diversity. Since seawater samples had many more T-RFs compared to the sediment samples for both endonucleases, T-RF richness strongly contributed to the separation of the samples from sediment verse seawater in the NMS ordination. The NMS ordination results and subsequent MRPP analysis (Fig. 5.2, Tables 5.4 and 5.5) supported that habitat (sediment versus seawater) is the major determinant of species composition for labyrinthulomycete communities in Raritan and Peconic Bays.

    Seasonal factors seemed to structure labyrinthulomycete communities in sediment and seawater. In temperate coastal environments such as Raritan and Peconic Bays, environmental factors that are strongly seasonal include temperature and dissolved oxygen. The NMS analysis of sediment data (Fig.5.2C and D) showed that temperature and dissolved oxygen concentration were the environmental variables most strongly related to the distribution of samples along Axis 2, although this ordination axis only represented 26 and 27% of total variation in the *HaeIII* and *Sau96I* data sets, respectively. MRPP analysis showed significant differences among sediment samples collected in different seasons. A seasonal pattern in thraustochytrid taxonomic composition was reported by Bongiorni and Dini (2002) in two sandy habitats in the Mediterranean Sea, based on AfDD method. They suggested that the seasonal changes were probably due to the major role played by temperature in regulating thraustochytrid proliferation in sediment. The labyrinthulomycete community structure in sediments also appears to be related to organic matter content. Bongiorni *et al.* (2005) studied the response of benthic labyrinthulomycetes to fish farm impact in seagrass and soft bottom sediments, and found that the labyrinthulomycete community in sediment impacted by biodeposition was dominated by smaller cells than less organic-rich sediments, indicating a change of species composition. Among the six sampling sites in Raritan and Peconic Bay included in T-RFLP analysis, sites having muddy bottom sediment (e.g. RB20, PB) are likely to have higher organic matter content than those having sandy sediment (RB1), and sites supporting higher clam density (e.g. RB20, RB21) probably have higher organic matter content than those supporting relatively low clam density (RB1, RB18). However, clam density was not strongly related to any NMS ordination axis and there was no significant difference in labyrinthulomycete communities among different sites or sites categorized by clam density (Tables 5.4 and 5.5). Overall, labyrinthulomycete community structure in the sediment samples did not show a spatial pattern in this study.

MRPP tests showed significant differences among seawater samples collected from different seasons. In the NMS diagrams, labyrinthulomycete communities in April, May and June were grouped separately from those in August and September along Axis 1 (Fig. 5.2E and F), and temperature was strongly correlated with Axis 1. The particulate and/or dissolved matter from phytoplankton or degradation of phytodetritus seems to play a role in supporting thraustochytrid proliferation in coastal areas (Raghukumar, 2002). A positive correlation between thraustochytrids and chlorophyll a concentrations or phytoplankton cells was detected by Naganuma *et al*. (1998), but such correlation was not detected by Kimura *et al*. (1999) in the Seto Inland Sea water or by Bongiorni and Dini (2002) in Mediterranean sea water. Strong seasonality of labyrinthulomycete species composition (and abundance) in the water column may reflect the dependence of labyrinthulomycetes on POM produced by seasonal phytoplankton blooms (Gaertner and Raghukumar, 1980; Raghukumar *et al*., 2001). In this study, it was unfortunate that neither phytoplankton chlorophyll concentration nor POM in the water were measured. Based on the annual reports of phytoplankton blooms prepared by the New Jersey Department of Environmental Protection (NJDEP) (http://www.nj.gov/dep/wms//bmw/reports.htm) in the Raritan Bay area from 2002 to 2005, phytoplankton blooms could be expected to happen during two periods between May and September: one in spring (May to June) dominated by dinoflagellates, and the other in mid-late summer (late July-early September) dominated by mixed diatoms. It is unknown whether the observed seasonal pattern in the labyrinthulomycete community in the NMS ordination (samples from April, May and June grouped separately from those in August and September) is related to the potential difference in species dominance of the phytoplankton bloom in different seasons or is independently driven by external environmental factors, such as temperature. Further detailed studies will also be needed to detect whether there are some biochemical components of particulate and/or dissolved organic matter from the phytoplankton bloom that are particularly responsible for the changes of labyrinthulomycete community in seawater (and in sediment). In the MRPP tests, no significant difference in seawater labyrinthulomycete communities among different sites or sites in different categories of clam density was detected. Clam density showed a weak correlation with Axis 2 in NMS ordination, but Axis 2 only explained 19 or 38% of total variation (Fig 5.2E and F), suggesting that the spatial pattern in labyrinthulomycete community structure in seawater samples was minor compared to temporal variation. As an index of community diversity, T-RF richness in seawater samples was strongly related to the distribution of samples along Axis 2. Since the seasonal pattern in NMS ordination was observed along Axis 1, labyrinthulomycete species richness seemed to have no distinct temporal pattern.

Labyrinthulomycete community structure was not related to the prevalence of QPX disease in clams in either NMS or subsequent MRPP analysis. QPX prevalence was determined by the histological method, which significantly underestimates QPX prevalence compared to qPCR assay (Chapter 2). Unfortunately, QPX prevalence determined by qPCR assay, which may be a better variable representing the severity of QPX disease in the clam samples, was only available for 3 sampling sites.

Identification of indicator groups in labyrinthulomycete communities

In silico TRFLP simulations were carried out for FAM-labeled Laby-A and HEX-labeled Laby-Y primers and either *HaeIII* or *Sau96I* restriction enzymes using previously published labyrinthulomycete 18S rRNA sequences. The predicted T-RF lengths of 53

representative species of 27 major phylogenetic subgroups of labyrinthulomycetes described by Collado-Mercado *et al.* (2010) are listed in Appendix 5.1.

Lengths of fluorescently labeled T-RFs were determined by capillary electrophoresis and comparison with an internal size standard run with each sample. Accurate fragment size determination is important, since one of our goals was to identify those labyrinthulomycete subgroups or species that have important contributions to the community composition by matching the sizes of observed T-RFs with the T-RF sizes predicted *in silico* from 18S rRNA gene sequences. The fluorophore attached to a T-RF affects its electrophoretic mobility, and the different dyes have different effects, causing errors in determining fragment sizes (Tu *et al.*, 1998). The sizes of T-RFs labeled with 6FAM or HEX are often underestimated, probably because DNA fragments labeled with a fluorescein dye, such as 6FAM and HEX, migrate faster than DNA fragment of the internal size standard (LIZ 600). In our preliminary experiment, the observed T-RFs of *in vitro* cultured QPX, *Thraustochytrium aureum* (ATCC34304) and *Schizochytrium aggregatum* (ATCC28209) were often 2-5 bases shorter than the T-RFs predicted from their sequences available in Genbank (Liu, unpublished data), which was consistent with the trends observed by Schutte *et al*. (2008). However, there is no way to correct for these migration discrepancies because the magnitude of the discrepancy is not constant across fragment sizes (Hahn *et al.*, 2001) and can be influenced by sequence composition (Kaplan and Kitts, 2003). In addition, run-to-run variability in T-RFLP analysis can also cause differences in estimated sizes of T-RF fragments from the same labyrinthulomycete species, although the consistent application of the automated procedure of aligning the T-RFs within ± 0.5 bp across all data sets probably allows an objective statistical analysis. Based on our preliminary results and previous studies which reported a range from 0 to 4 bases discrepancy between predicted and observed T-RF sizes (Wise and Osborn, 2001; Enright *et al.*, 2007), in this study, a conservative range of discrepancies between predicted and observed T-RF sizes of 0-5 bases was allowed to indentify plausible members of labyrinthulomycete communities (Appendix 5.1a and 5.1b). The possible contribution of each species and subgroup of labyrinthulomycetes to differences in community structure was evaluated based on the comparison of its predicted T-RFs and the observed T-RFs for both primers and both enzymes (Table 5.7).

Five species of 3 subgroups of labyrinthulomycetes possibly were not important contributors to any change of community structure (Table 5.7) because at least one of the four predicted T-RFs for each species was unique to this particular labyrinthulomycete, but not recognized to match any of those observed T-RFs that contribute to ordination patterns (Pearson correlation efficient $r^2 \geq 0.1$) (Appendix 5.1). Among the 40 observed T-RFs with the highest correlation coefficients with Axis 2 in sediment samples (both enzymes combined), 20 T-RFs (Table 5.6) contributed only to the seasonal pattern in sediment samples and not to other patterns. They possibly matched the predicted T-RFs from 37 representative species, covering a majority (23 of 27) of phylogenetic subgroups of labyrinthulomycetes in our database (Table 5.7). On the other hand, 6 observed T-RFs (*HaeIII*-B79, -G78 -G86 and *Sau96I*-B72, -B79 –B108; Table 5.6) exclusively contributed to the seasonal pattern in seawater samples, and possibly matched predicted T-RFs of 7 labyrinthulomycete species (6 *Aurantiochytrium spp*. and 1 *Thraust pachydermum spp.*; Table 5.7). Five of these 7 species may also have been important contributors to the seasonal pattern in the sediment samples, including four species from *Aurantiochytrium* subgroup and QPX. There are 10 representative species from 7 subgroups of labyrinthulomycetes including

3 *Aurantiochytrium* species, 2 *uLa5* species and 1 species each of subgroups *Labyrinthula, Oblongichytrium sp?*. *Sycioidochytrium uLa* 3 and 1 species between subgroups *uTH2* and *Aurantiochtyrium* possibly contributing to the difference in the community structure between sediment and seawater samples, but each of them was also a possible important contributor to the seasonal trends in either sediment or seawater samples. Among these subgroups, the *Oblongichytrium sp.?* group and the novel *uLa3* subgroup have been reported from sediment samples collected from Port Jefferson Harbor and Peconic Bay, and *uLa5* group consists of three species found in seawater samples (2 from Peconic Bay water and one from Mediterranean Sea surface water) (Collado-Mercado *et al.*, 2010), but no species were found exclusively contributing to the difference in labyrinthulomycete community between sediment and seawater samples.

Among the observed T-RFs having important contributions to either seasonal patterns or habitat differences, a majority did not match any predicted T-RFs of previously published labyrinthulomycetes. There were more unrecognized T-RFs among the important TRFs in the seawater data sets compared to the sediment data sets (16 vs 12 for *HaeIII* and 14 vs 7 for *Sau96I,* Table 5.6). These results suggested that species which have not been sequenced are an important component of the labyrinthulomycete community, particularly in seawater samples, and probably play an important role in determining the community structure in different habitats or in different seasons.

Sharing similar T-RFs, QPX of subgroup *T. pachydermum*, along with several representative species of *Aurantiochytrium* are the only indentified possible important contributors to the seasonal pattern in labyrinthulomycete community structure in seawater samples. As previously discussed, the sequences of the subgroup of *Aurantiochytrium* have 1-3 bases mismatched with primer Laby-Y, and possibly could not be amplified with Laby-A and Laby-Y primers in PCR. However, a few specific observed T-RFs among those important T-RFs for seasonal or habitat pattern in environmental samples, such as *HaeIII*-G72, -G86, -G87 and *Sau96I*-B71, -B72, did not match the predicted T-RFs of any labyrinthulomycete, except some species of *Aurantiochytrium*, preventing us from excluding the presence and contribution of this subgroup without further studies, although these specific observed important T-RFs could also be generated by other unpublished species (from other subgroups). Based on only T-RFLP results in this study, we cannot determine the presence of QPX or how much QPX contribute of QPX as a component of labyrinthulomycete community in the environment.

Table 5. 1. Categorization of environmental variables for nonmetric multidimensional scaling (NMS) and MRPP analysis. Clam density, QPX prevalence, TRF richness and labyrinthulomycete abundance determined by qPCR were categorized based on the relativized data (the original value for each sample divided by the maximum value of the variable).

Group#	Categorical variable						
	Sample type	Season	Site	Clam density	QPX prevalence	TRF richness	Labyrinthulomycete abundance by qPCR
1	sediment	April	RB1	0-0.10	0	0-0.20	BDL[a]
2	seawater	May	RB8	0.11-0.20	0.1-0.25	0.21-0.40	0.01-0.20
3		June	RB18	0.21-0.30	0.26-0.5	0.41-0.60	0.21-0.40
4		August	RB20	0.30-1	0.5-1	0.61-0.80	0.41-0.60
5		September	RB21			0.81-1	0.61-0.80
6			PB				0.81-1

[a] below detection limit of qPCR assay with Laby-A and Laby-Y primers.

Table 5. 2. Labyrinthulomycete abundance estimated by the qPCR assay using Laby-A and Laby-Y primers in sediment and seawater samples collected from 6 sampling sites in Raritan Bay (RB) and Peconic Bay (PB), New York, in 2006

Sampling site	Labyrinthulomycete abundance in sediment (18S rRNA copies ng^{-1} DNA extract/ cells mg^{-1})					Labyrinthulomycete abundance in seawater (18S rRNA copies ng^{-1} DNA extract /cells ml^{-1})				
	April	May	June	August	September	April	May	June	August	September
RB 1	111[a]/32[b]	153/2	111/11	140/9	0/0	0/0[c]	0/0	738/25	131/53	132/19
RB 8	254/31	0/0	1440/20	-[d]	0/0	299/21	0/0	237/8	142/26	0/0
RB 18	0/0	106/19	325/73	185/52	0/0	0/0	0/0	0/0	417/52	0/0
RB 20	152/16	118/22	83/62	224/63	0/0	223/21	461/56	0/0	159/17	224/53
RB 21	824/61	106/6	185/75	149/21	394/44	269/19	0/0	164/12	177/28	268/14
PB	139/18	180/18	0/0	0/0	0/0	212/22	77/22	176/3	191/12	141/23
Average	269 ± 321 / 33 ± 24 [e]					242 ± 150 / 25 ± 16[f]				

[a] Labyrinthulomycete 18S rRNA copies per ng DNA extract; 0 indicates below the detection limit of 100 copies.

[b] Labyrinthulomycete cells mg^{-1} sediment calculated by equation 8 where $a*$ equals to the total DNA content of each purified sediment DNA sample (ng); c= 537 copies per cell, d=5.38% and e varied among samples from 500 to 850 mg. 0 indicates below the detection limit of 7.4 ± 5.9 cells mg^{-1} sediment.

[c] Labyrinthulomycete cells ml^{-1} seawater calculated by equation 8 where $a*$ equals to the total DNA content of each purified seawater DNA sample (ng); c= 537 copies per cell, d=9.51 % and e varied among samples from 400 to 700 ml. 0 indicates below the detection limit of 7.4 ± 3.3 cells ml^{-1} seawater.

[d] No data available

[e] Averaged estimated labyrinthulomycete abundance (Mean ± STD) over the 20 positive sediment samples

[f] Averaged estimated labyirnhtulomycete abundance (Mean ± STD) over the 20 positive seawater samples
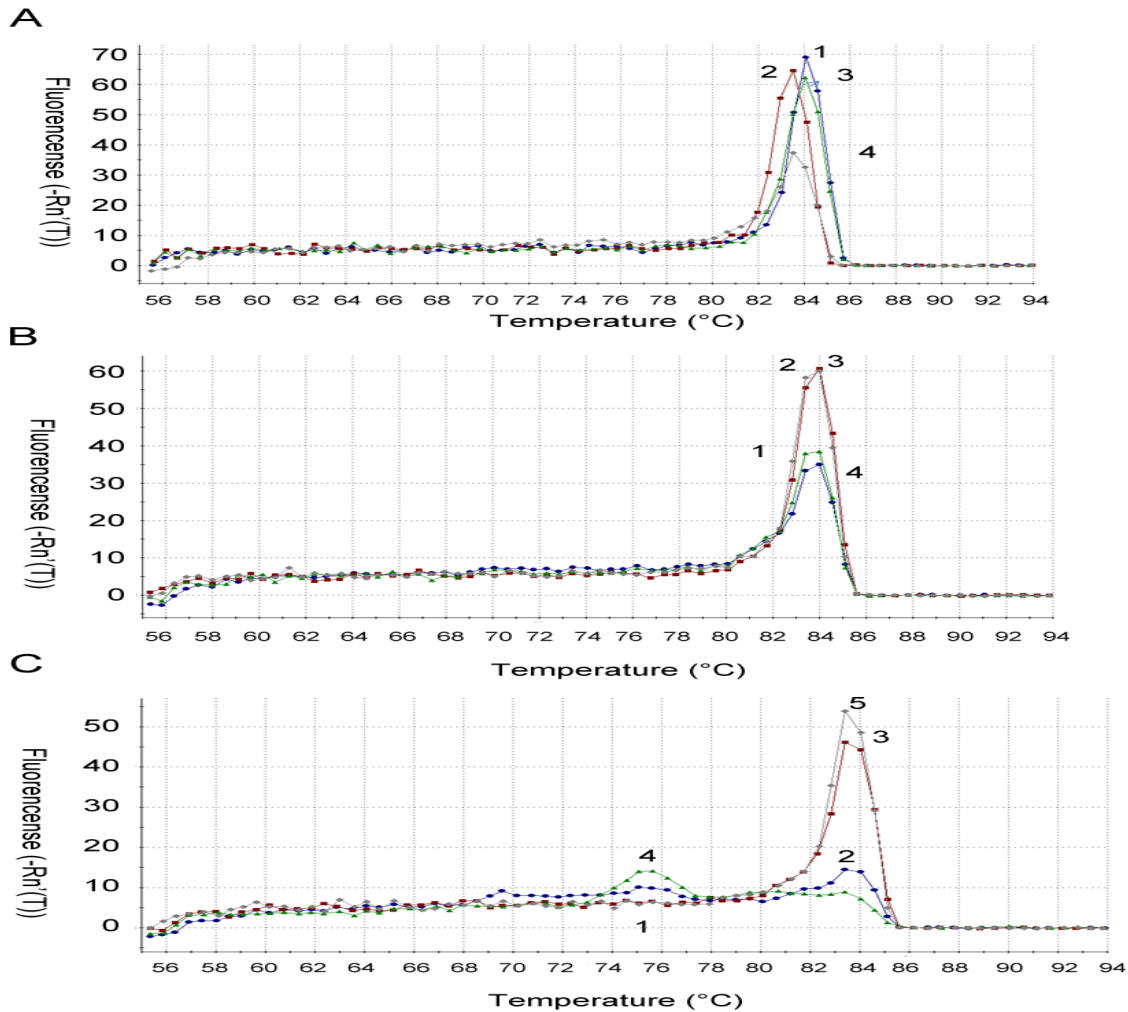
Figure 5. 1. Thermal dissociation curves of qPCR assay with Laby-A and Laby-Y primers.

(A) Control labyrinthulomycete-positive templates. Peak 1 at 84.1 °C (blue circles): plasmids containing cloned QPX 18S rRNA gene; Peak 2 at 83.5 °C (red rectangles): genomic DNA of QPX cells; Peak 3 at 84.0 °C (green triangles): genomic DNA of *Thraustochytrium aureum* (ATCC34304) ; Peak 4 at 83.5 °C (gray diamonds): genomic DNA of *Schizochytrium aggregatum* (ATCC28209).

(B) Labyrinthulomycete-positive environmental samples. Peak 1 at 84.0 °C (blue circles): DNA of Seawater sample from site 20 in September (SWSep20); Peak 2 at 83.5 °C (red rectangles): DNA of SWSep20 spiked with 1000 copies of plasmids containing QPX 18S rRNA gene; Peak 3 at 83.4 to 84.0 °C (green triangles): DNA of sediment sample collected from site 20 in May (SEDMay20); Peak 4 at 83.4 to 84.0 °C (gray diamonds): DNA of SEDMay20 spiked with 1000 copies of plasmids containing QPX 18S rRNA

(C) Environmental samples considered as labyrinthulomycete-negative. Peak 1 at 75.1 °C and peak 2 at 83.4 °C (blue circles): DNA of Seawater sample from site 18 in September (SWSep18); Peak 3 at 83.4 °C (red rectangles): DNA of SWSep18 spiked with 1000 copies of plasmids containing QPX 18S rRNA gene; Peak 4 at 75.6 °C (green triangles): DNA of Seawater sample from site 8 in May (SWMay8); Peak 5 at 83.5 °C (gray diamonds): DNA of SWMay8 spiked with 1000 copies of plasmids containing QPX 18S rRNA gene.

Table 5. 3. T-RF richness in T-RFLP profiles generated from environmental samples for two restriction enzymes

	HaeIII			*Sau96I*		
	Sediment	Seawater	total	Sediment	Seawater	total
T-RFs	70	84	111	58	90	112
Unique T-RFs	27 (39%)	41(49%)	68	22 (38%)	54 (60%)	76
Shared T-RFs	43 (61%)	43 (51%)	43	36 (62%)	36(40%)	36
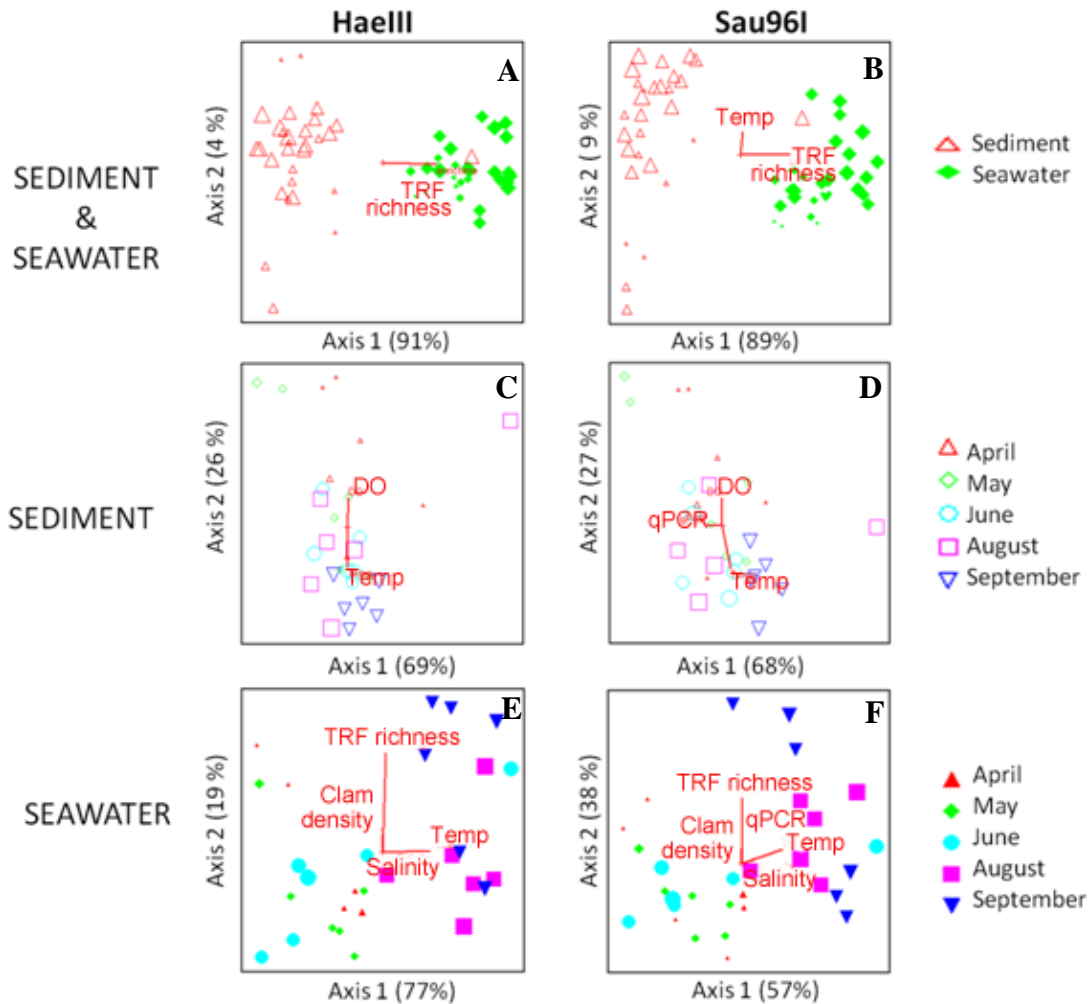
Figure 5. 2. NMS ordination of labyrinthulomycete communities in sediment (open symbols) and seawater (closed symbols). Vectors in the joint plots represent the environmental variables that have a Pearson r ≥ 0.3 or r ≤ -0.3 (also see Table 5.4), e.g. in Figure 5.2 (C), temperature (present as Temp) and dissolved oxygen concentration (present as DO) are two environment variables strongly correlated with Axis 2. Temperature is negatively correlated, having a Pearson r ≤ -0.3 and dissolved oxygen concentration is positively correlated, having a Pearson r ≥ 0.3. Symbol sizes increase with increasing temperature at the time the sediment and seawater samples were collected.

Table 5. 4. Pearson's r correlation coefficients for seven environmental factors with the axes of the non-metric multidimensional scaling (NMS) ordination for labyrinthulomycete communities as presented in Fig. 5.2. Pearson r ≥ 0.3 or r ≤ -0.3 are in bold.

| | SED and SW | | | | SED | | | | SW | | | |
| | HaeIII | | Sau96I | | HaeIII | | Sau96I | | HaeIII | | Sau96I | |
Axis	1	2	1	2	1	2	1	2	1	2	1	2
Temperature	-.113	-.139	.141	**.436**[a]	.041	**-.543**	.290	**-.587**	**.608**	.091	**.554**	.372
Salinity	-.056	.090	.076	.027	-.011	.056	-.082	-.032	**.333**	-.032	**.304**	.198
Dissolved oxygen	.013	.169	-.033	-.296	.141	**.459**	**-.050**	**.482**	-.060	-.094	-.282	.002
Clam density	.051	.150	-.052	.127	-.229	-.073	-.202	-.174	-.008	**.379**	-.062	**.334**
QPX prevalence	-.033	-.080	-.055	-.103	-.160	.011	-.159	.112	-.148	.032	-.041	.024
T-RF richness	**.646**	-.006	**.621**	.011	-.038	.102	.101	-.258	.165	**.889**	.026	**.707**
Labyrinthulomycete abundance	.156	.174	-.177	.046	-.181	.062	**-.336**	-.007	.169	.298	.051	**.415**

Table 5. 5. MRPP results from NMS analysis presented in Fig. 5.2. Comparisons were made between communities in sediment and seawater (sample type) and among sediment and seawater communities in different categories for each variable. *p<0.05, **p<0.01, ***p<0.001.

	SED and SW		SED		SW	
	HaeIII	*Sau96I*	*HaeIII*	*Sau96I*	*HaeIII*	*Sau96I*
Sample type	<0.0001***	<0.0001***	NA	NA	NA	NA
Season	0.1355	0.1158	0.0008***	0.0009***	<0.0001***	<0.0001***
Site	0.9982	0.9996	0.8975	0.8334	0.8867	0.8250
Clam density	0.8080	0.7794	0.5792	0.3856	0.4978	0.2774
QPX prevalence	0.9718	0.9686	0.5854	0.3538	0.9461	0.9464
TRF richness	<0.0001***	<0.0001***	0.0023**	0.2098	0.0104*	0.0014**
Labyrinthulomycete abundance	0.0262*	0.0132*	0.0147*	0.0065**	0.8790	0.6538

Table 5. 6. The T-RFs with the highest correlation strength with NMS ordination axis 1 in the sediment and seawater combined data set, axis 2 in the sediment data set and axis 1 in the seawater data set for each of *HaeIII* (a) and *Sau96I* (b). T-RFs in bold match the predicted T-RFs of previously published labyrinthulomycete sequences.

a			*HaeIII*		
Observed T-RF size	% SED samples peak found in	% SW samples peak found in	Correlation coefficient with axis 1 in SED&SW data set	Correlation coefficient with axis 2 in SED data set	Correlation coefficient with axis 1 in SW data set
B71[a]	60%	100%	0.89		
B79	43%	83%			**-0.87**
B84		66%			0.69
B86	7%	100%	0.93		
B87	10%	100%	0.94		
B89		97%	0.93		0.72
B97	83%	100%	0.92		
B103		55%			0.73
B104	7%	100%	0.9		0.97
B105		100%	0.93		0.89
B108		69%			0.73
B115	37%	100%	0.93		0.74
B122		83%			0.89
B123		79%			0.79
B132	13%	31%		0.47	
B133		83%	0.77		**0.81**
B136	23%			0.4	
B140	23%	48%			0.69
B141	13%	48%		0.52	
B202	80%			-0.61	
B211	100%	93%	-0.85	-0.83	-0.91
B212	100%	90%	-0.59	-0.86	-0.93
B273	13%			0.54	
B275	10%	10%		0.47	
B283	17%			**0.38**	
B285	10%			**0.42**	
B286	93%			**0.44**	
B287	43%			**0.55**	
B289	83%	41%		**0.71**	
B290	97%	24%	**-0.77**		
B291	97%			**0.64**	
G72[b]	47%	100%	**0.89**		
G78	100%	76%			**-0.71**
G79	83%	100%	**0.85**		
G86		100%	**0.94**		**0.78**

95

G87	13%	100%	**0.95**		
G98	13%	100%	0.97		
G105		93%	0.84		0.95
G106	7%	79%			0.76
G123		79%			0.79
G136	97%	52%	**-0.82**	**0.64**	
G201	80%			-0.49	
G210	80%			-0.61	
G211	100%	97%	-0.82	-0.74	-0.88
G212	90%	14%		-0.78	
G291	40%			0.41	

[a] TRFs showing blue peaks with FAM labeled primer Laby-A. [b] TRFs showing green peaks with HEX labeled primer Laby-Y

			Sau96I		
Observed T-RF size	% SED samples peak found in	% SW samples peak found in	Correlation coefficient with axis 1 in SED&SW data set	Correlation coefficient with axis 2 in SED data set	Correlation coefficient with axis 1 in SW data set
B71	38%	100%	**0.88**		
B72	48%	73%			**-0.82**
B77	93%	13%		-0.77	
B78	97%	100%	**0.79**		
B79	41%	87%			**-0.86**
B85		93%	**0.79**		**0.77**
B86		100%	**0.92**		
B87	7%	100%	**0.95**		
B90	10%	100%	0.92		0.72
B97	69%	100%	0.93		
B103		70%			0.79
B104		100%	0.86		0.93
B105		100%	**0.93**		**0.95**
B108		90%			**0.84**
B115	41%	100%	0.96		0.90
B122		77%			0.78
B123		83%			0.82
B133		93%			0.76
B202	72%			-0.6	
B211	100%	90%	-0.81	-0.85	-0.76
B212	100%	90%	-0.81	-0.79	-0.8
B219	97%			**0.44**	
B221	45%			**0.67**	
B222	97%	50%		**0.82**	
B223	100%	20%	**-0.8**	**0.57**	
B224	97%			**0.76**	
B229	45%	63%		**-0.48**	
G72	31%	100%	0.89		
G78	100%	83%		-0.67	-0.77
G79	83%	100%	0.88		
G86		97%	0.88		0.84
G87	10%	100%	0.93		
G98	17%	100%	0.96		
G105		73%			0.85
G106		87%	0.80		0.89
G116	55%	97%	0.81		0.75
G199	100%	83%		**0.82**	**-0.86**
G200	24%			**-0.45**	
G204	76%			**0.4**	
G210	83%			**-0.66**	

G211	100%	93%		**-0.61**
G212	83%	13%		**-0.83**
G220	34%			0.43
G222	34%	10%		0.58
G225	52%			0.53

Table 5. 7. Possible contributions of representative species of major subgroups of labyrinthulomycetes described in Collado-Mercado *et al*. (2010) to the change of community structure with seasonal change or habitat change.

Contribution to the pattern observed in community structure	subgroup	Genbank accession No and name of the representative species
Not to any pattern	*Aurantiochytrium*	DQ834737_Thraust_BP3_3_3
	Schizochytrium	AB022106_Schiz_aggregatum_ATCC_28209
		AB073309_Th_N4_103
	Ulkenia	AB022104_Japon_ATCC_28207
		DQ023615_Ulkenia_profunda_BUTRBG_111
Only to the seasonal pattern in sediment samples	*Aplanochytrium*	PBS07
	Aurantiochytrium	AB073308_Th_N1_27
		DQ374149_Th_ONC_T18
		AB073303_Thraustochytriidae_A5_20
		DQ836629_Th_T65
		AB183658_Th_MBIC11075*
		AY705763_Thraustochytriidae_sp_NIOS_1_haplotype_NIOS1_C05_3*
		AY758384_Schiz_FJU512*
		DQ023621_Schizochytrium_sp_BUCHAO_113*
	Between uTH2 and Aurantiochytrium	DQ367052_Th_32
	Labyrinthula	AB290457_Labyrinthula_sp_01_Jy_1b
		AB246795_Labyrinthula_N12
	Botryochytrium	AB022114_Ulkenia_profunda_Raghukumar_29
	Loides haliotidis	BBW042908_27
	Oblongichytrium (Y&H)	PBS02
	Parietichytrium	AB073305_Th_H1_14
		AB244715_Th_RT0049
	Schizochytrium	AB073306_Th_H6_16
		AB290578_Schiz_SEK_346
		AB052556_Thraust_KK17_3
	Thraust aureum	AB022110_Thraust_aureum_ATCC_34304
	Thraust Caudivorum	EF114354_Thraustochytrium_sp_caudivorum_strain_S4_clone_T41
	Thraust gaertnerium	AY705755_Th_NIOS6_A05_1
	Thraust kinnei	L34668_Thraust_kinnei_1694d
	Thraust Pachydermum	DQ641204_QPX_NY0313808CC1*
		AF474172_Th_C9G
	Thraust Striatum/motivum	AB022112_Thraust_striatum_ATCC_24473

	uLa 1	PJS101305_60
	uLa 2	PBS102405_10
	uLa 4	PBS102907_02
	uLa 6	DQ310278_uncult_euk_FV23_CilD7
	uLa 7	AY381171_uncult_euk_HE001005_112
	uLa 8	EF100247_Uncult_euk_D2P04B04
	Ulkenia	FJ010826_Thraustochytriidae_sp_AS4A1
		AB022116_Ulkenia_visurgensis_ATCC_28208
	uTH1	PBW102907_25
		AY256317_uncult_euk_D107
To the seasonal pattern in seawater samples	*Aurantiochytrium*	DQ023611_Schizochytrium_limacinum_isolate_BUCACD_032
		DQ834733_Thraust_TR1_4
		AB183658_Th_MBIC11075*
		AY705763_Thraustochytriidae_sp_NIOS_1_haplotype_NIOS1_C05_3*
		AY758384_Schiz_FJU512*
		DQ023621_Schizochytrium_sp_BUCHAO_113*
	Thraust Pachydermum	DQ641204_QPX_NY0313808CC1*
To the difference between sediment and seawater samples and to the seasonal pattern in sediment or seawater sample	*Aurantiochytrium*	DQ023611_Schizochytrium_limacinum_isolate_BUCACD_032
		DQ834738_Thraustochytrium_sp_1_3A4_1isolate2
		AY705742_Thraustochytriidae_sp_NIOS_4_haplotype_NIOS4_A00_2
	Between uTH2 and Aurantiochytrium	DQ367051_Th_thel2
	Labyrinthula	AB095092_Labyrinthula_L59
	Oblongichytrium sp.?	PBS102405_12
	Sycioidochytrium	AY870336_Thraustochytriidae_sp_Fng1
	uLa 3	PBS102405_38
	uLa 5	PBW102907_34
		AY381210_uncult_euk_BL010320_19

Chapter 6: Summary

In this study, a specific and sensitive real-time qPCR assay was developed for QPX detection in clams and environmental samples. A newly designed primer pair 5.8S24For and QPX-ITS2-R2 targeting the QPX ITS region of the rRNA operon was shown to be specific for QPX in standard PCR and exhibited a strong inverse relationship between C_T and the log_{10} number of plasmids containing cloned QPX ITS sequences in qPCR format. With this set of primers, qPCR assay was capable of reliably detecting as few as 10 QPX ITS copies in each reaction. Based on the experience of qPCR assay for QPX, a more general 18S rRNA-based qPCR assay with primers Laby-A and Laby-Y for labyrinthulomycetes, the group of ubiquitous but poorly studied marine protists to which QPX belongs, was developed to quantify the abundance of labyrinthulomycetes in sediment and seawater samples. With a primary standard curve constructed with 10-fold dilutions of a plasmid DNA containing a cloned QPX 18S rRNA gene, the conservative detection limit of this qPCR assay was 100 18S rRNA copies of QPX or other labyrinthulomycetes per reaction.

Using the same serial dilutions of QPX genomic DNA equivalent to 0.5, 1, 5, 50, 500 and 5000 QPX cells, the copy number of rRNA operons in each QPX cell was estimated to be 181 copies per cell by the ITS rRNA-based qPCR assay with primers 5.8S24For and QPX-ITS2-R2, but to be 537 copies per cell by the 18S rRNA-based qPCR assay with primers Laby-A and Laby-Y. This nearly 3-fold underestimate in the copy number of rRNA operons by the ITS rRNA-based qPCR assay was likely to be associated with the variability of the ITS2 region in QPX (Qian *et al.*, 2007). It suggested that there may be more sequence types of QPX ITS2 region than reported, and primer QPX-ITS2-R2 probably mismatches many of them.

Results of this study also show that sample processing and DNA extraction and purification methods critically influence the practical detection limits of qPCR assay in clam and environmental samples by influencing the PCR inhibition effect in DNA templates and the efficiency of recovering QPX DNA from samples. In this study, an "inhibition control reaction" approach, by adding a known amount of target DNA carried by plasmids to parallel PCR reactions, was used to detect and quantify PCR inhibition for each sample. PCR inhibition was much greater for sediment and seawater samples compared to clam samples. An extra DNA purification step with a commercial DNA cleanup or PCR purification kit combined with further 10-fold dilution was usually required to reduce PCR inhibition in the extracted sediment and seawater DNA. For templates with less than 50% inhibition, the qPCR assays were accepted as effective PCR amplifications, and the value of the PCR inhibition effect was used to correct the initial target gene abundance in the sample.

The QPX DNA recovery rates of different DNA extraction and purification procedures from clam, seawater and sediment samples were quantitatively estimated by measuring the efficiency of recovering DNA from those QPX cells added to tissue, sediment and seawater samples. Using the BD Nucleospin tissue kit, QPX recovery rate from clam tissue was estimated to be 16.31%, although large variation could exist when switching between kits. The Qbiogene FastDNA SPIN kit for soil was able to recover 5.38% QPX DNA from QPX-spiked sediment samples, and combining this kit with Galluzzi's crude lysis buffer (Galluzzi *et al.*, 2004) provided the highest recovery (9.51%) of QPX DNA from seawater samples among the six DNA extraction procedures tested.

In this study, the abundance of QPX or labyrinthulomycetes in each clam (only for QPX), sediment and seawater sample assayed by qPCR was estimated to be *(# target gene initial*

a*b)/(c*d*e), where # target gene $_{initial}$ is the initial number of targeted ITS or 18S rRNA copies in the assayed DNA template (1 μl) after correction for PCR inhibition; *a* is the dilution factor of DNA stock for the PCR reaction; *b* is the volume into which the DNA stock was resuspended (μl); *c* is the estimated copy number of target gene per QPX cell (cell^{-1}); *d* is the estimated DNA recovery rate of the extraction method; and *e* is the volume of seawater (ml) or the weight of sediment (mg) or the weight of clam tissue (mg) from which DNA was extracted. For the clam samples in the QPX clearance experiment and the temperature experiment discussed in Chapter 3, QPX DNA recovery rate was not taken into account for estimation of QPX abundance in clams because in those experiments, the clam tissues were preserved and processed differently from the procedure used for clam samples in other chapters for which DNA recovery rate was estimated. In Chapter 5, for the estimates of labyrinthulomycete abundance in environmental samples, DNA recovery rates estimated for QPX were used, under the assumption that DNA of other labyrinthulomycetes was recovered with the same efficiency as QPX.

In 2006, 15 groups of clams (~30 clams per group) collected on 5 sampling dates from three Raritan Bay sites (sites 8, 18 and 21) were analyzed by both histological and qPCR methods. Among all clams assayed, the qPCR assay found QPX abundance above the detection limit (0.5 cells per mg tissue assuming 0% inhibition in the qPCR reaction) in 74 clams, while only 18 of those were also diagnosed as QPX positive by histology. Prevalence determined by qPCR assay was significantly higher than prevalence determined by histology at all three surveyed sites through all sampling times, and the qPCR positive but histology-negative clams generally had low QPX loads, suggesting the qPCR assay is a more sensitive diagnostic tool for QPX especially when relatively few QPX cells are present.

Among the three Raritan Bay sites studied in 2006, QPX in clams seemed to have two different temporal patterns. At site 18, QPX prevalence determined by histology and qPCR assay were significantly correlated. The prevalence data, together with the weighted prevalence determined by qPCR assay (which is a quantitative evaluation of average QPX load), revealed a seasonal pattern: QPX prevalence and weighted prevalence were relatively low in April, increased in May to June, and peaked in August before declining in September. The significant correlation between QPX weighted prevalence at site 18 and temperature at the time of sampling, along with the distinct progression of QPX loads with the season, suggested a seasonal transmission and development pattern of QPX disease at this site. At site 8, although a decline of QPX prevalence and weighted prevalence in June, which was likely a result of sampling error, prevented the weighted prevalence from showing a significant relationship with water temperature in the regression analysis, the general pattern of QPX prevalence and weighted prevalence through the year and the general trend of R^2 values in regression tests suggested that QPX in clams in this site had a similar temporal pattern to that at site 18. On the other hand, clams seemed to have a different temporal pattern of QPX disease at site 21. Unusually (compared to the other sites) high QPX prevalence and weighted prevalence were present in April, did not change much through May and June, and declined in August and September. The relationship between weighted prevalence and temperature was different at site 21 than site 18, with the best correspondence found with a 105 day lag by regression analysis (Table 2.2) or 120 day lag by correlation analysis (Fig. 2.7). It is unclear what might cause two different seasonal patterns in the three sampling sites which were basically experiencing the same environmental conditions.

In temperate coastal environments such as Raritan and Peconic Bays, temperature is a major environmental factor that shows strong seasonality. To better understand the temporal patterns of QPX infection observed in field clams, laboratory-based experiments were conducted to study the effect of temperature on the progression of QPX disease in terms of parasite abundance and mortality in clams. The lowest temperature tested, 13 °C, had a distinct effect on the interaction between clams and QPX compared to the higher temperatures (21 °C and 27 °C. Both QPX-injected clams and naturally infected clams kept at 13 °C always showed higher prevalence and weighted prevalence compared to those at 21 and 27 °C after 2 or 4 months incubation. For QPX-challenged clams, no mortality was observed during 4 months incubation. Increasing QPX loads was only observed in clams incubated at 13 °C, while clams incubated at 21 °C and 27 °C exhibited a clear recovery process. For naturally infected clams with high initial QPX prevalence and QPX loads, even though the significantly higher mortality at 13 °C might have removed the most heavily infected clams from this sample, the remaining clams at 13 °C still showed the highest QPX prevalence and parasite loads throughout the incubation, while the clams at 21 °C and 27 °C were experiencing a healing process. These results suggested that under lab conditions (30 psu and oxygen saturation), low temperature could be more advantageous for QPX than for its host, while higher temperature favors the clams and facilitates the clearance of QPX from infected individuals.

Using qPCR assay, QPX was detected at abundances between 34 and 215 cells mg^{-1} in four of 43 sediment samples collected from Raritan and Peconic Bays in 2006, but no QPX was detected in any of the 40 seawater samples. This is the first report of quantitative detection of QPX in sediment, suggesting sediment, as the habitat of clams and an environmental reservoir for QPX, may play a role in the natural transmission of QPX disease. Based on this finding, together with the results of the temperature experiment that infected clams incubated at 13 °C tended to retain a higher QPX abundance in tissue and experienced a higher mortality (may be associated with disease development) than those at room temperature, we incorporated sediment in the QPX transmission experiments conducted with cohabitated naturally infected clams and susceptible clams and tested the possibility of low temperature being favorable for QPX transmission.

QPX cells were detected by qPCR assay in sediment samples collected from transmission experiments conducted both at room temperature and 13 °C. In the transmission experiment at 13 °C, QPX cells were also detected in all seawater samples. These are the only seawater samples in which QPX abundance was found above the detection limit of qPCR assay. Some QPX-positive environmental samples were collected before the first clam mortality occurred in the experiments, strongly supporting the hypothesis that release of QPX from live, infected (likely severely infected) clams is a source of parasites in the environment, and may be an important mode of parasite release prior to clam death. On the other hand, no clear correlation was observed between QPX abundance in environmental samples and the mortalities of infected clams. Due to the limited knowledge about the release mechanism of QPX from infected clams, and about the persistence of QPX cells in the environment after release from infected clams, we could not differentiate the contributions of QPX potentially released from live, infected clams versus dead clams to the detected QPX abundance in the environmental samples. Based on results in the transmission experiments, the hypothesis that the death of infected hosts with consequent release of parasite cells from disintegrating host tissue is also a source of pathogen in the environment cannot be supported or rejected. As

studies on other marine bivalve parasites have shown that the death of infected hosts, with consequent release of parasite cells from disintegrating host tissue into the environment, is the main source of infectious forms (Ragone Calvo *et al.*, 2003; Bushek *et al.*, 2002), QPX release from decayed infected tissue needs to be further investigated.

The detection of QPX in sediment and seawater samples collected from the transmission experiments suggests an effect of infected clams on the distribution and abundance of QPX in the environment. Using a DGGE method, Gast *et al.* (2008) examined water, sediment, seaweeds, seagrass and various macrophytes and invertebrates in Virginia and Massachusetts and detected QPX in almost all different sample types throughout the year. They also showed that the frequency of positive samples was higher in enzootic sites in MA as opposed to VA. However, in our field study in Raritan and Peconic Bays, all QPX-positive sediment samples were from enzootic sampling sites (the DGGE assay is more sensitive because it uses many more PCR cycles). These investigations, combined with our laboratory study of QPX persistence in sediment, suggest that QPX organisms may be widely distributed in the coastal environment, but probably at very low abundances below the detection limit of our qPCR assay unless infected clams (live or dead) are actively releasing QPX cells.

The transmission experiments conducted in this study also revealed an effect of temperature on QPX transmission between cohabitated infected clams and susceptible clams. No QPX was detected by qPCR in susceptible clams after being co-incubated with naturally infected clams, which initially had high QPX prevalence and parasite loads, at room temperature. This result was consistent with a previous laboratory transmission experiment (Dahl and Allam, 2007) which did not detect QPX infection by histology in susceptible clams after being cohabitated with infected adult clams for 10 months at room temperature, although sediment as an environmental reservoir was incorporated in our experiment, and the more sensitive qPCR detection method was applied in our study. On the contrary, in the transmission experiment at 13 °C, some susceptible clams acquired QPX cells at rare to moderate levels of abundance after 2 to 3 months cohabitation with naturally infected clams, suggesting the occurrence of QPX transmission between clams. Because of the unavailability of tissue samples from these susceptible clams for histological examination, whether the parasite acquisition in those clams led to active QPX infection was not confirmed by histology. However, the results of our transmission experiment, agreeing with the results of the temperature experiments presented in Chapter 3, suggested that room temperature may not be a conducive environment for parasite acquisition or establishment of infection in the susceptible hosts while a colder environment may impair host defenses against QPX and help the parasite breaching host barriers to establish an infection.

The findings of laboratory-based *in vivo* experiments enable us to better interpret and understand the temporal patterns of QPX prevalence and infection intensity revealed by field studies of Raritan Bay clams. During April to August, especially from April to June when water temperature was mostly below 20°C, the seasonal patterns at Raritan Bay site 8 and 18 showed increased QPX prevalence and infection intensity. At the same time, a large proportion of clams were also found to have rare to light infections, suggesting the concurrence of parasite acquisition from environment, establishment of new infections and development of existing infections was likely related to the effect of relatively low temperature. At Raritan Bay site 21, although the pattern of infection looked different from the other two sites, the relatively higher and less variable QPX prevalence and infection intensity during April to June seemed to also suggest an effect of lower temperature probably

combined with the stress associated with higher clam density: new infection acquisition and progression might start earlier or occur more rapidly under low temperature; a colder environment in the spring may also promote disease development in those infected clams surviving from previous year. On the other hand, when temperature remained relatively high (≥21°C) after June, especially during August and September, QPX prevalence and weighted prevalence started to decline. Although some established infections might have continued to develop due to the possible time lag in response of parasite-host interaction to the temperature changes, the simultaneous decline in the proportion of clams with lighter infection suggested that new parasite acquisition was reduced or hindered and clam healing was promoted, probably because of the advantageous effect of higher temperature on hosts in the host-pathogen interaction.

In many marine invertebrate diseases, temperature is a major environmental factor that can explain spatial and temporal variation of disease prevalence (Harvell *et al.*, 1999). High water temperature has been frequently described to be a key factor influencing the severity of bacterial and protistan diseases in several bivalve species. Many major shellfish diseases become more severe with higher temperatures, and experimental challenge with pathogens has shown that high temperatures enhance prevalence (Lacoste *et al.*, 2001; Ragone Calvo *et al.*, 2003; Carnegie *et al.*, 2008). A few papers have examined the implications of climate change for marine parasites (Harvell *et al.*, 1999; Marcogliese, 2001). One famous case is that of *Perkinsus marinus*, cause of Dermo disease in the eastern oyster, *Crassostrea virginica*, showing a dramatic range extension associated with a recent warming trend (Ford and Smolowitz, 2007). However, a few cold water diseases have also been reported in bivalves. For instance, *Mikrocytos mackini*, the agent of the Denman Island disease in the oyster *Crassostrea gigas*, did not develop in oysters held at temperatures above 14 °C. Temperatures below 10 °C are required for the development of the disease and associated mortalities (Hervio et al. 1996; Bower et al. 1997). A study on the brown ring disease affecting the clam *Ruditapes philippinarum* also demonstrated that the clams challenged by *Vibrio tapetis,* the etiological agent of the disease, had lower prevalence at higher temperature (21 °C) compared to those kept at 8 °C and 14 °C (Paillard *et al.*, 2004). Our study suggested QPX disease is likely a cold water disease, in accordance with the distribution of this disease along the east coasts of Canada and the U.S.: QPX disease is reported mainly in areas where seawater temperature is relatively low in summer (in Canada, i.e. Prince Edward Island and New Brunswick, and in U.S, i.e. Massachusetts, New York, New Jersey and Virginia) (Drinnan and Henderson, 1963; Whyte *et al.*, 1994; Ragone Calvo *et al.*, 1998; Smolowitz *et al.*, 1998; MacCallum and McGladdery, 2000; Ford *et al.*, 2002; Dove *et al.*, 2004). QPX has never been reported south of Virginia even though clam aquaculture is extensive along the southeastern United States coast. The apparent absence of QPX in this region is likely due to the relatively higher temperature in summer since our study showed that the transmission and progression of QPX disease in clams are likely to be facilitated by lower temperature, and long-term exposure to higher temperature probably promotes clam healing.

QPX is believed to be an opportunistic pathogen and has been widely detected in seawater and sediment or associated with aggregates, macrophytes and invertebrates but rarely shows high abundance outside its clam host (Lyons *et al*. 2005; 2006; Gast *et al*. 2008). In our field study, QPX was only above the qPCR detection limit in 4 of 43 sediment samples, and not in any of the 40 seawater samples collected from the Raritan and Peconic Bay areas

in 2006. The limited number of QPX-positive environmental samples prevented us further studying the QPX dynamics in the environment or the relationship between the abundance of QPX in the environment and QPX prevalence in clams. QPX belongs to a group of ubiquitous but poorly understood marine protists, the labyrinthulomycetes, and in particular is a member of the group of thraustochytrids (or thraustochytrid phylogenetic group, TPG). Although the labyrinthulomycetes appear to play an important role in the mineralization of particle organic matter in the ocean, their significance as a component of the marine ecosystem has been underappreciated, mainly due to the limited knowledge of some basic questions such as their abundance and diversity. In this study, we investigated the abundance and diversity of labyrinthulomycete communities in sediment and seawater samples collected Raritan and Peconic Bays in 2006, when and where the dynamics of QPX in the clam and environmental samples was also investigated, to provide more information about these organisms related to QPX for a better understanding the dynamics of QPX in the natural environment.

The labyrinthulomycete community structure (abundance and species composition) in the environmental samples were examined by using 18S rRNA-based qPCR and T-RFLP techniques. The primer pair Laby-A and Laby-Y was used in both methods. The alignment of available 18S rRNA sequences of labyrinthulomycetes and a previous field study (Collado-Mercado *et al.*, 2010) suggested that this primer pair probably cannot amplify all labyrinthulomycetes, because the sequences of a few phylogenetic subgroups of labyrinthulomycetes mismatch primer Laby-Y. However, the possible contribution of these subgroups to the abundance and diversity of labyrinthulomycete communities in this study cannot be excluded, because a few specific T-RFs that can only be generated by some representative species in these subgroups were present in our T-RFLP profiles and may have important contributions to determining the seasonal pattern of labyrinthulomycete communities in sediment and seawater samples.

Labyrinthulomycete abundance was estimated to be 33 ± 24 cells per mg sediment, ranging from 2 to 75 cells mg^{-1} in 20 of 29 sediment samples (Table 5.2). These estimates fell in the same range with the previously reported labyrinthulomycete abundance in sediment samples measured by microscopy-based MPN or AfDD methods (Raghukumar *et al.*, 1995; Bongiorni *et al.*, 2005). In seawater, our qPCR assay detected labyrinthulomycetes at abundance of 25 ± 16 cells ml^{-1} (ranging from 3 to 56 cells ml^{-1}; Table 5.2), which was comparable to those reported in the Sea of Japan and coastal Seto Inland Sea (Naganuma *et al.*, 1998; Kimura *et al.*, 1999), but lower than those in some samples from the Arabian Sea (Raghukumar *et al.*, 2001). There were no seasonal or spatial trends observed in the abundance of labyrinthulomycetes determined by our qPCR assay.

NMS analysis of T-RFLP profiles revealed temporal trends in labyrinthulomycete community structure in both sediment and seawater samples, although the pattern was more distinct in seawater. Likewise, MRPP tests showed significant differences among sediment and seawater samples collected from different seasons. A previous study suggested that labyrinthulomycete community structure is related to organic matter content seasonally and spatially (Bongiorni and Dini 2002). However, the lack of data on organic matter content in sediment and seawater made us unable to test this hypothesis. The seasonality of labyrinthulomycete species composition and abundance in the water column has been suggested to reflect the dependence of labyrinthulomycetes on POM produced by seasonal phytoplankton blooms (Gaertner, 1968; Gaertner and Raghukumar, 1980; Raghukumar *et al.*,

2001; Bongiorni and Dini, 2002). In this study, neither phytoplankton chlorophyll concentration nor POM in the water was measured. Phytoplankton blooms dominated by different phytoplankton during two periods through spring to fall were often reported in Raritan Bay area by NJDEP. This difference in species dominance of the phytoplankton bloom in different seasons might be related to the observed seasonal pattern in the labyrinthulomycete community in the seawater samples revealed by NMS ordination (samples from April, May and June grouped separately from those in August and September), but further detailed studies would be need to test this hypothesis.

NMS and MRPP results also indicated that the composition of labyrinthulomycete communities in sediment was significantly different from those in seawater samples. This result may be related to the relatively higher diversity of labyrinthulomycete communities in seawater, because T-RF richness, which is an index of diversity, was much higher in seawater than in sediment and was the most important environmental variable influencing the difference in labyrinthulomycete communities in sediment and seawater. However, although the seawater samples generally had many more T-RFs and more T-RFs that had important contributions to the seasonal pattern or habitat difference in the labyrinthulomycete community structure, fewer observed T-RFs in the seawater data sets were identified to possibly match the predicted T-RFs of previously published labyrinthulomycete sequences. This result suggested that species which have not been sequenced are an important component of the labyrinthulomycete community, particularly in seawater samples, and the seasonal pattern in seawater samples may be mainly determined by the unidentified labyrinthulomycetes.

In this study, labyrinthulomycete communities did not show significant differences among sites or among sites categorized by clam density. The labyrinthulomycete community structure was not related to the prevalence of QPX disease in clams determined by histology, either. As histological method tends to underestimate QPX prevalence, QPX prevalence or weighted prevalence determined by qPCR assay would be a better environmental variable to represent the severity of QPX disease in the clam population in future studies.

As a representative species of subgroup that also includes *Thraustochytrium pachydermum,* QPX does not generate its own specific T-RFs that can be used to specifically indentify it in the *HaeIII* and *Sau96I* T-RFLP data sets. Instead it always shares similar length T-RFs with some species of *Aurantiochytrium.* Besides these species of *Aurantiochytrium*, QPX was the only identified species possibly having an important contribution to the seasonal pattern of labyrinthulomycete community structure in seawater. It was also among the 37 representative species of 23 phylogenetic subgroups of labyrinthulomycetes that were possibly important contributors to the seasonal pattern of labyrinthulomycete community in sediment. In this study, the presence and contribution of QPX in the labyrinthulomycete community cannot be determined without excluding the presence of certain species of *Aurantiochytrium.* A further PCR test with cloning and sequencing probably could determine whether the sequences of subgroup *Aurantiochytrium* were able to be amplified by primer Laby-A and Laby-Y. If the mismatch between sequence and primer does not allow the amplification of *Aurantiochytrium spp.,* the contribution of QPX to the seasonal pattern of labyrinthulomycete community could be determined, at least in the assayed Raritan and Peconic Bay seawater samples.

References

Abdo, Z., Schuette, U. M. E., Bent, S. J., Williams, C. J., Forney, L. J. and Joyce, P. (2006) Statistical methods for characterizing diversity of microbial communities by analysis of terminal restriction fragment length polymorphisms of 16S rRNA genes. *Environmental Microbiology* **8,** 929-938.

Allam, B. and Pawagi, S. (2004) The incidence of QPX disease in hard clams from different locations in New York State. In *Report submitted to the New York State Departmetn of Environmental Conservation.*

Allam, B. and Pawagi, S. (2005) The incidence of QPX disease in hard clams from different locations in New York State. In *Report submitted to the New York State Departmetn of Environmental Conservation.*

Allam, B. and Pawagi, S. (2006) The incidence of QPX disease in hard clams from different locations in New York State. In *Report submitted to the New York State Departmetn of Environmental Conservation.*

Alvarez, I. and Wendel, J. F. (2003) Ribosomal ITS sequences and plant phylogenetic inference. *Molecular Phylogenetics and Evolution* **29,** 417-434.

Anbu, P., Kim, D. U., Jeh, E. J., Jeong, Y. S. and Hur, B. K. (2007) Investigation of the physiological properties and synthesis of PUFAs from thraustochytrids and its electrophoretic karyotypes. *Biotechnology and bioprocess engineering* **12,** 720-729.

Anderson, R. S., Kraus, B. S., McGladdry, S. E. and Smolowitz, R. (2003) QPX, a pathogen of quahogs (hard clams), employs mucoid secretions to resist host antimicrobial agents. *Journal of Shellfish Research* **22,** 205-208.

Ansell, A. D. (1964) *Venus mercenaria* (L.) in Southhampton Water. *Ecology* **44,** 396-397.

Ansell, A. D. (1968) The rate of growth of the hard clam Mercenaria mercenaria (L.) throughout the geographic range. *J. Cons.Perm. Intl. Explor. Mer.* **31,** 364-409.

Audemard, C., Ragone Calvo, L. M., Paynter, K. T., Reece, K. S. and Burreson, E. M. (2006) Real-time PCR investigation of parasite ecology: in situ determination of oyster parasite *Perkinsus marinus* transmission dynamics in lower Chesapeake Bay. *Parasitology* **132,** 827-842.

Audemard, C., Reece, K. S. and Burreson, E. M. (2004) Real-time PCR for detection and quantification of the protistan parasite *Perkinsus marinus* in environmental waters. *Applied and Environmental Microbiology* **70,** 6611-6618.

Baldwin, A. J., Moss, J. A., Pakulski, J. D., Catala, P., Joux, F. and Jeffrey, W. H. (2005) Microbial diversity in a Pacific Ocean transect from the Arctic to Antarctic circles. *Aquatic Microbial Ecology* **41,** 91-102.

Bardach, J. E., Ryther, J. H. and McLarney, W. O. (1972) Aquaculture: The farming and husbandry of freshwater and marine organisms, Wiley-Interscience, New York.

Bongiorni, L. and Dini, F. (2002) Distribution and abundance of thraustochytrids in different Mediterranean coastal habitats. *Aquatic Microbial Ecology* **30,** 49-56.

Bongiorni, L., Mirto, S., Pusceddu, A. and Danovaro, R. (2005) Response of benthic protozoa and thraustochytrid protists to fish farm impact in seagrass (*Posidonia oceanica*) and soft-bottom sediments. *Microbial Ecology* **50,** 268-276.

Bower, S. M. (1987) Pathogenicity and host specificity of *Labyrinthuloides haliotidis* (*Protozoa, Labyrinthomorpha*), a parasite of juvenile abalone. *Canadian Journal of Zoology* **65,** 2008-2012.

Bowles, R. D., Hunt, A. E., Bremer, G. B., Duchars, M. G. and Eaton, R. A. (1999) Long-chain n-3 polyunsaturated fatty acid production by members of the marine protistan group the thraustochytrids: screening of isolates and optimisation of docosahexaenoic acid production. *Journal of Biotechnology* **70,** 193-202.

Brousseau, D. J. (1996) Epizootiology of the parasite, Perkinsus marinus (Dermo) in intertidal oyster populations from Long Island Sound. *Journal of Shellfish Research* **15,** 583-587.

Buggé, D. M. and Allam, B. (2007) Effects of starvation and macroalgae extracts on the survival and growth of quahog parasite unknown (QPX). *Journal of Experimental Marine Biology and Ecology* **348,** 60-69.

Burreson, E. M. and Ragone Calvo, L. M. (1996) epizooticology of *Perkinsus marinus* disease of oysters in Chesapeake Bay, with emphasis on data since 1985. *Journal of Shellfish Research* **15,** 17-34.

Bushek, D., Ford, S. E. and Chintala, M. M. (2002) Comparison of in vitro-cultured and wild-type *Perkinsus marinus*. III. Fecal elimination and its role in transmission. *Diseases of Aquatic Organisms* **51,** 217-225.

Carmona, M. L., Naganuma, T. and Yamaoka, Y. (2003) Identification by HPLC-MS of carotenoids of the Thraustochytrium CHN-1 strain isolated from the Seto Inland Sea. *Bioscience Biotechnology and Biochemistry* **67,** 884-888.

Carnegie, R. B., Barber, B. J., Culloty, S. C., Figueras, A. J. and Distel, D. L. (2000) Development of a PCR assay for detection of the oyster pathogen *Bonamia ostreae*

and support for its inclusion in the *Haplosporidia*. *Diseases of Aquatic Organisms* **42,** 199-206.

Carnegie, R. B., Stokes, N. A., Audemard, C., Bishop, M. J., Wilbur, A. E., Alphin, T. D., Posey, M. H., Peterson, C. H. and Burreson, E. M. (2008) Strong seasonality of *Bonamia sp.* infection and induced *Crassostrea ariakensis* mortality in Bogue and Masonboro Sounds, North Carolina, USA. *Journal of Invertebrate Pathology* **98,** 335-43.

Cavalier-Smith, T., Allsopp, M. T. E. P. and Chao, E. E. (1994) Traustochytrids are chromists, not Fungi: 18S rRNA signinatures of Heterokonta. *Philosophical Transactions of the Royal Society London B* **346,** 387-397.

Collado-Mercado, E., Radway, J. C. and Collier, J. L. (2010) Novel uncultivated labyrinthulomycetes revealed by 18S rDNA sequences from seawater and sediment samples. *Aquatic Microbial Ecology* **58,** 215-228.

Cook, K. L. and Britt, J. S. (2007) Optimization of methods for detecting *Mycobacterium avium* subsp *paratuberculosis* in environmental samples using quantitative, real-time PCR. *Journal of Microbiological Methods* **69,** 154-160.

Culman, S. W., Bukowski, R., Gauch, H. G., Cadillo-Quiroz, H. and Buckley, D. H. (2009) T-REX: software for the processing and analysis of T-RFLP data. *BMC Bioinformatics* **10,** 171.

Culman, S. W., Gauch, H. G., Blackwood, C. B. and Thies, J. E. (2008) Analysis of T-RFLP data using analysis of variance and ordination methods: a comparative study. *Journal of Microbiological Methods* **75,** 55-63.

Dahl, S. F. and Allam, B. (2007) Laboratory transmission studies of QPX disease in the northern quahog (=hard clam): Development of an infection procedure. *Journal of Shellfish Research* **26,** 383-389.

Dahl, S. F., Perrigault, M. and Allam, B. (2008) Laboratory transmission studies of QPX disease in the hard clam: Interactions between different host strains and pathogen isolates. *Aquaculture* **280,** 64-70.

Dahl, S. F., Thiel, J. and Allam, B. (2010) Field performance and QPX disease progress in cultured and wild-type strains of *Mercenaria mercenaria* in New York waters. *Journal of Shellfish Research* **29,** 83-90.

Dove, A. D. M., Bowser, P. R. and Cerrato, R. M. (2004) Histological analysis of an outbreak of QPX disease in hard clams *Mercenaria mercenaria* in New York. *Journal of Aquatic Animal Health* **16,** 246-250.

Drinnan, R. and Henderson, E. (1963) 1962 mortalities and a possible disease organism in Neguac quahaugs, Biological Station, St. Andrews, New Brunswick, Canada.

Enright, A. M., Collins, G. and O'Flaherty, V. (2007) Temporal microbial diversity changes in solvent-degrading anaerobic granular sludge from low-temperature (15 degrees C) wastewater treatment bioreactors. *Systematic and Applied Microbiology* **30,** 471-482.

Ford, S. E., Kraeuter, J. N., Barber, R. D. and Mathis, G. (2002) Aquaculture-associated factors in QPX disease of hard clams: density and seed source. *Aquaculture* **208,** 23-38.

Ford, S. E. and Smolowitz, R. (2007) Infection dynamics of an oyster parasite in its newly expanded range. *Marine Biology* **151,** 119-133.

Frostegard, A., Courtois, S., Ramisse, V., Clerc, S., Bernillon, D., Le Gall, F., Jeannin, P., Nesme, X. and Simonet, P. (1999) Quantification of bias related to the extraction of DNA directly from soils. *Applied and Environmental Microbiology* **65,** 5409-5420.

Gaertner, A. (1968) Eine Methode des quantitativen Nachweises niederer mit Pollen koederbarer Pilze im Meerwasser und im sediment. *Veroeff Institute Meeresforsch Bremerhav Supplement* **3,** 75-92.

Gaertner, A. and Raghukumar, S. (1980) Ecology of the thraustochytrids (lower marine fungi) in the Falden Ground and other parts of the North Sea I. *Meteor Forsch Ergebn A* **22,** 165-185.

Galluzzi, L., Penna, A., Bertozzini, E., Vila, M., Garces, E. and Magnani, M. (2004) Development of a real-time PCR assay for rapid detection and quantification of *Alexandrium minutum* (a dinoflagellate). *Applied and Environmental Microbiology* **70,** 1199-1206.

Gast, R. J., Cushman, E., Moran, D. M., Uhlinger, K. R., Leavitt, D. and Smolowitz, R. (2006) DGGE-based detection method for Quahog Parasite Unknown (QPX). *Diseases of Aquatic Organisms* **70,** 115-122.

Gast, R. J., Moran, D. M., Audemard, C., Lyons, M. M., DeFavari, J., Reece, K. S., Leavitt, D. and Smolowitz, R. (2008) Environmental distribution and persistence of Quahog Parasite Unknown (QPX). *Diseases of Aquatic Organisms* **81,** 219-229.

Ginzinger, D. G. (2002) Gene quantification using real-time quantitative PCR: An emerging technology hits the mainstream. *Experimental Hematology* **30,** 503-512.

Gu, W. and Levin, R. E. (2006) Quantitative detection of *Plesiomonas shigelloides* in clam and oyster tissue by PCR. *International Journal of Food Microbiology* **111,** 81-86.

Hahn, M., Wilhelm, J. and Pingoud, A. (2001) Influence of fluorophor dye labels on the migration behavior of polymerase chain reaction-amplified short tandem repeats during denaturing capillary electrophoresis. *Electrophoresis* **22,** 2691-2700.

Harvell, C. D., Kim, K., Burkholder, J. M., Colwell, R. R., Epstein, P. R., Grimes, D. J., Hofmann, E. E., Lipp, E. K., Osterhaus, A., Overstreet, R. M., Porter, J. W., Smith, G. W. and Vasta, G. R. (1999) Review: Marine ecology - Emerging marine diseases - Climate links and anthropogenic factors. *Science* **285,** 1505-1510.

Haugland, R. A., Brinkman, N. and Vesper, S. J. (2002) Evaluation of rapid DNA extraction methods for the quantitative detection of fungi using real-time PCR analysis. *Journal of Microbiological Methods* **50,** 319-323.

Higuchi, R., Fockler, C., Dollinger, G. and Watson, R. (1993) Kinetic PCR analysis: real-time monitoring of DNA amplification reactions. *Bio-Technology* **11,** 1026-1030.

Honda, D., Yokochi, T., Nakahara, T., Raghukumar, S., Nakagiri, A., Schaumann, K. and Higashihara, T. (1999) Molecular phylogeny of labyrinthulids and thraustochytrids based on the sequencing of 18S ribosomal RNA gene. *Journal of Eukaryotic Microbiology* **46,** 637-647.

Huang, J. Z., Aki, T., Yokochi, T., Nakahara, T., Honda, D., Kawamoto, S., Shigeta, S., Ono, K. and Suzuki, O. (2003) Grouping newly isolated docosahexaenoic acid-producing thraustochytrids based on their polyunsaturated fatty acid profiles and comparative analysis of 18S rRNA genes. *Marine Biotechnology* **5,** 450-457.

Kaplan, C. W. and Kitts, C. L. (2003) Variation between observed and true Terminal Restriction Fragment length is dependent on true TRF length and purine content. *Journal of Microbiological Methods* **54,** 121-125.

Kimura, H., Fukuba, T. and Naganuma, T. (1999) Biomass of thraustochytrid protoctists in coastal water. *Marine Ecology-Progress Series* **189,** 27-33.

Kleeman, S. N. and Adlard, R. D. (2000) Molecular detection of *Marteilia sydneyi*, pathogen of Sydney rock oysters. *Diseases of Aquatic Organisms* **40,** 137-146.

Kleinschuster, S. J., Smoloxitz, R. and Parent, J. (1998) *In Vitro* life cycle and propagation of Quahog Parasite Unknown. *Journal of Shellfish Research* **17,** 75-78.

Kraeuter, J. N., Ford, S. E., Barber, R. D. and Mathis, G. (1998) Effects of planting density and depth on proliferation of QPX in hard clams. *Journal of Shellfish Research* **17,** 358.

Kumon, Y., Yokoyama, R., Yokochi, T., Honda, D. and Nakahara, T. (2003) A new labyrinthulid isolate, which solely produces n-6 docosapentaenoic acid. *Applied Microbiology and Biotechnology* **63,** 22-28.

Lacoste, A., Jalabert, F., Malham, S., Cueff, A., Gelebart, F., Cordevant, C., Lange, M. and Poulet, S. A. (2001) A *Vibrio splendidus* strain is associated with summer mortality of juvenile oysters *Crassostrea gigas* in the Bay of Morlaix (North Brittany, France). *Diseases of Aquatic Organisms* **46,** 139-145.

Leander, C. A. and Porter, D. (2001) The Labyrinthulomycota is comprised of three distinct lineages. *Mycologia* **93,** 459-464.

Leander, C. A., Porter, D. and Leander, B. S. (2004) Comparative morphology and molecular phylogeny of aplanochytrids (Labyrinthulomycota). *European journal of protistology* **40,** 317-328.

Lewis, T. E., Mooney, B. D., McMeekin, T. A. and Nichols, P. D. (1998) New Australia sources of polyunsaturated fatty acids. *Chemistry in Australia* **65,** 37-39.

Lewis, T. E., Nichols, P. D. and McMeekin, T. A. (1999) The biotechnological potential of thraustochytrids. *Marine Biotechnology* **1,** 580-587.

Liu, Q., Allam, B. and Collier, J. L. (2009) Quantitative real-time PCR assay for QPX (Thraustochytriidae), a parasite of the hard clam (*Mercenaria mercenaria*). *Applied and Environmental Microbiology* **75,** 4913-4918.

Liu, W. T., Marsh, T. L., Cheng, H. and Forney, L. J. (1997) Characterization of microbial diversity by determining terminal restriction fragment length polymorphisms of genes encoding 16S rRNA. *Applied and Environmental Microbiology* **63,** 4516-4522.

Lyons, M. M., Smolowitz, R., Dungan, C. F. and Roberts, S. B. (2006) Development of a real time quantitative PCR assay for the hard clam pathogen Quahog Parasite Unknown (QPX). *Diseases of Aquatic Organisms* **72,** 45-52.

Lyons, M. M., Smolowitz, R., Gomez-Chiarri, M. and Ward, J. E. (2007) Epizootiology of Quahog Parasite unknown (QPX) disease in northern quahogs (=hard clams) *Mercenaria mercenaria*. *Journal of Shellfish Research* **26,** 371-381.

Lyons, M. M., Ward, J. E., Smolowitz, R., Uhlinger, K. R. and Gast, R. J. (2005) Lethal marine snow: Pathogen of bivalve mollusc concealed in marine aggregates. *Limnology and Oceanography* **50,** 1983-1988.

Maas, P. A. Y., Kleinschuster, S. J., Dykstra, M. J., Smolowitz, R. and Parent, J. (1999) Molecular characterization of QPX (Quahog Parasite Unknown), a pathogen of *Mercenaria mercenaria*. *Journal of Shellfish Research* **18,** 561-567.

MacCallum, G. S. and McGladdery, S. E. (2000) Quahog Parasite Unknown (QPX) in the northern quahog *Mercenaria mercenaria* (Linnaeus, 1758) and *M. mercenaria* var.

notata from Atlantic Canada, survey results from three maritime provinces. *Journal of Shellfish Research* **19,** 43-50.

Marcogliese, D. J. (2001) Implications of climate change for parasitism of animals in the aquatic environment. *Canadian Journal of Zoology-Revue Canadienne De Zoologie* **79,** 1331-1352.

Marsh, A. G., Gauthier, J. D. and Vasta, G. R. (1995) A semiquantitative PCR assay for assessing *Perkinsus marinus* infections in the easter oyster, *Crassostrea virginica*. *Journal of Parasitology* **81,** 577-583.

McCune, B. and Grace, J. B. (2002) Analysis of ecological communities, MjM Software Design, Gleneden Beach, OR.

Medlin, L., Elwood, H. J., Stickel, S. and Sogin, M. L. (1988) The characterization of enzymatically amplified eukaryotic 16S-like rRNA-coding regions. *Gene* **71,** 491-499.

Mo, C. Q., Douek, J. and Rinkevich, B. (2002) Development of a PCR strategy for thraustochytrid identification based on 18S rDNA sequence. *Marine Biology* **140,** 883-889.

Morris, R. M., Vergin, K. L., Cho, J. C., Rappe, M. S., Carlson, C. A. and Giovannoni, S. J. (2005) Temporal and spatial response of bacterioplankton lineages to annual convective overturn at the Bermuda Atlantic Time-series Study site. *Limnology and Oceanography* **50,** 1687-1696.

Naganuma, T., Takasugi, H. and Kimura, H. (1998) Abundance of thraustochytrids in coastal plankton. *Marine Ecology-Progress Series* **162,** 105-110.

Nelson, J. D., Boehme, S. E., Reimers, C. E., Sherrell, R. M. and Kerkhof, L. J. (2008) Temporal patterns of microbial community structure in the Mid-Atlantic Bight. *FEMS Microbiology Ecology* **65,** 484-493.

Oliver, L. M., Fisher, W. S., Ford, S. E., Calvo, L. M. R., Burreson, E. M., Sutton, E. B. and Gandy, J. (1998) *Perkinsus marinus* tissue distribution and seasonal variation in oysters *Crassostrea virginica* from Florida, Virginia and New York. *Diseases of Aquatic Organisms* **34,** 51-61.

Paillard, C., Allam, B. and Oubella, R. (2004) Effect of temperature on defense parameters in Manila clam *Ruditapes philippinarum* challenged with *Vibrio tapetis*. *Diseases of Aquatic Organisms* **59,** 249-262.

Park, T. G., de Salas, M. F., Bolch, C. J. S. and Hallegraeff, G. A. (2007) Development of a real-time PCR probe for quantification of the heterotrophic dinoflagellate *Cryptoperidiniopsis brodyi* (Dinophyceae) in environmental samples. *Applied and Environmental Microbiology* **73,** 2552-2560.

Perrigault, M., Bugge, D. M. and Allam, B. (2010) Effect of environmental factors on survival and growth of quahog parasite unknown (QPX) *in vitro*. *Journal of Invertebrate Pathology*.

Perrigault, M., Bugge, D. M., Hao, C. C. and Allam, B. (2009) Modulatory effects of hard clam (*Mercenaria mercenaria*) tissue extracts on the in vitro growth of its pathogen QPX. *Journal of Invertebrate Pathology* **100,** 1-8.

Prokopowich, C. D., Gregory, T. R. and Crease, T. J. (2003) The correlation between rDNA copy number and genome size in eukaryotes. *Genome* **46,** 48-50.

Qian, H., Liu, Q., Allam, B. and Collier, J. L. (2007) Molecular genetic variation within and among isolates of QPX (Thraustochytridae), a parasite of the hard clam *Mercenaria mercenaria*. *Diseases of Aquatic Organisms* **77,** 159-168.

Ragan, M. A., MacCallum, G. S., Murphy, C. A., Cannone, J. J., Gutell, R. R. and McGladdery, S. E. (2000) Protisan parasite QPX of hard-shell clam *Mercenaria mercenaria* is a member of *Labyrinthulomycota*. *Diseases of Aquatic Organisms* **42,** 185-190.

Raghukumar, S. (2002) Ecology of the marine protists, the Labyrinthulomycetes (Thraustochytrids and Labyrinthulids). *European journal of protistology* **38,** 127-145.

Raghukumar, S., Ramaiah, N. and Raghukumar, C. (2001) Dynamics of thraustochytrid protists in the water column of the Arabian Sea. *Aquatic Microbial Ecology* **24,** 175-186.

Raghukumar, S., Sathepathak, V., Sharma, S. and Raghukumar, C. (1995) Thraustochytrid and fungal component of marine detritus. III. Field studies on decomposition of leaves of the mangrove *Rhizophora apiculata*. *Aquatic Microbial Ecology* **9,** 117-125.

Raghukumar, S. and Schaumann, K. (1993) An epifluorescence microscopy method for direct detection and enumeration of the fungilike marine protists, the thraustochytrids. *Limnology and Oceanography* **38,** 182-187.

Ragone Calvo, L. M., Dungan, C. F., Roberson, B. S. and Burreson, E. M. (2003) Systematic evaluation of factors controlling *Perkinsus marinus* transmission dynamics in lower Chesapeake Bay. *Diseases of Aquatic Organisms* **56,** 75-86.

Ragone Calvo, L. M., Ford, S. E., Kraeuter, J. N., Leavitt, D. F., Smolowitz, R. and Burreson, E. M. (2007) Influence of host genetic origin and geographic location on QPX disease in Northern quahogs (=hard clams), *Mercenaria mercenaria*. *Journal of Shellfish Research* **26,** 109-119.

Ragone Calvo, L. M., Walker, J. G. and Burreson, E. M. (1998) Prevalence and distribution of QPX, Quahog Parasite Unknown, in hard clams, *Mercenaria mercenaria* in Virginia, USA. *Diseases of Aquatic Organisms* **33,** 209-219.

Ragone, L. M. and Burreson, E. M. (1993) Effect of salinity on infection progression and pathogenicity of *Perkinsus marinus* in the easter oyster, *Crassostrea virginica. Journal of Shellfish Research* **12,** 1-7.

Rinkevich, B. (1999) Cell cultures from marine invertebrates: obstacles, new approaches and recent improvements. *Journal of Biotechnology* **70,** 133-153.

Santangelo, G., Bongiorni, L. and Pignataro, L. (2000) Abundance of thraustochytrids and ciliated protozoans in a Mediterranean sandy shore determined by an improved, direct method. *Aquatic Microbial Ecology* **23,** 55-61.

Schutte, U. M., Abdo, Z., Bent, S. J., Shyu, C., Williams, C. J., Pierson, J. D. and Forney, L. J. (2008) Advances in the use of terminal restriction fragment length polymorphism (T-RFLP) analysis of 16S rRNA genes to characterize microbial communities. *Applied Microbiology and Biotechnology* **80,** 365-380.

Schwalbach, M. S. and Fuhrman, J. A. (2005) Wide-ranging abundances of aerobic anoxygenic phototrophic bacteria in the world ocean revealed by epifluorescence microscopy and quantitative PCR. *Limnology and Oceanography* **50,** 620-628.

Selesi, D., Pattis, I., Schmid, M., Kandeler, E. and Hartmann, A. (2007) Quantification of bacterial RubisCO genes in soils by *cbbL* targeted real-time PCR. *Journal of Microbiological Methods* **69,** 497-503.

Skovhus, T. L., Ramsing, N. B., Holmstrom, C., Kjelleberg, S. and Dahllof, I. (2004) Real-time quantitative PCR for assessment of abundance of *Pseudoalteromonas* species in marine samples. *Applied and Environmental Microbiology* **70,** 2373-2382.

Smith, C. J., Danilowicz, B. S., Clear, A. K., Costello, F. J., Wilson, B. and Meijer, W. G. (2005) T-Align, a web-based tool for comparison of multiple terminal restriction fragment length polymorphism profiles. *FEMS Microbiology Ecology* **54,** 375-380.

Smolowitz, R., Leavitt, D. and Perkins, F. (1998) Observations of a protistan disease similar to QPX in *Mercenaria mercenaria* (hard clams) from the coast of Massachusetts. *Journal of Invertebrate Pathology* **71,** 9-25.

Stoeck, T., Taylor, G. T. and Epstein, S. S. (2003) Novel eukaryotes from the permanently anoxic Cariaco Basin (Caribbean sea). *Applied and Environmental Microbiology* **69,** 5656-5663.

Stokes, N. A. and Burreson, E. M. (1995) A sensitive and specific DNA probe for the oyster pathogen *Haplosporidium Nelsoni. Journal of Eukaryotic Microbiology* **42,** 350-357.

Stokes, N. A., Ragone Calvo, L. M., Reece, K. S. and Burreson, E. M. (2002) Molecular diagnostics, field validation, and phylogenetic analysis of Quahog Parasite Unknown (QPX), a pathogen of the hard clam *Mercenaria mercenaria*. *Diseases of Aquatic Organisms* **52,** 233-247.

Travers, M. A., Basuyaux, O., Le Goic, N., Huchette, S., Nicolas, J. L., Koken, M. and Paillard, C. (2009) Influence of temperature and spawning effort on *Haliotis tuberculata* mortalities caused by *Vibrio harveyi*: an example of emerging vibriosis linked to global warming. *Global Change Biology* **15,** 1365-1376.

Tu, O., Knott, T., Marsh, M., Bechtol, K., Harris, D., Barker, D. and Bashkin, J. (1998) The influence of fluorescent dye structure on the electrophoretic mobility of end-labeled DNA. *Nucleic Acids Research* **26,** 2797-2802.

Van der Auwera, G., Chapelle, S. and De Wachter, R. (1994) Structure of the large ribosomal subunit RNA of *Phytophthora megasperma*, and phylogeny of the oomycetes. *FEBS Letters* **338,** 133-136.

Vigil, P., Countway, P. D., Rose, J., Lonsdale, D. J., Gobler, C. J. and Caron, D. A. (2009) Rapid shifts in dominant taxa among microbial eukaryotes in estuarine ecosystems. *Aquatic Microbial Ecology* **54,** 83-100.

Watson, R. J. and Blackwell, B. (2000) Purification and characterization of a common soil component which inhibits the polymerase chain reaction. *Canadian Journal of Microbiology* **46,** 633-642.

Whyte, S. K., Cawthorn, R. J. and McGladdery, S. E. (1994) QPX (Quahaug Parasite X), a pathogen of northern quahaug *Mercenaria mercenaria* from the Gulf of St.Lawrence, Canada. *Diseases of Aquatic Organisms* **19,** 129-136.

Will-Wolf, S., Geiser, L. H., Neitlich, P. and Reis, A. H. (2006) Forest lichen communities and environment - How consistent are relationships across scales? *Journal of Vegetation Science* **17,** 171-184.

Wise, M. J. and Osborn, A. M. (2001) TRUFFLER: programs to study microbial community composition and flux from fluorescent DNA fingerprinting data. In *bioinformatics and bioengineering Conference*, pp. 129-135.

Yi, H., Kim, H. J., Kim, C. G., Harn, C. H., Kim, H. M. and Park, S. (2009) Using T-RFLP to assess the impact on soil microbial communities by transgenic lines of watermelon rootstock resistant to Cucumber Green Mottle Mosaic Virus (CGMMV). *Journal of Plant Biology* **52,** 577-584.

Zhang, H. and Lin, S. J. (2005) Development of a cob-18S rRNA gene real-time PCR assay for quantifying *Pfiesteria shumwayae* in the natural environment. *Applied and Environmental Microbiology* **71,** 7053-7063.

Zhang, T. and Fang, H. H. P. (2006) Applications of real-time polymerase chain reaction for quantification of microorganisms in environmental samples. *Applied Microbiology and Biotechnology* **70,** 281-289.

Zhu, F., Massana, R., Not, F., Marie, D. and Vaulot, D. (2005) Mapping of picoeucaryotes in marine ecosystems with quantitative PCR of the 18S rRNA gene. *FEMS Microbiology Ecology* **52,** 79-92.

Appendix

Appendix 5. 1. The predicted T-RF lengths and their possible matches with observed T-RFs presented in Table 5.6, of representative species of major subgroups of labyrinthulomycetes described in Collado-Mercado *et al*. (2010). "NT" indicates a predicted fragment smaller than 70 bases, the smallest T-RF size in the T-RFLP profile. "NI" indicates a predicted fragment that could not match any observed TRF among the TRFs contributing to any pattern in sediment or seawater samples. T-RF* indicates a predicted fragment that could not match any of the observed T-RF presented in Table 5.6, but could match some other observed T-RF among the important TRFs (Pearson correlation efficient $r^2 \geq 0.1$) contributing to the either seasonal patterns or habitat differences

a	*HaeIII*				
Subgroup	Genbank accession number and name of the representative species	Predicted fragment length (bases)		Possible matching observed fragment length (bases)	
		blue	green	blue	green
Aurantiochytrium	DQ023611_Schizochytrium_limacinum_isolate_BUCACD_032	80	75		72
	AB183658_Th_MBIC11075	79	82	79	
	AY705763_Thraustochytriidae_sp_NIOS_1_haplotype_NIOS1_C05_3	80	82		
	AY758384_Schiz_FJU512	81	82		
	AB073308_Th_N1_27	288	81	283, 285, 286, 287	78,79
	DQ374149_Th_ONC_T18	292	81	287, 289, 290, 291	
	AY705742_Thraustochytriidae_sp_NIOS_4_haplotype_NIOS4_A00_2	292	82		
Thraust Caudivorum	EF114354_Thraustochytrium_sp_caudivorum_strain_S4_clone_T41	291	79	286, 287, 289, 290, 291	
Between uTH2 and Aurantiochytrium	DQ367051_Th_thel2	291	79		
Thraust Pachydermum	AF474172_Th_C9G	297*	81	292, 295*	
Aurantiochytrium	DQ023621_Schizochytrium_sp_BUCHAO_113	80	87		86, 87
Thraust Pachydermum	DQ641204_QPX_NY0313808CC1	79	138	79	
	AB022113_Thraust_pachydermum	79	138		
Aurantiochytrium	DQ834737_Thraust_BP3_3_3	80	141		
	DQ834733_Thraust_TR1_4	81	142		
Oblongichytrium sp.?	PBS102405_12	134	137	132, 133	136
Ulkenia	AB022104_Japon_ATCC_28207	179	137	NI	
Schizochytrium	AB073309_Th_N4_103	282	140		
	AB073306_Th_H6_16	287	137	283, 285, 286, 287	

uLa 3	PBS102405_38	290	138	285, 286, 287, 289, 290	
Labyrinthula	AB095092_Labyrinthula_L59	290	136		
Thraust gaertnerium	AY705755_Th_NIOS6_A05_1	291	141	286, 287, 289, 290, 291	
Schizochytrium	AB022106_Schiz_aggregatum_ATCC_28209`	291	141		
uLa 4	PBS102907_02	292	138	287, 289, 290, 291	
Aplanochytrium	PBS07	292	138		
uLa 5	PBW102907_34	292	136		
Sycioidochytrium	AY870336_Thraustochytriidae_sp_Fng1	292	138		
Botryochytrium	AB022114_Ulkenia_profunda_Raghukumar_29	292	139		
Thraust kinnei	L34668_Thraust_kinnei_1694d	292	138		
Schizochytrium	AB290578_Schiz_SEK_346	292	138		
	AB052556_Thraust_KK17_3	292	141		
Loides haliotidis	BBW042908_27	292	138		
uTH1	PBW102907_25	292	138		
Thraust Striatum/motivum	AB022112_Thraust_striatum_ATCC_24473	292	140		
Ulkenia	DQ023615_Ulkenia_profunda_BUTRBG_111	292	139		
Oblongichytrium (Y&H)	PBS02	293	138	289, 290, 291	
uLa7	AY381171_uncult_euk_HE001005_112	293	138		
uLa 2	PBS102405_10	293	138		
uLa 8	EF100247_Uncult_euk_D2P04B04	293	138		
uLa 5	AY381210_uncult_euk_BL010320_19	293	137		
uLa1	PJS101305_60	293	138		
uLa6	DQ310278_uncult_euk_FV23_CilD7	294	138		
Ulkenia	AY256317_uncult_euk_D107	294	138		
Between uTH2 and Aurantiochytrium	DQ367052_Th_32	295	138	290, 291	
Ulkenia	FJ010826_Thraustochytriidae_sp_AS4A1	296	139	291	
	AB022116_Ulkenia_visurgensis_ATCC_28208	297*	139	292, 295*	
Thraust aureum	AB022110_Thraust_aureum_ATCC_34304	295	64	290,291	NT
Parietichytrium	AB244715_Th_RT0049	292	144*	287, 289, 290, 291	141*
Labyrinthula	AB290457_Labyrinthula_sp_01_Jy_1b	290	135	285, 286, 287, 289, 290	133, 135*
	AB246795_Labyrinthula_N12				

b	Sau96I					
Subgroup	Genbank accession number and name of the representative species	Predicted fragment length (bases)		Possible matching observed fragment length (bases)		
		blue	green	blue	green	
Schizochytrium	AB022106_Schiz_aggregatum_ATCC_28209	66	143	NT	NI	
Aurantiochytrium	DQ834737_Thraust_BP3_3_3	79	142	77, 78, 79		
	DQ834733_Thraust_TR1_4	80	144			
	DQ023611_Schizochytrium_limacinum_isolate_BUCACD_032	79	201		199, 200	
	AB073308_Th_N1_27	76	203	71, 72		
Ulkenia	AB022104_Japon_ATCC_28207	184	204	NI		
uLa 3	PBS102405_38	227	203	222, 223, 224		
uLa 5	PBW102907_34	227	203			
Labyrinthula	AB246795_Labyrinthula_N12	225	202	221, 222, 223, 224		
Between uTH2 and Aurantiochytrium	DQ367051_Th_thel2	226	203			
Labyrinthula	AB290457_Labyrinthula_sp_01_Jy_1b	225	204	223, 224	199, 200, 204	
Oblongichytrium sp.?	PBS102405_12	228	204			
uLa 5	AY381210_uncult_euk_BL010320_19	228	204			
Thraust aureum	AB022110_Thraust_aureum_ATCC_34304	231	204	229		
Thraust pachydermum	DQ641204_QPX_NY0313808CC1	79	205	77, 78, 79	200, 204	
Schizochytrium	AB073306_Th_H6_16	222	205	219, 221, 222		
	AB290578_Schiz_SEK_346	227	205	222, 223, 224		
Thraust Caudivorum	EF114354_Thraustochytrium_sp_caudivorum_strain_S4_clone_T41	227	205			
Loides haliotidis'	BBW042908_27	227	205			
Thraust kinnei	L34668_Thraust_kinnei_1694d	227	205			
uLa 4	PBS102907_02	227	205			
Aplanochytrium	PBS07	227	205			
uTH1	PBW102907_25	227	205			
Sycioidochytrium	AY870336_Thraustochytriidae_sp_Fng1	227	205			
uLa 8	EF100247_Uncult_euk_D2P04B04	228	205	223, 224		
Oblongichytrium (Y&H)	PBS02	228	205			
uLa 2	PBS102405_10	228	205			
uLa7	AY381171_uncult_euk_HE001005_11	228	205			

	2				
uLa6	DQ310278_uncult_euk_FV23_CilD7	229	205	224, 229	
uTH1	AY256317_uncult_euk_D107	229	205		
Ulkenia	DQ023615_Ulkenia_profunda_BUTRBG_111	293	206	NI	204
Aurantiochytrium	DQ374149_Th_ONC_T18	78	207	77, 78	
	AB183658_Th_MBIC11075	78	208		
	AY705763_Thraustochytriidae_sp_NIOS_1_haplotype_NIOS1_C05_3	79	208	77, 78, 79	
	AY758384_Schiz_FJU512	80	208		
	AB073303_Thraustochytriidae_A5_20	89	207	85, 86, 87	
Schizochytrium	AB073309_Th_N4_103	110	207	105, 108	
Thraust gaertnerium	AY705755_Th_NIOS6_A05_1	226	207	221, 222, 223, 224	
Botryochytrium	AB022114_Ulkenia_profunda_Raghukumar_29	227	206	222, 223, 224	
Thraust Striatum/motivum	AB022112_Thraust_striatum_ATCC_24473	227	207		
Schizochytrium	AB052556_Thraust_KK17_3	227	208		
Parietichytrium	AB244715_Th_RT0049	229	209	224, 229	
Ulkenia	FJ010826_Thraustochytriidae_sp_AS4A1	231	206	229	
	AB022116_Ulkenia_visurgensis_ATCC_28208	232	206		
Thraust Pachydermum	AF474172_Th_C9G	232	207		
Parietichytrium	AB073305_Th_H1_14	231	207		
Between uTH2 and Aurantiochytrium	DQ367052_Th_32	230	67		NT
Aurantiochytrium	DQ836629_Th_T65	78	211	77, 78	210, 211
uLa1	PJS101305_60	229	213	224, 229	210, 211, 212
Aurantiochytrium	DQ023621_Schizochytrium_sp_BUCHAO_113	79	217	77, 78,79	212